เอทานอลดีไฮเดรชันบนตัวเร่งปฏิกิริยาอะลูมินาที่ปรับปรุงด้วยฟอสฟอรัสและโลหะมีตระกูล

นางสาวมุจลินลฐ์ ลิ้มแหลมทอง

วิทยานิพนธ์นี้เป็นส่วนหนึ่งของการศึกษาตามหลักสูตรปริญญาวิศวกรรมศาสตรมหาบัณฑิต
สาขาวิชาวิศวกรรมเคมี ภาควิชาวิศวกรรมเคมี
คณะวิศวกรรมศาสตร์ จุฬาลงกรณ์มหาวิทยาลัย
ปีการศึกษา 2559

ETHANOL DEHYDRATION OVER ALUMINA CATALYSTS WITH PHOSPHORUS AND NOBLE METAL MODIFICATION

Miss Mutjalin Limlamthong

A Thesis Submitted in Partial Fulfillment of the Requirements
for the Degree of Master of Engineering Program in Chemical Engineering
Department of Chemical Engineering
Faculty of Engineering
Chulalongkorn University
Academic Year 2016

Thesis Title	ETHANOL DEHYDRATION OVER ALUMINA CATALYSTS WITH PHOSPHORUS AND NOBLE METAL MODIFICATION
By	Miss Mutjalin Limlamthong
Field of Study	Chemical Engineering
Thesis Advisor	Professor Bunjerd Jongsomjit, Ph.D.

Accepted by the Faculty of Engineering, Chulalongkorn University in Partial Fulfillment of the Requirements for the Master's Degree

.....Dean of the Faculty of Engineering
(Associate Professor Supot Teachavorasinskun, D.Eng.)

THESIS COMMITTEE

.....Chairman
(Associate Professor Muenduen Phisalaphong, Ph.D.)

.....Thesis Advisor
(Professor Bunjerd Jongsomjit, Ph.D.)

.....Examiner
(Chutimon Satirapipathkul, D.Eng.)

.....External Examiner
(Ekrachan Chaichana, D.Eng.)

มุจลินลฐ์ ลิ้มแหลมทอง : เอทานอลดีไฮเดรชันบนตัวเร่งปฏิกิริยาอะลูมินาที่ปรับปรุงด้วยฟอสฟอรัสและโลหะมีตระกูล (ETHANOL DEHYDRATION OVER ALUMINA CATALYSTS WITH PHOSPHORUS AND NOBLE METAL MODIFICATION) อ .ที่ปรึกษาวิทยานิพนธ์หลัก: ศ. ดร. บรรเจิด จงสมจิตร, 160 หน้า.

ตัวรองรับอะลูมินาซึ่งประกอบด้วยเฟสแกมมาและไคน์ในอัตราส่วนโดยปริมาตรเท่ากับ 1:1 ถูกเตรียมด้วยวิธีโซลโวเทอร์มอล โดยใช้สารผสมระหว่างโทลูอีนและ1-บิวทานอลเป็นตัวทำละลาย ตัวรองรับดังกล่าวถูกนำไปปรับปรุงด้วยกรดฟอสฟอริกและสารตัวแทนโลหะมีตระกูล ตัวเร่งปฏิกิริยาที่ได้ถูกตรวจสอบผลของปริมาณฟอสฟอรัสและชนิดของโลหะมีตระกูลซึ่งส่งผลต่อคุณสมบัติและประสิทธิภาพในการเร่งปฏิกิริยาของตัวเร่งปฏิกิริยา ความสามารถในการเร่งปฏิกิริยาของตัวเร่งปฏิกิริยาถูกวินิจฉัยผ่านปฏิกิริยาดีไฮเดรชันของเอทานอลในวัฏภาคแก๊ส ที่ความดันบรรยากาศและอุณหภูมิ 200 ถึง 400 องศาเซลเซียส ผลการทดลองพบว่าการเติมฟอสฟอรัสส่งผลต่อความเป็นกรดของตัวเร่งปฏิกิริยาโดยลดปริมาณกรดปานกลางถึงแก่และเพิ่มปริมาณกรดอ่อน ปริมาณกรดอ่อนที่มากขึ้นส่งผลทำให้ตัวเร่งปฏิกิริยามีความสามารถในการทำปฏิกิริยาดีไฮเดรชันเพื่อเปลี่ยนเอทานอลไปเป็นไดเอทิลอีเทอร์ได้มากขึ้น ตัวรองรับอะลูมินาในวัฏภาคผสมซึ่งปรับปรุงด้วยฟอสฟอรัสปริมาณ 5 เปอร์เซ็นต์โดยน้ำหนัก แสดงประสิทธิภาพในการเร่งปฏิกิริยาที่สูงที่สุดในตัวเร่งปฏิกิริยาอะลูมินาซึ่งผ่านการปรับปรุงด้วยฟอสฟอรัสอื่นๆ โดยให้ปริมาณไดเอทิลอีเทอร์เท่ากับ 34.41 เปอร์เซ็นต์ นอกจากนี้ การปรับปรุงโลหะมีตระกูลต่างชนิดกันพบว่าส่งผลอย่างมีนัยยะสำคัญต่อความสามารถในการเร่งปฏิกิริยาของตัวเร่งปฏิกิริยา ตัวเร่งปฏิกิริยา 5P/Al_2O_3 ซึ่งปรับปรุงด้วยพาลาเดียมแสดงประสิทธิภาพในการเร่งปฏิกิริยาที่สูงที่สุดในตัวเร่งปฏิกิริยาที่ศึกษาทั้งหมด โดยให้ปริมาณไดเอทิลอีเทอร์สูงถึง 57.68 เปอร์เซ็นต์ ปริมาณไดเอทิลอีเทอร์ที่สูงที่สุดเท่ากับ 42.50 เปอร์เซ็นต์ ได้รับจากการใช้ตัวเร่งปฏิกิริยา Pd5P/Al_2O_3 ในระบบอุณหภูมิคงที่เป็นเวลา 10 ชั่วโมง แม้ว่าปริมาณไดเอทิลอีเทอร์ที่ได้รับจะมีค่าสูง แต่ทั้งตัวเร่งปฏิกิริยา 5P/Al_2O_3 และ Pd5P/Al_2O_3 ต่างเกิดปริมาณคาร์บอนที่เกาะที่ผิวของตัวเร่งปฏิกิริยาขึ้นน้อยกว่าเมื่อเปรียบเทียบกับตัวเร่งปฏิกิริยาอะลูมินาที่ไม่ผ่านการปรับปรุง

ภาควิชา วิศวกรรมเคมี ลายมือชื่อนิสิต .....

สาขาวิชา วิศวกรรมเคมี ลายมือชื่อ อ.ที่ปรึกษาหลัก .....

ปีการศึกษา 2559

5870225521 : MAJOR CHEMICAL ENGINEERING
KEYWORDS: MIXED PHASE ALUMINA / ETHANOL DEHYDRATION / DIETHYL ETHER

MUTJALIN LIMLAMTHONG: ETHANOL DEHYDRATION OVER ALUMINA CATALYSTS WITH PHOSPHORUS AND NOBLE METAL MODIFICATION. ADVISOR: PROF. BUNJERD JONGSOMJIT, Ph.D., 160 pp.

The mixture of 1:1 volume ratio of gamma and chi crystalline phase alumina support was prepared via the solvothermal technique using the mixed solution between toluene and 1-butanol. The support was brought to modify with phosphoric acid and noble metal agents. These catalysts were investigated on the effect of both phosphorus loading and types of noble metal on catalytic characteristic and catalytic activity. The catalytic performance was identified through ethanol dehydration reaction in gas phase process at 1 atm and temperature of 200°C to 400°C. The results were found that the phosphorus modification had an effect on catalytic acidity by decreasing the amount of medium to strong acid sites and raised quantity of weak acid sites. The higher amount of weak acid brought the catalysts to demonstrate the higher catalytic activity through the ethanol dehydration to diethyl ether. The mixed phase of alumina supports modified with 5 wt% of phosphorus exhibited the highest catalytic activity among other P-modified alumina catalysts giving the diethyl ether yield of 34.41%. In addition, the different types of noble metal modification were found to have a significant effect on catalytic performance. The 5P/Al_2O_3 catalyst deposited by palladium showed the highest catalytic activity through all of the studied catalysts reached 57.68% of diethyl ether yield. The highest average yield of diethyl ether of 42.50% was obtained from using Pd5P/Al_2O_3 catalyst in time on stream system for 10 h. Despite of high diethyl ether yield obtained, both 5P/Al_2O_3 and Pd5P/Al_2O_3 catalysts had the lower coke formation when compared to non-modified alumina supports.

Department:	Chemical Engineering	Student's Signature	.....
Field of Study:	Chemical Engineering	Advisor's Signature	.....
Academic Year:	2016		

ACKNOWLEDGEMENTS

The author would like to evince the greatest appreciation to her advisor, Professor Bunjerd Jongsomjit for his continuous support, counsel and invaluable encouragement along this research. In addition, the author is also grateful for chairman of the committee, Associate Professor Muenduen Phisalaphong and members of the thesis committee, Chutimon Satirapipathkul and Ekrachan Chaichana for their dedicated in spending the time for her research suggestion.

Furthermore, the author would like to thank for the Thailand Research Fund (TRF) and Department of Chemical Engineering, Chulalongkorn University for the financial support of this research.

Most of all, the author would like to express the gratefully acknowledge to her parents and friends both in Center of Excellence on Catalysis and Catalytic Reaction Engineering and others for their supporting and encouragement throughout the times of the research.

CONTENTS

Page

Page

Page

Page

Page

FIGURE CONTENTS

TABLE CONTENTS

SCHEME CONTENTS

Chapter 1
INTRODUCTION

1.1 General introduction

In recent times, about 85% of the providing energy in the world comes from fossil fuels [1]. However, the usage of fossil fuels tends to create anthropogenic emissions of greenhouse gases, which significantly cause the global climate change [2]. To decrease the global warming effect, ethanol which currently the biggest biofuel in the world is employed to use as alternative fuels instead of fossil fuels. Although, the use of ethanol as fuel still has many problems such as corrosiveness and low solubility in fossil fuels, which cause the variation of fuel properties [3]. In addition, diethyl ether (DEE) can improve cetane number by adding to diesel fuels and can reduce NO_x and particulate emissions, which is observed to be about 89% and 85%, respectively [4]. Therefore, in this research, we are interested in turning ethanol into diethyl ether towards dehydration reaction.

Alumina (Al_2O_3) has been found significantly interesting as support due to its thermal stability, easy to synthesize and high surface area. Khom-in et al. investigated activities of mixed γ- and χ-phase Al_2O_3 supports in dehydration reaction [5]. They discovered that mixed γ- and χ-phase Al_2O_3 supports have higher activities towards dehydration reaction compared to single γ-Al_2O_3 or χ-Al_2O_3 supports. Therefore, we used mixed γ- and χ-phase Al_2O_3 supports in the ratio of 1:1 in this study. Ramesh et al. [6] reported the effect of phosphorus modified H-ZSM-5 catalyst in ethanol dehydration reaction. They proposed that the modification of phosphorus on H-ZSM-5 catalyst increases the activity and stability of the catalyst (stability is up to 110 h). In addition, they found diethyl ether as main product at low temperature. Furthermore, from Golay et al. [7] and Zaki [8] investigation, solid acid catalysts considered to have higher activity for ethanol dehydration reaction compared to solid catalysts with basic character.

From the studies, the ethanol dehydration reaction at low temperature causes low ethanol conversion and diethyl ether yield; consequently, the noble metals (Pt, Pd and Ru) were added into catalysts to improve the catalytic activity for diethyl ether production. Therefore, this research aims to investigate the catalytic properties and catalytic performance of P-modified and noble metal modified P/Al_2O_3 catalysts, which were synthesized by acid activation and incipient wetness impregnation techniques, respectively.

1.2 Research objectives

1) To investigate the effect of catalysts characteristics related to the catalytic performance towards ethanol dehydration reaction.
2) To compare the effect of P-modified and addition of noble metal (Pt, Pd and Ru) on alumina supports in catalytic dehydration of ethanol activities.
3) To compare the catalytic stability between Al_2O_3 supports, P-modified Al_2O_3 catalyst and noble metal modified P/Al_2O_3 catalyst in ethanol dehydration reaction for 10 h.
4) To compare the effect of noble metal addition on alumina supports and noble metal addition on P-modified alumina catalyst to catalytic performance of ethanol dehydration reaction.

1.3 Research scopes

1) Synthesis of the Al_2O_3 supports by solvothermal method.
2) Synthesis of the P-modified Al_2O_3 catalysts by varying phosphorus loading at 0-20 wt% using acid activation technique.

3) Reaction study of 0-20 wt% P-modified Al_2O_3 catalysts in ethanol dehydration reaction, which is carried out in a fixed-bed reactor under atmospheric pressure and temperature range of 200-400°C.
4) Determining the most suitable P-modified Al_2O_3 catalyst and reaction condition, which gives the highest diethyl ether yield.
5) Modification of the chosen P-modified Al_2O_3 catalyst with different noble metals including Pt, Pd and Ru using the incipient wetness impregnation technique.
6) Reaction study of noble metal modified P/Al_2O_3 catalysts in ethanol dehydration reaction, which is carried out in a fixed-bed reactor under atmospheric pressure and temperature range of 200-400°C.
7) Determining the most suitable noble metal modified P/Al_2O_3 catalyst and reaction condition, which gives the highest diethyl ether yield.
8) Reaction study of the Al_2O_3 supports, the chosen P-modified Al_2O_3 catalyst and the chosen noble metal modified P/Al_2O_3 catalyst under atmospheric pressure and its most suitable temperature for 10 h.
9) Comparison of the catalytic performance in time on stream system between the Al_2O_3 supports, the chosen P-modified Al_2O_3 catalyst and the chosen noble metal modified P/Al_2O_3 catalyst.
10) Preparation of the chosen noble metal modified Al_2O_3 catalyst using the incipient wetness impregnation technique.
11) Reaction study of noble metal modified Al_2O_3 catalysts in ethanol dehydration reaction, which is carried out in a fixed-bed reactor under atmospheric pressure and temperature range of 200-400°C.
12) Comparison of the catalytic performance in time on stream system between the chosen P-modified Al_2O_3 catalyst and the chosen noble metal modified Al_2O_3 catalyst.

13) Characterization of Al_2O_3 supports, P/Al_2O_3 catalysts, noble metal modified Al_2O_3 catalyst and noble metal modified P/Al_2O_3 catalysts by using the following methods;

- X-ray diffraction (XRD)
- X-ray fluorescence (XRF)
- Inductively coupled plasma (ICP)
- Scanning electron microscope (SEM) and energy dispersive X-ray spectroscopy (EDX)
- N_2 physisorption
- Ammonia temperature-programmed desorption (NH_3-TPD)
- X-ray photoelectron spectroscopy (XPS)
- Thermal gravimetric and differential thermal analysis (TG/DTA)

1.4 Research methodology

Part I : The characteristic and catalytic activity of the Al_2O_3 catalysts modification with different loading of phosphorus (0-20 wt% P)

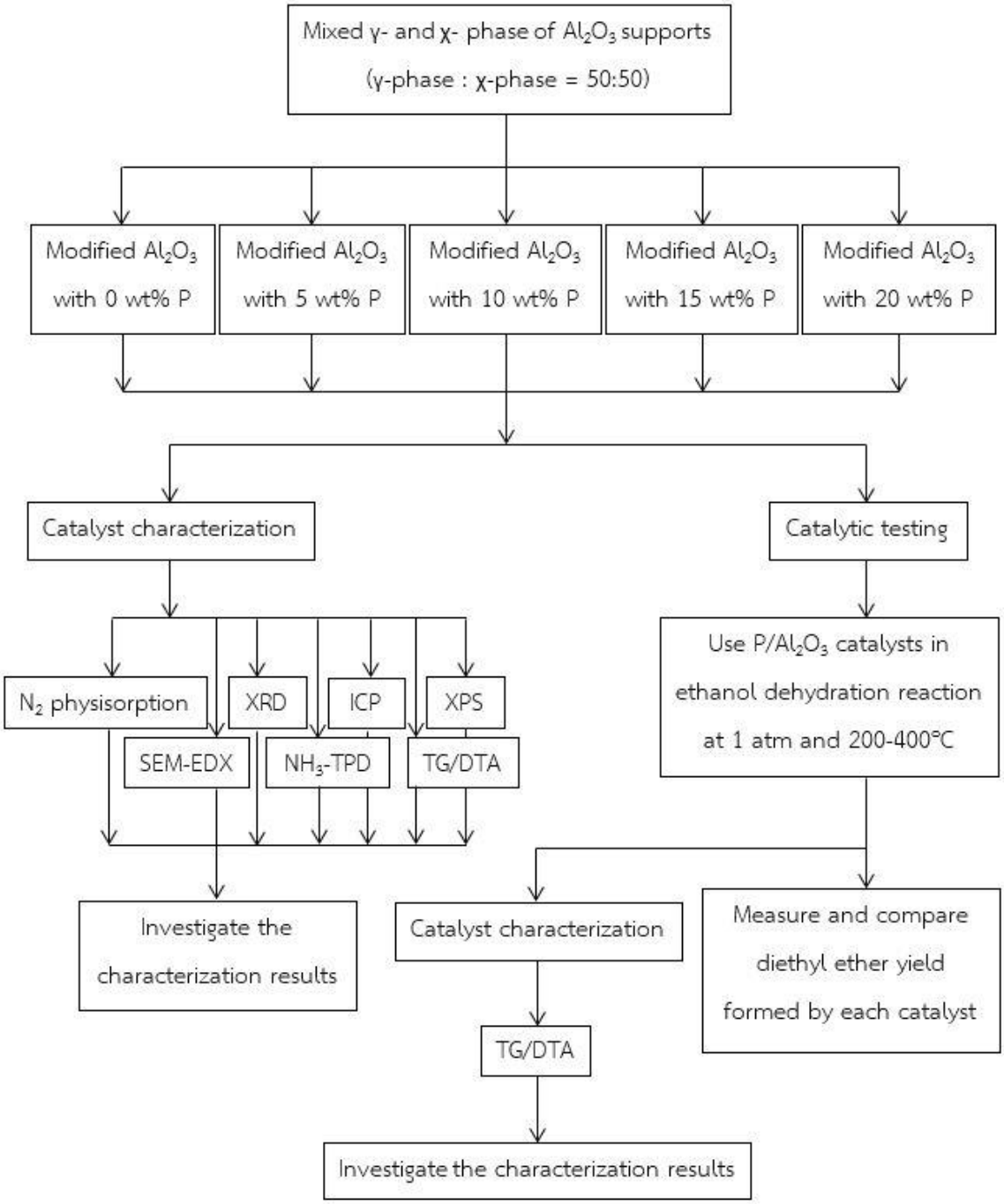

Part II : The characteristic and catalytic activity of the P/Al_2O_3 catalysts modification with different noble metals (Ru, Pt and Pd)

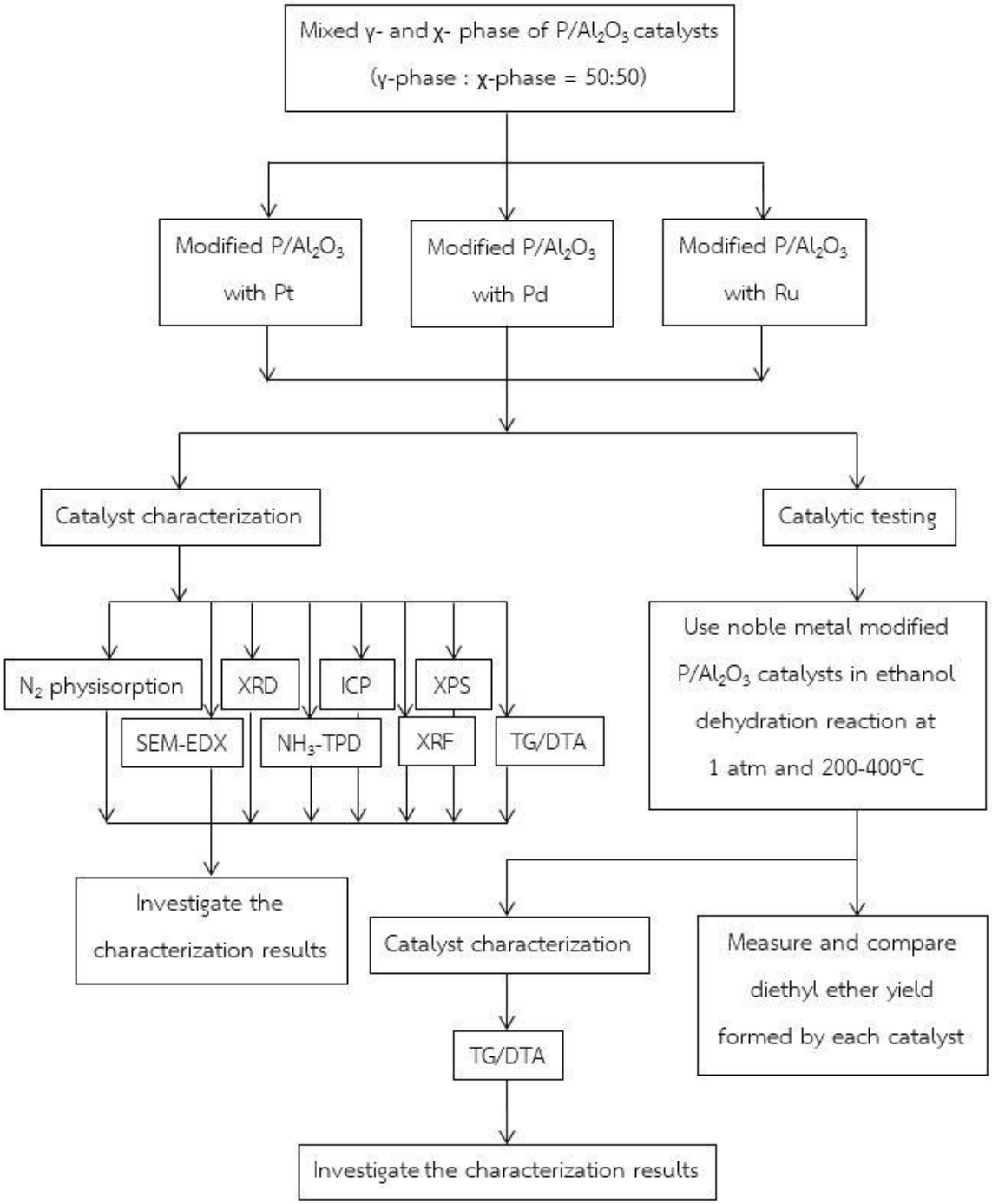

Part III : The comparison of the catalytic post-reaction properties and catalytic performance in time on stream system between Al_2O_3 supports, P-modified Al_2O_3 catalyst and the noble metal modified P/Al_2O_3 catalyst which was observed the highest diethyl ether yield.

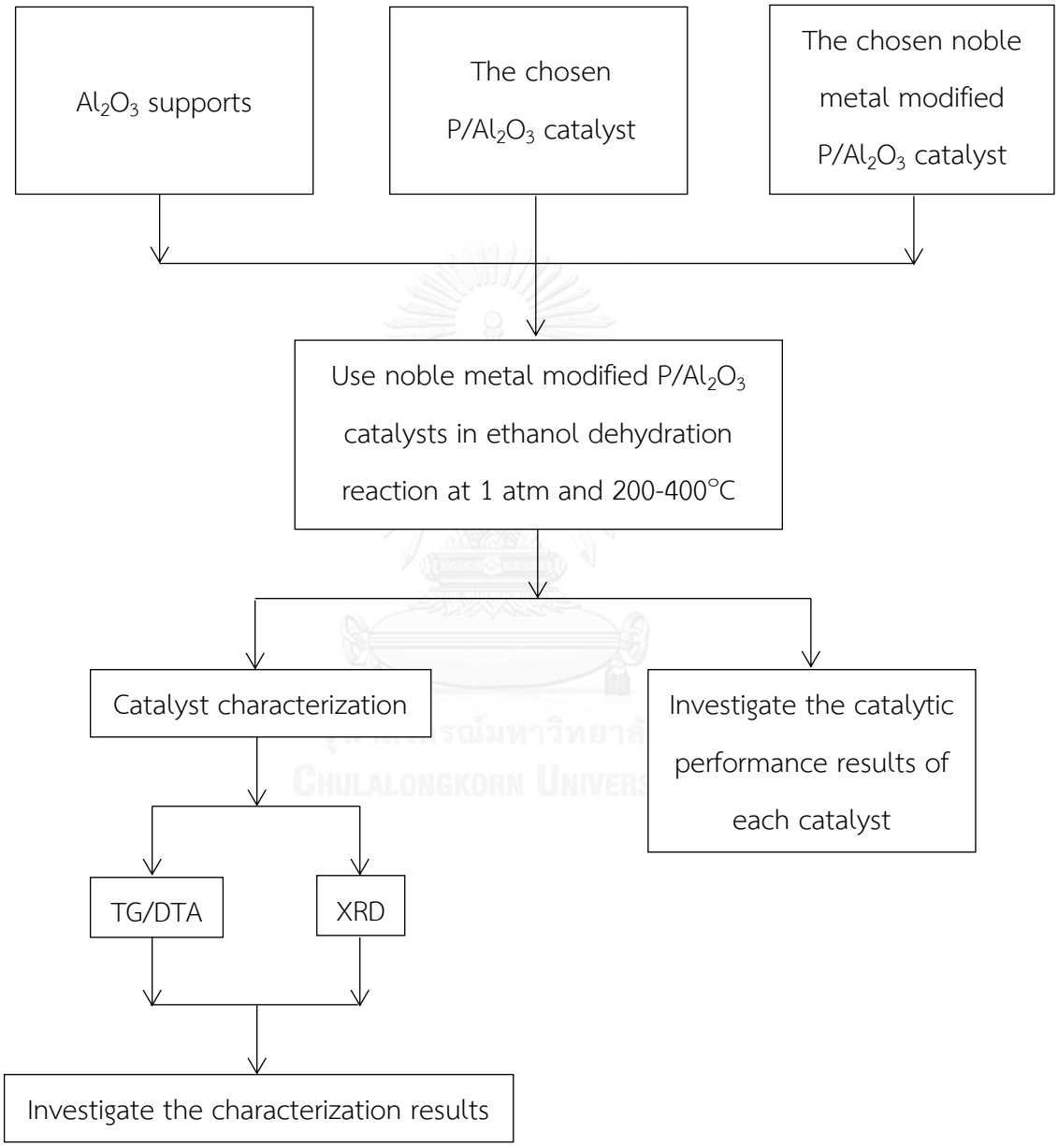

Part IV : Comparison of the characteristics and catalytic activity between the chosen noble metal modified Al_2O_3 catalyst and the chosen noble metal modified P/Al_2O_3 catalyst.

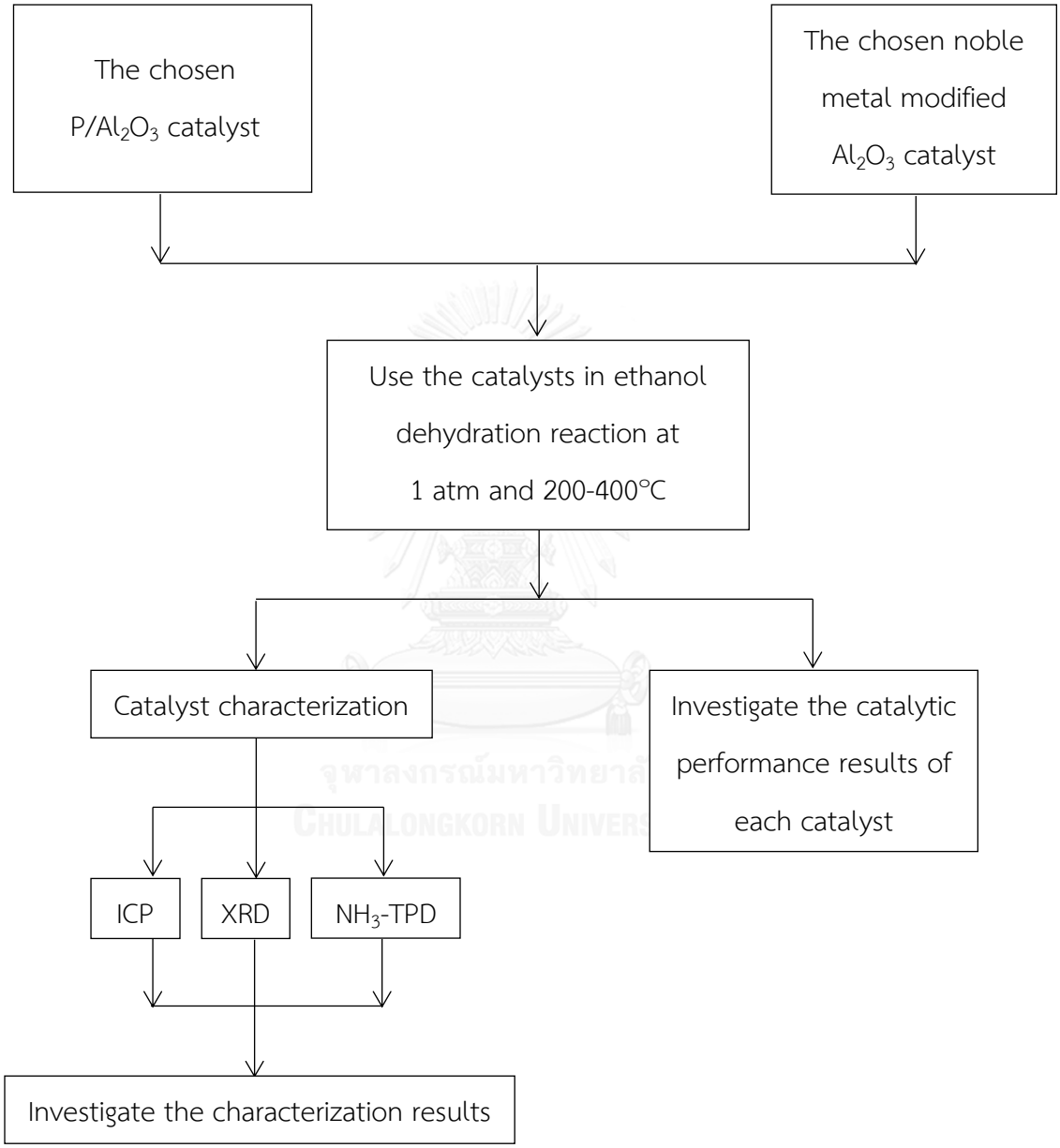

Chapter 2
THEORIES

2.1 Alumina

2.1.1 Property of alumina

Alumina, Al_2O_3, is one of the most important chemical compounds used in a variety of applications. Because of its high attrition resistance, high chemical resistance, high thermal resistance and high dielectric strength, alumina is widely used in temperature or electrical resistance applications and also served as catalyst support for many industries [9]. Alumina has a white solid appearance, a molar mass of 101.96 g mol^{-1}, a density of 3.95-4.10 g cm^{-3} and insoluble in water, diethyl ether and ethanol. Alumina also has melting and boiling points of 2072° C and 2977° C, respectively.

Each metastable crystalline structure of alumina (η-, γ-, δ-, θ-, β-, κ-, χ, and α-alumina) depends on the calcination condition of the precursor hydroxide through the thermal dehydration reaction. The precursor includes gibbsite, boehmite, bayerite, nordstrandite and diaspore [10, 11]. The phase transform of precursors into transition alumina is shown in **Figure 1** as follows;

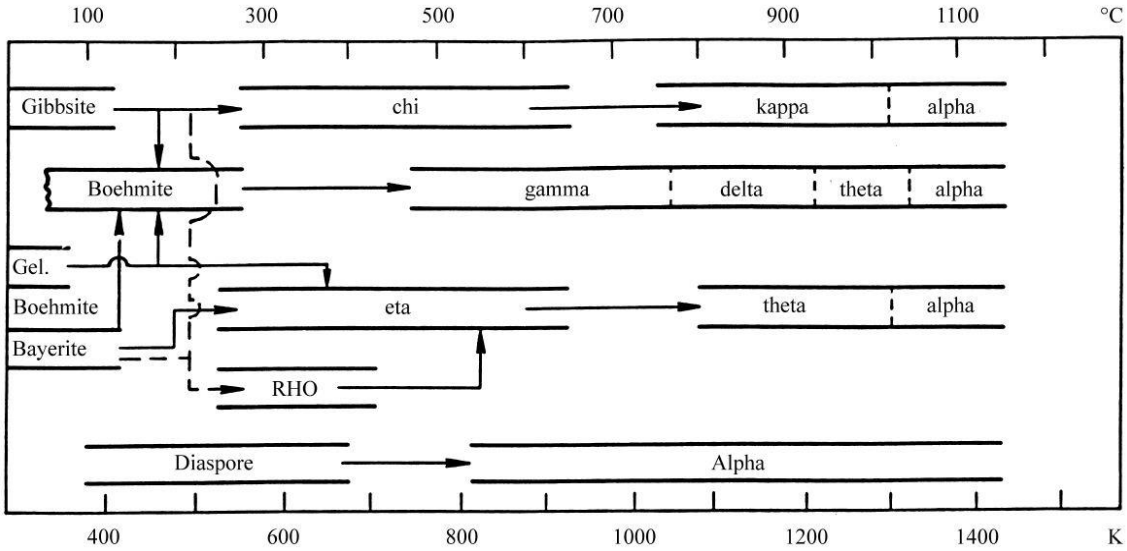

Figure 1 The sequence of aluminum hydroxide transformation [10].

Alumina has acid and basic sites on its surface. The acidity and basicity of alumina depend on the water treatment of alumina as depicted in **Figure 2**. When treated the alumina with the sufficient quantity of water, Al^{3+} ion in alumina converted Lewis acid sites into Brønsted acid sites, while the basic sites are determined from the O^{2-} anion [12].

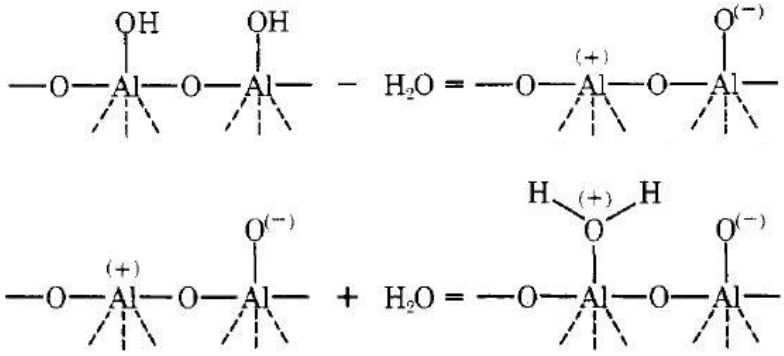

Figure 2 The effect of water addition on alumina acidity [12].

2.1.2 Synthesis of alumina: Solvothermal method

Alumina can be prepared by using various methods such as precipitation, sol-gel and solvothermal techniques [13]. Because of long synthesis time and

complexity of precipitation and sol-gel techniques, the synthesis by solvothermal method was picked up as an interesting technique.

The solvothermal synthesis is a method for preparing various materials under high pressure. The solvent used during synthesis determined the reaction's name. For the example, if water is used as the solvent, the process is called "hydrothermal synthesis". Solvothermal technique gains the advantage from sol-gel route in controlling of size, shape distribution and crystallinity of particle. These characteristics can be modified, by changing experimental conditions (precursor type, solvent type, reaction temperature and reaction time). Because the operation must be carried in closed system with high pressure condition; therefore, stainless steel autoclave is usually used as the reactor. Autoclave structure is representing in **Figure 3** as follow;

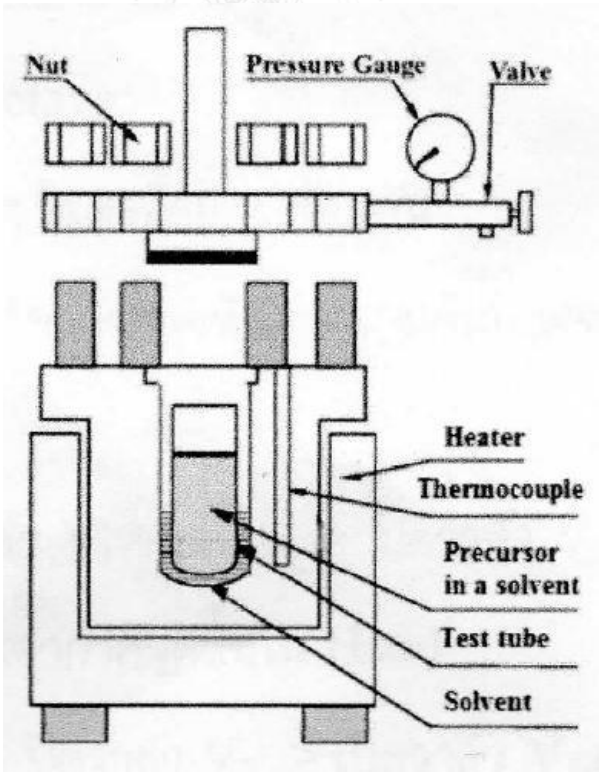

Figure 3 Stainless steel autoclave structure

2.2 Phosphorus

Phosphorus (P) is a chemical element with atomic number of 15. As a free element, phosphorus exists in many forms, which each form exhibits significantly different in properties as described in **Table 1**. Two major allotropes of phosphorus are white phosphorus and red phosphorus. Because of its high reactivity, it has never found as a free element, but found in oxidized state as phosphate rocks. In this study, the phosphorus is used to modify alumina support in the form of phosphoric acid in order to increase catalytic activity.

Table 1 Phosphorus properties

Properties	Specification
Appearance	colorless, waxy white, yellow, scarlet, red, violet, black
Group, block	group 15 (pnictogens), p-block
Atomic weight (±) (A_r)	30.974
Phase	solid
Density near r.t.	white: 1.823 g·cm^{-3} red: ≈ 2.2–2.34 g·cm^{-3} violet: 2.36 g·cm^{-3} black: 2.69 g·cm^{-3}
Heat of fusion	white: 0.66 kJ/mol
Heat of vaporization	white: 51.9 kJ/mol
Molar heat capacity	white: 23.824 J/(mol·K)

2.2 Promoter

Promoter is a substance which is added to solid catalyst in small amount but can significantly improve catalytic activity. Promoter itself has no or little effect on the catalytic activity. Considering from role of promoter, the promoter can be distinguished into two groups which are 1) Escalating the catalyst activity by facilitating the desired process and 2) Escalating the catalyst selectivity by poisoning the undesired reactions. Moreover, the promoter in the first group can be either structure-forming promoters, which form in particle as inert substances to prevent particle sintering or activating promoters, which create the addition active sites on the catalyst [14-16]. Generally, alkali, alkali earth, halogen group and noble metal such as Pt, Pd, Ru, Rh, Au, Ag and so on are often used as chemical promoter.

2.4 Ethanol dehydration reaction

Formerly, ethanol is normally used as a solvent. Since the discovery of dehydration reaction, ethanol can be used to produce a variety of products such as ethylene, diethyl ether (DEE), acetaldehyde and so on via catalytic dehydration reaction of ethanol.

Ethanol dehydration reaction occurs when the reaction reaches an optimal temperature with the existence of a suitable catalyst. The optimal temperature in ethanol dehydration reaction is in a range of 180°C to 500°C [17].

Two mainly competitive ways of ethanol dehydration are depicted as follows;

$C_2H_5OH \longleftrightarrow C_2H_4 + H_2O$.....+44.9 kJ/mol (1)

$2C_2H_5OH \longleftrightarrow C_2H_5OC_2H_5 + H_2O$..... –25.1 kJ/mol (2)

From Eq. (1) and (2), reaction (1) is a dehydration of ethanol to ethylene while reaction (2) is a dehydration of ethanol to diethyl ether. The reaction (1) is

favored at moderate to high temperature because it is endothermic reaction, contrasted with reaction (2) which is exothermic reaction and favors to occurred at low to moderate temperature [18].

In addition to the main products generated, ethanol dehydration reaction produces the small amount of byproducts such as acetaldehyde [19], hydrocarbons [20], light based-groups [21] and etc.

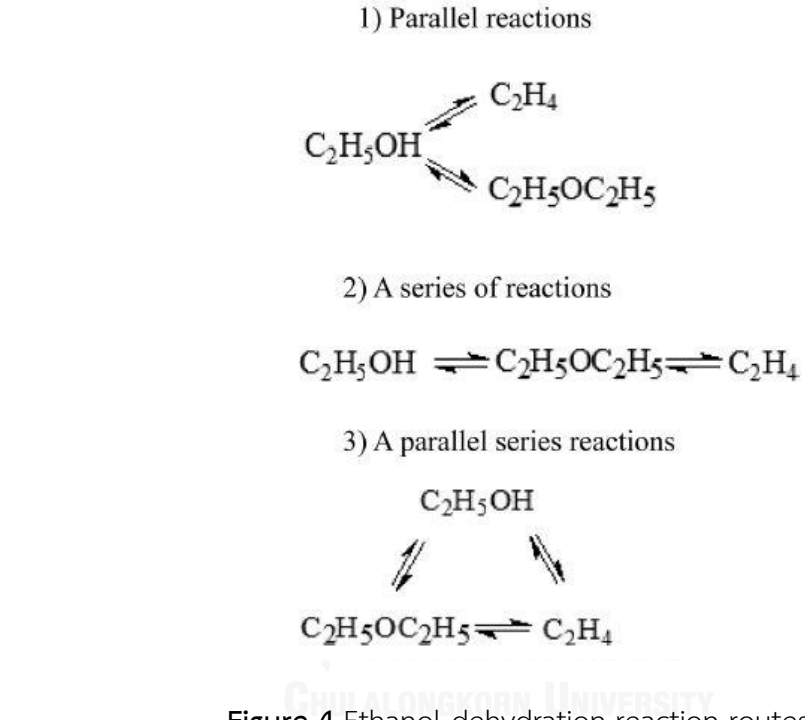

Figure 4 Ethanol dehydration reaction routes [22]

Figure 4 represents main mechanism of ethanol dehydration reaction. The mechanism of ethanol dehydration reaction can be summarized into 3 routes which are (1) parallel reactions (2) a series of reactions and (3) a parallel series reactions.

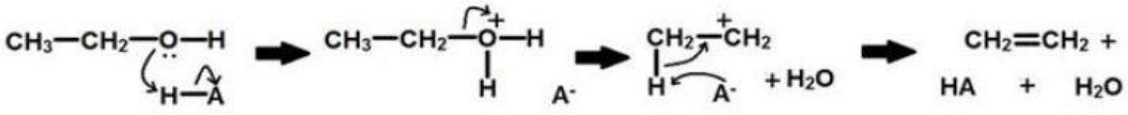

Figure 5 The mechanism of dehydration of ethanol to ethylene [17]

Considering the mechanism of ethanol dehydration to ethylene in **Figure 5**, one molecule of ethanol of ethylene required one molecule of ethanol to generate carbocation during the process. At first, an acid site (Brønsted acid site) in the solid catalyst protonates the hydroxyl group in ethanol molecule to remove a water molecule. Then, the methyl group is deprotonated by a conjugate base on the catalyst and rearranges the molecule into ethylene [17].

To illustrate the mechanism of dehydration reaction of ethanol to diethyl ether, there are two pathways of ethanol to form diethyl ether; (1) dissociative pathway (2) associative pathway. Both pathways require two molecule of ethanol to generate one diethyl ether molecule.

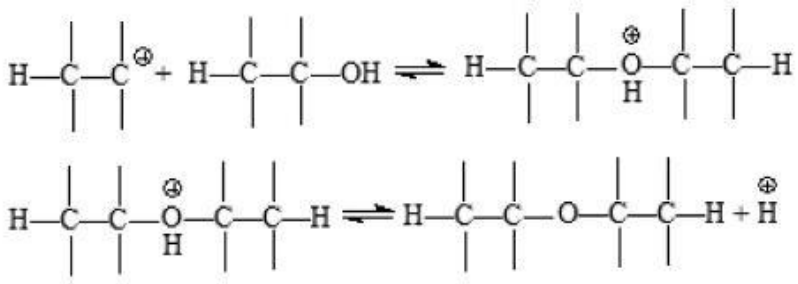

Figure 6 The mechanism of dehydration of ethanol to diethyl ether –Dissociative pathway [23]

Figure 6 displays the mechanism of dissociative pathway. One molecule of ethanol dissociates to carbonation and leaves –OH group. After that, the carbonation attacks with reactant molecule and leaves proton.

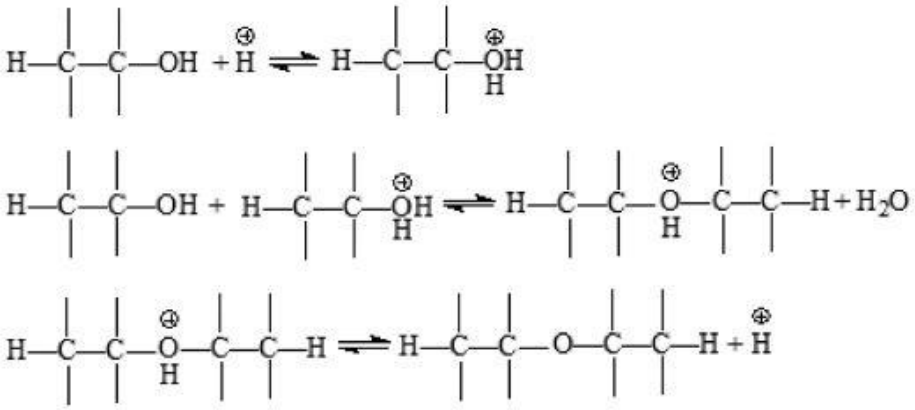

Figure 7 The mechanism of dehydration of ethanol to diethyl ether –Associative pathway [23]

In associative pathway as depicted in **Figure 7**, the mechanism starts when an acid site (Brønsted acid site) on the solid catalyst protonates the hydroxyl group of the first ethanol molecule to be electrophilic. Then, the resulting molecule attacks with another ethanol molecule, forms an intermediate, removes water and base-group, respectively [23].

2.5 Determining chemical activity formulas

The ethanol conversion, rate of reaction, selectivity towards each product and product yield were defined as follows;

$$\text{Conversion (\%)} = \frac{\text{Moles of reacted ethanol}}{\text{Moles of fed ethanol}} \times 100$$

$$\text{Selectivity (\%)} = \frac{\text{Moles of each product}}{\text{Total moles of the products}} \times 100$$

$$\text{Yield (\%)} = \text{Conversion} \times \text{Selectivity (\%)}$$

$$\text{Rate of reaction (mole ethanol/g cat. h)} = \frac{\text{Ethanol feed rate (mole ethanol/h)} \times \text{Ethanol conversion at studied temperature (\%)}}{\text{0.0821 (l.atm/mol.K)} \quad \text{Studied temperature (K)} \quad \text{Amount of catalyst used (g)}}$$

Chapter 3
LITERATURE REVIEWS

Many catalysts such as activated alumina, silicon oxide, activated carbon, clay, magnesium oxide, zirconium oxide, phosphate, heteropoly salt, and molecular sieve, etc. have been studied through ethanol dehydration reaction [23]. To classify type of catalysts, the catalysts can be divided into four main categories, which are phosphoric acid catalyst, oxide catalyst, molecular sieve catalyst and heteropolyacid catalyst [23].

3.1 Phosphoric acid catalyst

Phosphoric acid catalyst is the first catalyst used in industries. It has an advantage in high purity of product obtained; however, the catalyst is easily deactivated because of the formation of coke. In the 1930s, British Imperial Chemical (ICI) [24] started to load phosphate on clay or coke. After that, in 1981, Donald et al. [25] investigated the effect of reaction condition and reactant concentration on ethanol dehydration to ethylene by using phosphoric acid as catalyst. Since 1950s onwards, there was no usage of this catalyst.

3.2 Oxide catalyst

Oxide catalyst is generally referred to active alumina based catalysts. It is often used as supported catalyst or catalyst itself via many chemical reactions such as dehydration, alkylation, and isomerization, etc. [26] Alumina has the advantage that it offers high stability. Therefore, it leads to longer catalyst lifetime.

3.3 Molecular sieve catalyst

Because molecular sieves have high surface area and unique acidic-basic properties, they are widely used as catalysts in order to bring about high catalytic ability. The molecular sieves including ZSM-5 type, Si-Al phosphate (SAPO) type, etc. have been studied as the catalysts since 1980s. The most interested molecular sieve catalyst nowadays is ZSM-5 molecular sieve catalyst.

3.4 Heteropolyacid catalyst

Heteropolyacid consists of oxygen atom bridging with multi acid in the molecule. As the catalyst, heteropolyacid catalyst can lower reaction temperature. Unfortunately, it normally decreases the conversion of catalyst and has the problems in high catalyst loss.

The interesting reviews of alcohol dehydration reaction over solid catalyst sequencing from publication year are shown as follows;

Mao, R. et al. (1989) [27] reported about the improvement of ethanol dehydration reaction by modified ZSM-5 catalyst with trifluoromethanesulfonic acid. The researchers found that at temperature lower than 200° C and using low concentration of reactant, the modified catalyst stability is remained constant. In addition to the catalytic ability, the modification of catalyst with trifluoromethanesulfonic acid could enhance both ethanol conversion (from 96% to 98%) and ethylene selectivity (from 49% to 99%) when considered at reaction temperature, WHSV and feed ethanol of 400°C, 3.2 h^{-1}, and 15 vol%, respectively.

Xu, M. et al. (1997) [28] studied the effects of hydrogen and helium on catalytic activity of methanol dehydration reaction to dimethyl ether (DME) using 10 wt%

Pt/Cab-O-Sil as catalyst. The results showed that at the temperature range of 225°C to 280°C, methanol conversion was increased from 38% to 77%, but DME selectivity was decreased from 78% to 47%. The existence of hydrogen in the system increased the catalytic stability; however, it lowered the catalytic ability. Contrast with the effect of hydrogen, the presence of helium in the reaction increased the catalyst activity by enhanced methanol conversion from 32% to 37%.

Takahara, I. et al. (2005) [29] reported the ethanol dehydration reaction over solid catalysts including H-mordernites (HM20 and HM90), H-ZSMH zeolites (HZSM5-25 and HZSM5-90), H-beta-zeolite (HB25), H-Y zeolite (HY5.5) and silica-alumina (SA) at the temperature range of 453 K to 573 K and atmospheric pressure. Considering the activity results, the catalytic activity found to decrease as following order: HM20>HM90>HZSM5-25>HB25>HZSM5-90>HY5.5>SA. In addition to the percentage of Brønsted acid sites observed on HM20, HM90, HZSM5-25, HZSM5-90, HB25, HY5.5 and SA catalysts, it found to be 83%, 95%, 94%, 92%, 33%, 83% and 50%, respectively. Since observed the amount of carbonaceous species on the post-reaction catalysts, HM20 had the amount of carbonaceous species equal to 6 mg C/g cat, while the carbonaceous species in HM90 was too low to measure. Therefore, H-mordenites were found to have the highest activity in the study and the catalytic activity of catalyst was related to the amount of Brønsted acid sites deposited on the post-reaction catalysts.

Chen, G. et al. (2007) [30] investigated the modification of TiO_2 effect and the influence of operation parameter on γ-Al_2O_3 catalyst over ethanol dehydration reaction by using micro channel as the reactor. The results demonstrated that the 10 wt% of TiO_2-doped catalyst had higher ethanol conversion, ethylene selectivity and ethylene yield when compared to undoped catalyst. The 10 wt% TiO_2/γ-Al_2O_3 catalyst was reported to have highest ethanol conversion, ethylene selectivity and ethylene yield of 99.96%, 99.34%, and 72.7%, respectively.

Li, Y. et al. (2007) [31] reported the experimental study of ethanol dehydration to ethylene over γ-Al_2O_3 catalyst. The objective of this study was to investigate the influence of varying reaction temperature, feed flow rate and ethanol concentration. The results indicated that at the reaction temperature of 410° C to 440° C and the beginning of the reaction, selectivity towards ethylene enhanced with increasing in reaction temperature and then the selectivity remained constant. According to the feed flow rate effect, the faster feed flow rate had positive effect on ethanol conversion, but had negative effect on the ethylene selectivity. Considering the results, the optimum temperature, feed flow rate and ethanol concentration in the study are 420°C, 1.0 mL/min, and 50% to 100%, respectively.

Varisli, D., T. et al. (2007) [32] investigated the production of ethylene and diethyl ether through ethanol dehydration reaction over heteropolyacid catalysts including tungstophosphoricacid (TPA), sillicontungsticacid (STA) and molybdophosphoricacid (MPA). The reaction temperature observed in the study was in the range of 140° C to 250° C. The activity results found that at the same temperature, the catalytic activity trend was decrease as follow; STA>TPA>MPA. The presence of water vapor in the reaction was decrease the catalytic ability.

Khom-in et al. (2008) [5] reported the methanol dehydration reaction over a wide range of nanocrystalline Al_2O_3 with mixed γ- and χ- phases. The γ-Al_2O_3, χ-Al_2O_3 and mixed γ- and χ-Al_2O_3 which comprised of 0, 10, 20, 50, 80, 90 and 100% χ- phases were prepared by solvothermal method. It was found that Al_2O_3 acidity had a significantly effect on catalytic ability of the catalyst which the total acidity and catalytic activity were following the order: 20% χ-Al_2O_3 > 0% χ-Al_2O_3 >100% χ-Al_2O_3 > 10% χ-Al_2O_3 > 0% χ-Al_2O_3 > 90% χ-Al_2O_3 > 80% χ-Al_2O_3. Therefore, the mixed phase of γ- and χ-Al_2O_3 contained appropriate amount of χ-Al_2O_3 found to have higher acidity and catalytic activity pure γ-Al_2O_3 and χ-Al_2O_3.

Wannaborworn, M. et al. (2008) [33] experimented ethanol dehydration reaction over alumina catalysts. The investigated alumina catalysts were prepared by solvothermal and sol-gel method and were brought to compare the catalytic activity through the dehydration of ethanol. The results showed that the alumina synthesized by solvothermal method exhibited the higher activity than sol-gel method. It was due to its higher surface area and higher amount of acid site. The alumina synthesized by solvothermal method had the highest catalytic activity at 350°C with 100% of ethanol conversion and 100% of ethylene selectivity.

Zhang, D. et al. (2008) [34] studied the phosphorus modification on HZSM-5 zeolite catalysts to the catalytic activity of ethanol dehydration to ethylene. The addition of phosphorus found to decrease strong acid sites. The P-modified HZSM-5 zeolite catalysts with phosphorus content higher than 3.4 wt% which observed only weak acid site showed the good catalytic performance in dehydration reaction of ethanol to ethylene.

Remesh, K. et al. (2009) [35] studied the catalytic ability of phosphorus modified H-ZSM-H catalysts (using phosphoric acid as the phosphorus source) for ethanol dehydration reaction. The results showed that increasing phosphoric acid loadings from 5 to 20 wt% could increase both catalyst activity and selectivity towards ethylene. Moreover, it found that reaction temperature and space velocity (WHSV) also had the positive effect on catalytic activity and ethylene selectivity.

Remesh, K. et al. (2010) [6] reported further experimental including the stability testing and effect of lowered reactant concentration study of the phosphorus modified H-ZSM-5 catalysts in catalytic ethanol dehydration reaction. From the stability results, the phosphorus modified catalysts were found to be stable after used in the reaction more than 200 h. The phosphorus modified catalysts were also showed high selectivity toward ethylene (about 98%) when decreased the ethanol concentration to 10 wt%.

Bi, J. et al. (2010) [36] experimented the bio-ethanol dehydration comparing the catalytic stability between nanoscale HZSM-5 zeolite catalyst and microscale HZSM-5 zeolite catalyst. The catalytic stability of the nanoscale HZSM-5 zeolite catalyst found to be higher than microscale HZSM-5 zeolite catalyst. In addition, the nanoscale
HZSM-5 zeolite catalyst also had lower coke formation than microscale HZSM-5 zeolite catalyst. Therefore, the improvement of HZSM-5 zeolite catalyst by reducing the catalyst size is an attractive option.

Han, Y. et al. (2011) [37] investigated the effect of calcination temperature and relationship between activity/selectivity and the catalyst surface acidity on catalytic activity of ethanol dehydration reaction using 5 wt% Mo/HZSM-5 as catalyst. The results showed that 5 wt% Mo/HXSM-5 catalyst which calcined at 500°C had higher catalytic performance compared to undoped HZSM-5 catalyst. The 5 wt% Mo/HXSM-5 catalyst was also observed to have the highest weak and medium acidity which lead to have the highest activity than other catalysts in the study.

Liu, D. et al. (2011) [38] studied the modification of γ-Al_2O_3 catalyst with niobium oxide and ammonium sulfate which were tested in dehydration of methanol to dimethyl ether. The results found that the niobium oxide and ammonium sulfate modification on γ-Al_2O_3 catalyst tended to reduce the acid sites strength whereas increase the number of acid sites. Thus, it enhanced the catalytic activity of the modified catalysts through the methanol dehydration reaction.

Rahmanian, A. and H.S. Ghaziaskar (2013) [39] reported the usage of aluminum phosphate–hydroxyapatite catalyst on the catalytic performance of ethanol dehydration to diethyl ether (DEE) under sub and supercritical condition. This study aims to investigate the effect of temperature, pressure and ethanol flow rate on the dehydration reaction. The catalytic results indicated that the modification of aluminum phosphate on hydroxyapatite catalyst could increase ethanol conversion,

diethyl ether selectivity and diethyl ether yield to 78%, 96% and 75%, respectively. The other results found that the higher pressure of process tended to enhance the liquid selectivity and also found that the most favorable condition of the study which gave the highest diethyl ether yield is at 340° C, 200 bar and 0.17 mL min^{-1} reactant flow rate.

Valdez, R. et al. (2013) [40] investigated the effects of (1) acid-basic properties and (2) Pt, Pd and Pt-Pd (1:1) modification on the catalytic activity via 2-propanol dehydration reaction. The results showed that basic Pt/Al_2O_3 catalyst was suitable to synthesize diisopropyl ether (DIPE) towards 2-propanol dehydration reaction at a temperature of 523 K (2-propanol conversion obtained was 100% with DIPE selectivity of 100%) In addition to produce propene, using the weakly acidic Pt-Pd /Al_2O_3 catalyst is the most favorable choice because it gave 2-propanol conversion of 100% with propene selectivity reached 100%. Using Pt and bimetallic catalysts could prolong the reaction lifetime, but Pd catalyst did not.

From all of the above mentioned, we can conclude that various forms of phosphorus as same as many types of noble metal play significant role on escalating the catalyst activity. Therefore, the effect of phosphorus and noble metal addition on catalytic ability over ethanol dehydration reaction are needed for a further study.

Chapter 4
EXPERIMENTAL

This chapter explains the research methodology consisting of catalyst preparation, ethanol dehydration reaction experiment and catalyst characterization techniques including X-ray diffraction (XRD), X-ray fluorescence (XRF), inductively coupled plasma (ICP), scanning electron microscope (SEM) and energy dispersive X-ray spectroscopy (EDX), N_2 physisorption, ammonia temperature-programmed desorption (NH_3-TPD), X-ray photoelectron spectroscopy (XPS) and thermal gravimetric and differential thermal analysis (TG/DTA).

4.1 Catalyst Preparation

4.1.1 Synthesis of Al_2O_3 supports

Al_2O_3 supports were prepared by using solvothermal method as reported by Wannaborworn, M. et al [33]. In the solvothermal method, aluminum isopropoxide (AIP) and the mixture of toluene and 1-butanol with toluene to 1-butanol ratio of 1:1 by volume were used as Al_2O_3 precursor and organic solvent, respectively.

At first, the mixture between toluene and 1-butanol was prepared and filled in small and large test tube for 100 and 30 cm^3, respectively. Then, 25 g of AIP was added into the small test tube. After mixed the solution, the test tube was put into 300 cm^3 autoclave and then purged by nitrogen gas in order to remove air impurities inside the autoclave. The mixture was heated to 300° C for 2 h at heating rate of 2.5°C/min and held constant at that temperature for 2 h. After the autoclave reactor was cooled to room temperature, the resulting powder was washed twice by methanol, dried at 110°C overnight and calcined at 600°C for 6 h.

The chemicals used to synthesize Al_2O_3 supports are shown in **Table 2** as follows;

Table 2 The chemicals used for Al_2O_3 supports synthesis

Chemical	Supplier
Aluminum isopropoxide ($[(CH_3)_2CHO]_3Al$) 98%	Aldrich
Toluene ($C_6H_5CH_3$) 99%	Merch
1-Butanol ($C_4H_{10}O$) 99%	Fluka
Methanol (CH_3OH)	Merch
Ultra high purity nitrogen gas 99.99%	TIG

4.1.2 Synthesis of P/Al_2O_3 catalysts

The P-modified Al_2O_3 catalysts were prepared by acid activation technique. A 100 ml of solution containing suitable amount of 85 wt% phosphoric acid in deionized water was added to the solution and stirred at room temperature for 30 minute. The precipitate was filter, dried at 110°C overnight and calcined at 600°C for 6 h to obtain the catalyst powder.

4.1.3 Synthesis of noble metal modified P/Al_2O_3 catalysts

The noble metal modified P/Al_2O_3 catalysts were prepared by the incipient wetness impregnation technique. Based on 1 g of catalyst obtained in each preparation, a noble metal precursor was dissolved in deionized water. Then, the aqueous solution equal to the pore volume of P/Al_2O_3 catalyst was added drop-wise to the catalyst to reach 0.5 wt% loadings of noble metal. After the impregnation, the resulting catalyst was dried at 110°C overnight and calcined at 600°C for 6 h.

The chemicals used to synthesize P/Al_2O_3 and noble metal modified P/Al_2O_3 catalysts are described in **Table 3** as follows;

Table 3 The chemicals used for Al_2O_3 supports synthesis P/Al_2O_3 and noble metal modified P/Al_2O_3 catalysts

Chemical	Supplier
Orthophosphoric acid (H_3PO_4)	Carlo Erba
Tetraammineplatinum (II) chloride hydrate $[PtCl_2(NH_3)_4.H_2O]$ 99.99%	Aldrich
Tetraamminepalladium (II) nitrate $[Pd(NH_3)_4(NO_3)_2]$ 10%	Aldrich
Ruthenium (III) nitrosyl nitrate $(N_4O_{10}Ru)$; Ru 1.5%	Aldrich
Ultra high purity nitrogen gas 99.99%	TIG

4.2 Ethanol dehydration reaction

The chemicals used in ethanol dehydration reaction are displayed in **Table 4**. The ethanol dehydration reaction was carried out in a borosilicate glass fixed-bed reactor with an inside diameter of 0.7 cm. To achieve the reaction study, 0.05 g of catalyst and 0.01 g of quartz wool were packed in the reactor. Then, pretreated the catalyst at 200°C for 1 h under atmospheric pressure and 50 mL/min of argon. After finished the pretreat step, the vaporized ethanol was fed into the reactor. The products were analyzed in a temperature range of 200 to 400° C and atmospheric pressure by using a gas chromatograph with flame ionization detector (FID), which had the operating conditions as shown in **Table 5.**

Table 4 The chemicals used in ethanol dehydration reaction

Chemical	Supplier
Ethanol (C_2H_5OH) 99.99%	Merch
Argon	TIG
Ultra high purity hydrogen gas 99.99%	TIG
Ultra high purity nitrogen gas 99.99%	TIG

Table 5 The operating conditions in gas chromatograph

Gas chromatograph	Shimadzu GC-14A
Detector	FID
Capillary column	DB-5
Carrier gas	Nitrogen (99.99 vol%)
	Hydrogen (99.99 vol%)
Column temperature	Initial : 40°C
	Final : 40°C
Injector temperature	150°C
Detector temperature	150°C
Time analysis	8 min

4.3 Catalyst characterization

4.3.1 X-ray diffraction (XRD)

The bulk crystalline phase and crystalline size of the catalysts were determined by using a SIEMENS D5000 X-ray diffractometer with CuKα (λ = 1.54439 Å) and Ni filter in the 2θ range of 10° to 80°.

4.3.2 X-ray fluorescence (XRF)

The quantities of noble metal in the catalysts were measured by Panaanalytical MINIPAL 4 instrument using 1 g of sample in each analysis.

4.3.3 Inductively coupled plasma (ICP)

The phosphorus and noble metal contents in the catalysts were measured by Perkin Elmer OPTIMA 2000^{TM} instrument. The instrument used energy from inductive coupled plasma to stimulate the transition of atoms from ground state to excited state and collected the energy released when returning to ground state by DBI-CCD (Dual backside-illuminated charge-coupled device).

4.3.4 Scanning electron microscope (SEM) and energy dispersive X-ray spectroscopy (EDX)

The morphologies and elemental distribution of the catalysts were determined by JEOL mode JSM-6400 scanning electron microscope and Link Isis Series 300 program energy dispersive X-ray spectroscopy, respectively. Before the analysis, the samples were treated at 110°C for 24 h to eliminate moisture.

4.3.5 N_2 physisorption

The surface area (using the stand BET method), average pore volume, average pore size (using the BJH desorption analysis), hysteresis loop (using the adsorption-desorption isotherms) and pore size distribution of the catalysts were investigated using a Micromeritics ASAP 2000 automated system. The samples were thermally treated at 110°C for 24 h before the analysis.

4.3.6 Ammonia temperature-programmed desorption (NH_3-TPD)

The acid properties of the catalysts were determined by using a Micromeritics Pulse Chemisorp 2750 instrument. Prior to the analysis, 0.1 g of sample and quartz wool were packed in glass tube and pretreated at 200° C by using heating rate of 10° C/min. After cooled the temperature down to 40° C, the sample was saturated with 15% NH_3 for 30 minutes and heated to 400°C at heating rate of 10°C/min.

4.3.7 X-ray photoelectron spectroscopy (XPS)

The binding energy of each element in the catalysts was determined by using a Shimadzu AMICUS instrument. The small amount of samples was brought to pretreat at 110°C for 24 h before the analysis.

4.3.8 Thermal gravimetric and differential thermal analysis (TG/DTA)

The thermal decomposition of pre-reaction catalyst and the amount of carbon (coke) in the catalysts after reaction test were analyzed by TA Instruments SDTQ 600 analyzer in the temperature range of 36-8 0 0 ° C. The small amount of samples which had pretreated at 110°C for 24 h was required for each analysis.

4.4 Research plan

Table 6 The research plan

Research plan	Year 2558					Year 2559										
	8	9	10	11	12	1	2	3	4	5	6	7	8	9	10	11	12
Studied about the theory related to ethanol dehydration reaction and experiment.	◄	———	———	———	———	———	———	———	———	———	———	———	———	———	———	———	►
Considered the variables associated with the experiment.		◄	———	►													
Determined the experimental duration.		◄	———	———	►												
Prepared the catalysts.						◄	———	———	►								
Characterized the catalysts.						◄	———	———	———	►							
Studied the catalysts activities via ethanol dehydration reaction.						◄	———	►			◄	———	►				
Analyzed the results and discussion.											◄	———	———	———	►		
Concluded the results, determined the problems and proposed solutions to the problem.														◄	———	►	
Prepared the report for presentation.									◄	►				◄	———	———	►

Note: Black arrow (◄——►) refers to the duration of each experiment planned.

Gray arrow (◄——►)refers to the duration of each experiment done.

CHAPTER 5
RESULTS AND DISCUSSION

This chapter describes the characteristic and catalytic activity of mixed γ- and χ-phase Al_2O_3 supports, P-modified Al_2O_3 catalysts, noble metal modified Al_2O_3 catalyst and noble metal modified P/Al_2O_3 catalysts in ethanol dehydration reaction. All of the mention contents are divided into four parts. The first part explains the characteristic and catalytic activity of the mixed γ- and χ-phase Al_2O_3 supports modification with different loading of phosphorus (0-20 wt% P). The second part explains the characteristic and catalytic activity of the P/Al_2O_3 catalysts which has the highest diethyl ether yield modification with different type of noble metal (Ru, Pt and Pd). The third part explains the characteristic and catalytic performance in time on stream system of Al_2O_3 supports, the chosen P-modified Al_2O_3 catalyst and the chosen noble metal modified P/Al_2O_3 catalyst. The last part explains the characteristic and catalytic activity in the comparison between the chosen noble metal modified Al_2O_3 catalyst and the chosen noble metal modified P/Al_2O_3 catalyst.

Part I : The characteristic and catalytic activity of the Al_2O_3 catalysts modification with different loading of phosphorus (0-20 wt% P)

The P-modified alumina catalysts were synthesized by solvothermal and acid activation techniques and then brought to determine both catalytic properties and performance in ethanol dehydration reaction. All of the results are described in **Topic 5.1.1** to **5.1.9** as follows;

5.1.1 Inductively coupled plasma (ICP)

After modified Al_2O_3 catalyst with different loading of phosphoric acid by acid activation technique, the P-modified Al_2O_3 catalysts were brought to determine the amount of phosphorus contained in bulk catalyst by inductively coupled plasma (ICP). The amount of phosphorus in each bulk sample is shown in **Table 7** as follows;

Table 7 The amount of phosphorus contained in the catalysts bulk

H_3PO_4 used in acid activation (wt%)	**Amount of P in catalyst bulk (wt%)**
0	0
5	5
10	12
15	14
20	20

Therefore, in this report, the Al_2O_3 catalysts contained phosphorus in amount of 0, 5, 12, 14 and 20 wt% are called Al_2O_3, $5P/Al_2O_3$, $12P/Al_2O_3$, $14P/Al_2O_3$ and $20P/Al_2O_3$, respectively.

5.1.2 X-ray diffraction (XRD)

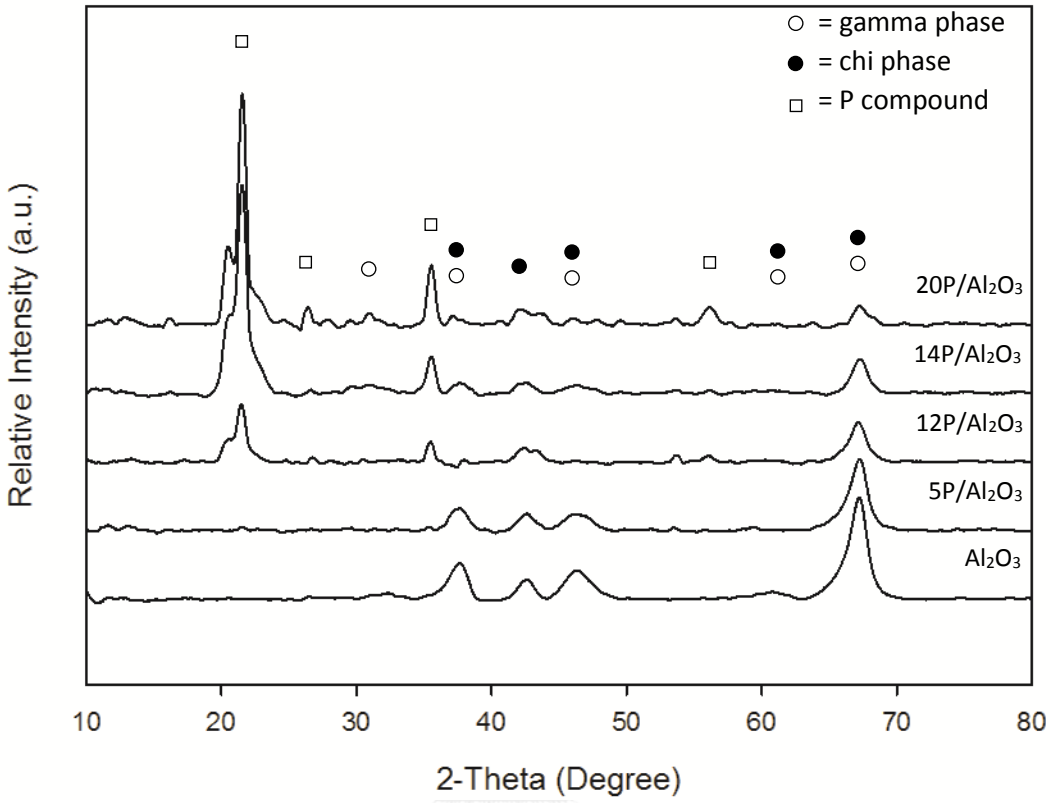

Figure 8 XRD patterns of Al_2O_3 and P-modified Al_2O_3 catalysts

Figure 8 displays XRD patterns of mixed γ- and χ-phase of alumina catalyst and mixed γ- and χ-phase of alumina catalyst modified with various loading of phosphorus prepared by solvothermal and acid activation technique, respectively. From XRD patterns, the results was observed for both γ- and χ-phase of alumina catalyst as specified in the report of Khom-in et al. [5]. The γ- and χ-phase of alumina supports were noticed the γ-phase at 2θ of 32°, 37°, 46°, 61° and 67° and χ-phase at 2θ of 37°, 43°, 46°, 61° and 67°, while the phosphorus species were observed in XRD patterns at 2θ of 22°, 27°, 36° and 56° as the report of Jeong-Hee Choi et al. [41]. The 5 wt% of phosphorus modified alumina catalyst seemed to exhibit a similar XRD pattern as alumina supports. This can be suggested that phosphorus species were well dispersed on alumina supports or had their crystalline size smaller than 3-5 nm. Therefore, it led these two samples to have the similar pattern of XRD.

5.1.3 Scanning electron microscope (SEM) and energy dispersive X-ray spectroscopy (EDX)

To identify the morphology of the catalysts and elemental distribution on the catalysts surface, the catalysts were brought to investigate using scanning electron microscope (SEM) and energy dispersive X-ray spectroscopy (EDX), respectively.

The morphology of mixed **γ**- and **χ**-phase alumina catalysts modified with various loading of phosphorus (0-20 wt%) were observed by scanning electron microscope (SEM) and illustrated in **Figure 9**.

From SEM images of Al_2O_3 and P-modified Al_2O_3 catalysts, it was found that all of the studied catalysts had irregular shape. In addition, the amount of phosphorus doping into the catalysts did not affect the catalyst morphologies or it could be said that all of the studied catalysts showed the similar morphological features.

(a)

(b)

(c)

(d)

(e)

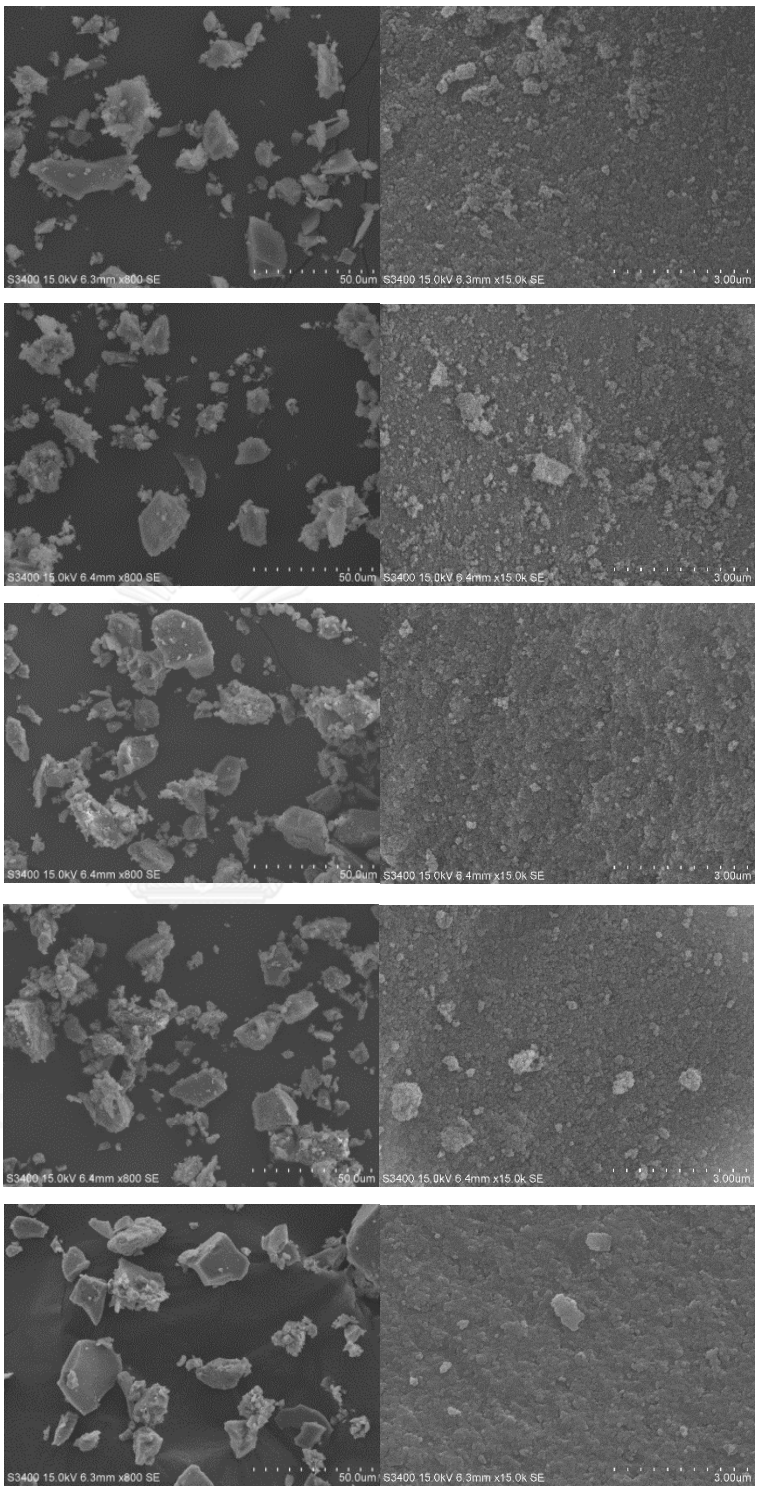

Figure 9 SEM micrograph of Al_2O_3 and P-modified Al_2O_3 catalysts;
(a) Al_2O_3 (b) 5P/Al_2O_3 (c) 12P/Al_2O_3 (d) 14P/Al_2O_3 (e) 20P/Al_2O_3

The elemental dispersion of Al_2O_3 and P-modified Al_2O_3 catalysts, which were studied through energy dispersive X-ray spectroscopy (EDX) technique, is displayed in elemental distribution mapping (EDX mapping) of each catalyst. The EDX mappings of each catalyst are shown in **Figure 10** to **Figure 14** as follows;

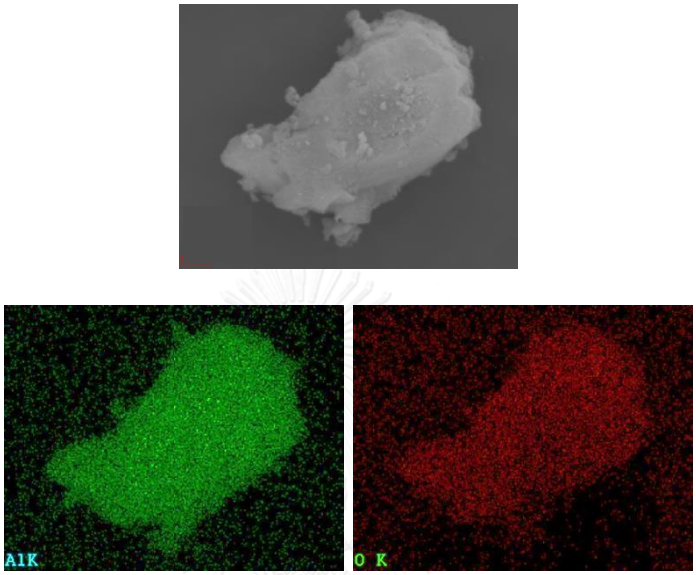

Figure 10 EDX mapping of Al_2O_3

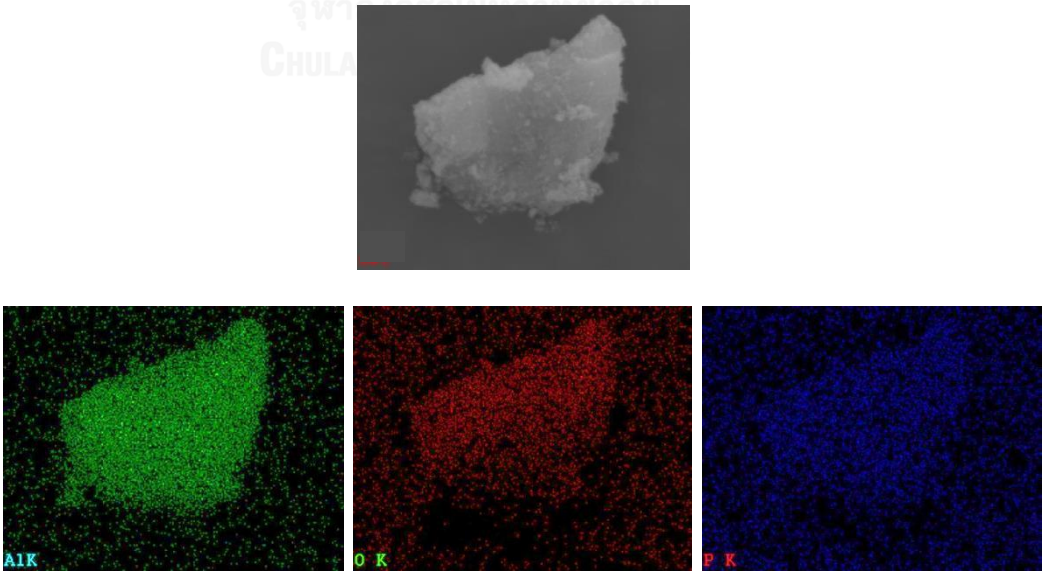

Figure 11 EDX mapping of 5P/Al_2O_3

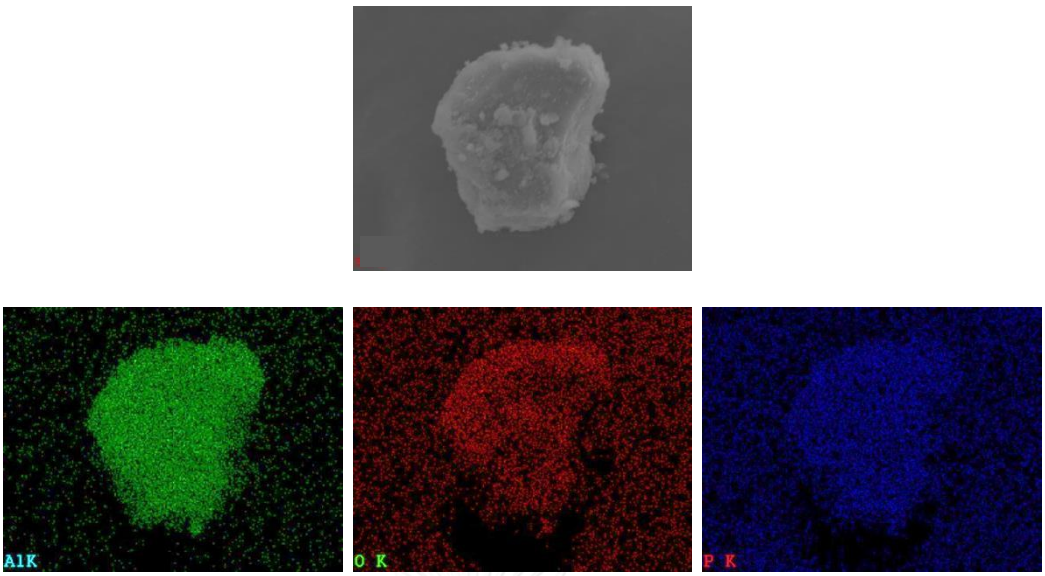

Figure 12 EDX mapping of 12P/Al_2O_3

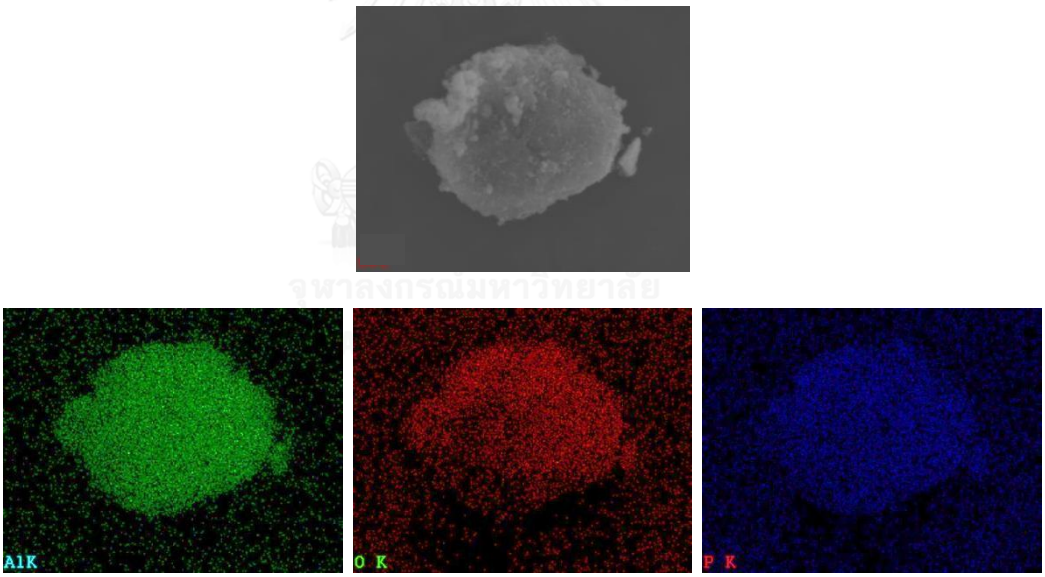

Figure 13 EDX mapping of 14P/Al_2O_3

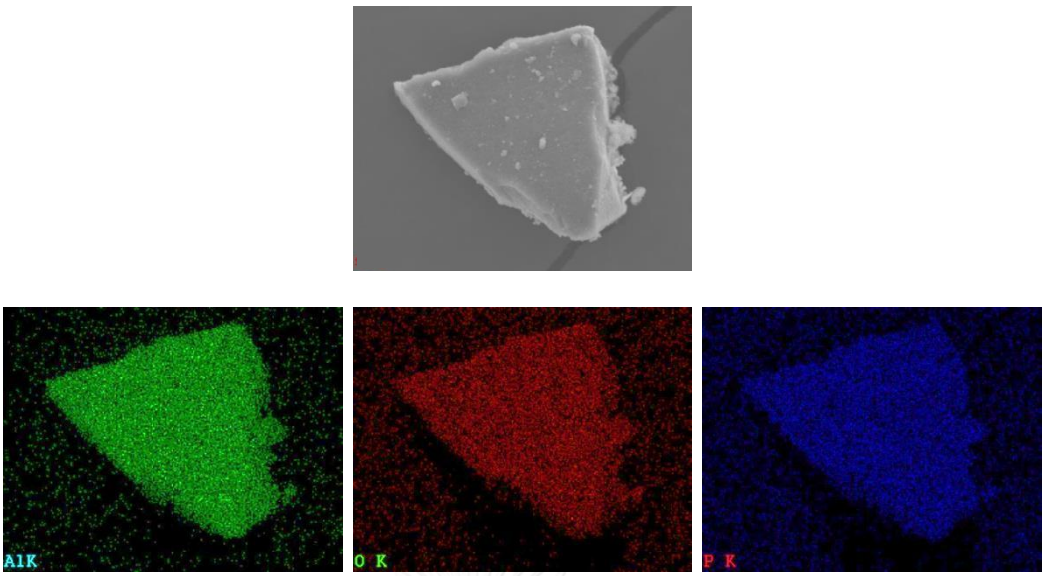

Figure 14 EDX mapping of 20P/Al_2O_3

From the EDX mappings show in **Figure 10** to **Figure 14**, the results were found that alumina (green color), oxygen (red color) and phosphorus (blue color) distribution on the surface of studied catalysts were all well dispersed. The amount of elemental distribution (Al, O and P) in weight percent and atom percent over each catalyst surface are demonstrated in **Table 8**.

Table 8 The amount of elemental distribution on the catalysts surface

Catalysts	Amount of element on surface (wt%)			Amount of element on surface (at%)		
	Al	O	P	Al	O	P
Al_2O_3	56.67	43.33	-	43.68	56.32	-
5P/Al_2O_3	55.43	31.11	13.46	46.33	43.87	9.80
12P/Al_2O_3	51.19	29.23	19.58	43.56	41.93	14.51
14P/Al_2O_3	47.58	31.56	20.85	39.99	44.74	15.27
20P/Al_2O_3	39.82	39.81	20.37	31.93	53.84	14.23

From the mention results of ICP and EDX, it can be suggested that phosphorus species modified on the alumina catalyst had larger size than pore size of the catalysts. Therefore, the deposited phosphorus was found to be dispersed on the catalysts surface instead of dispersed in the catalysts pore. The amount of phosphorus detected on the catalysts surface and bulks catalysts are presented in **Table 9** as follow;

Table 9 The amount of phosphorus comparing between catalysts surface and bulk catalysts

Catalyst	Amount of phosphorus on catalysts surface identified by EDX (wt%)	Amount of phosphorus in bulk catalysts identified by ICP (wt%)
5P/Al_2O_3	13.46	4.84
12P/Al_2O_3	19.58	11.63
14P/Al_2O_3	20.85	13.82
20P/Al_2O_3	20.37	20.43

5.1.4 N_2 physisorption

The nitrogen physisorption technique was used to determine the surface area, porosity structure and isotherm of mixed γ- and χ-phase of alumina catalyst modified with different loading of phosphorus (0-20 wt%). The surface area, pore volume and pore size of each studied catalyst is summarized in **Table 10** as follows;

Table 10 The surface area, pore volume and pore size of Al_2O_3 and P-modified Al_2O_3 catalysts

Catalysts	Surface Area[a] (m^2/g)	Pore Volume[b] (cm^3/g)	Pore Size[c] (Å)
Al_2O_3	199	0.661	107.6
$5P/Al_2O_3$	151	0.486	114.9
$12P/Al_2O_3$	47	0.126	99.3
$14P/Al_2O_3$	37	0.099	112.9
$20P/Al_2O_3$	6	0.002	197.5*

[a] Determined from BET method

[b,c] Determined from BJH desorption method

* Average pore size of the catalyst

The catalyst surface area, pore volume and pore size described in **Table 10** were observed with a significant decrease of surface area and pore volume of the studied catalysts with increasing the loading of contained phosphorus. These results indicated that the phosphorus species deposited on the catalysts were clogged up both on the catalyst surface and dispersed inside catalyst pore. This phenomenon brought the catalysts to have lower surface area and pore volume.

In addition, the nitrogen adsorption-desorption isotherms of all studied catalysts which are shown in **Figure 15** revealed that all catalysts exhibited a similar isotherms; type-IV isotherms (classified by IUPAC: International Union of Pure and Applied Chemistry) and displayed hysteresis loop, indicating that there were the formation of mesoporous structure in the catalysts. Furthermore, alumina catalyst was observed to have the highest nitrogen adsorption capacity, which associated to its highest amount of pore volume compared to P-modified alumina catalysts.

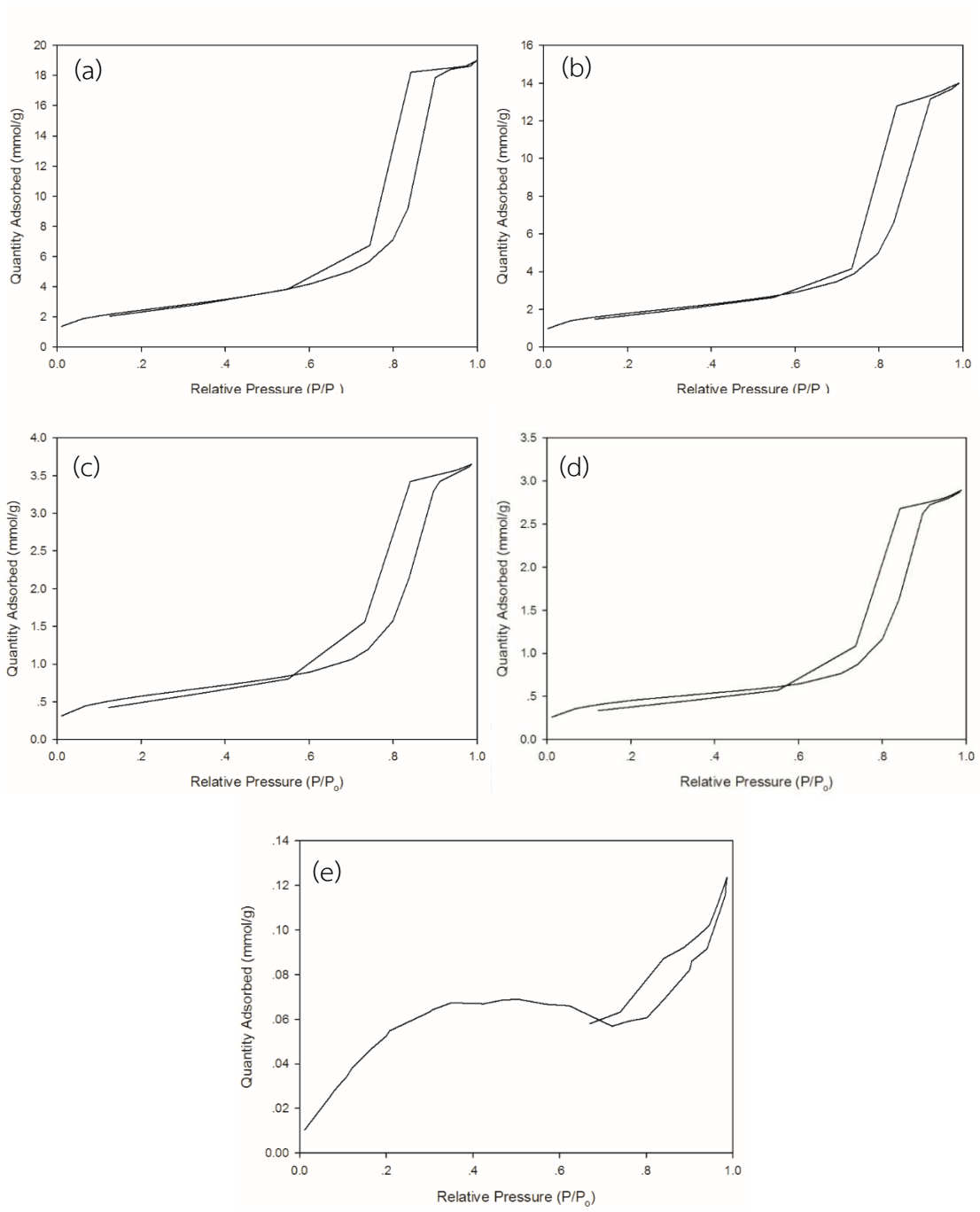

Figure 15 The N_2 adsorption-desorption isotherms at −196°C of the catalysts; (a) Al_2O_3 (b) 5P/Al_2O_3 (c) 12P/Al_2O_3 (d) 14P/Al_2O_3 (e) 20P/Al_2O_3

The pore size distributions of all studied catalysts are displayed in **Figure 16** as follows;

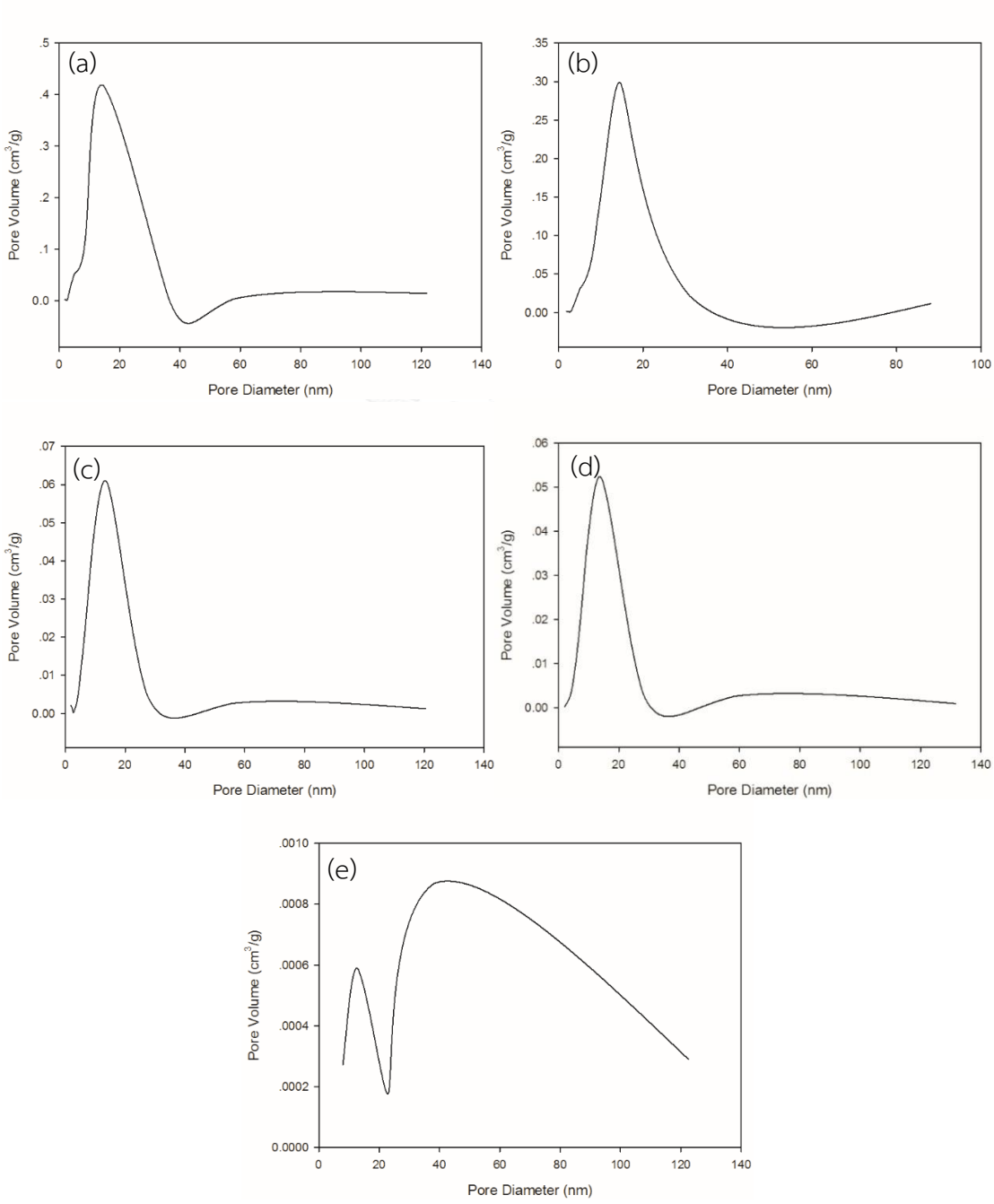

Figure 16 The pore size distribution of the catalysts;
(a) Al_2O_3 (b) 5P/Al_2O_3 (c) 12P/Al_2O_3 (d) 14P/Al_2O_3 (e) 20P/Al_2O_3

Pore size distribution of each catalyst showed that P-modified alumina catalysts, which had phosphorus loading in the amount of 0 to 14 wt% revealed unimodal distribution. However, P-modified alumina catalysts, which had phosphorus loading in the amount of 20 wt% was observed to have bimodal distribution with the presence of significant larger pore size. This indicates the pore blockage of alumina with 20 wt% of P loading.

5.1.5 Ammonia temperature-programmed desorption (NH_3-TPD)

Ammonia temperature-programmed desorption technique was used to determine the surface acidity of mixed **γ**- and **χ**-phase Al_2O_3 supports modification with different loading of phosphorus. The acid strength of each catalyst can be determined from the desorption temperature. The obtained desorption peaks were brought to calculate amount of acid site as shown in **Table 11**. The weak and medium to strong acid sites were estimated from the desorption peak in the temperature below 200°C and temperature range of 200 to 400°C, respectively. The NH_3-TPD profiles of each studied catalyst are depicted in **Figure 17** as follows;

The NH_3-TPD profiles of all catalysts, excepting $20P/Al_2O_3$ catalyst were observed to have two desorption peaks. It was found that modification of the alumina supports with phosphorus tended to decrease the amount of medium to strong acid sites. In addition, it can be noticed that the desorption temperature of each catalyst was shift to the higher temperature when increasing the loading of phosphorus. These phenomena indicated that the catalysts, which contained higher amount of phosphorus would have a lower coke formation, which is according to Kwak, B.S. et al. [42].

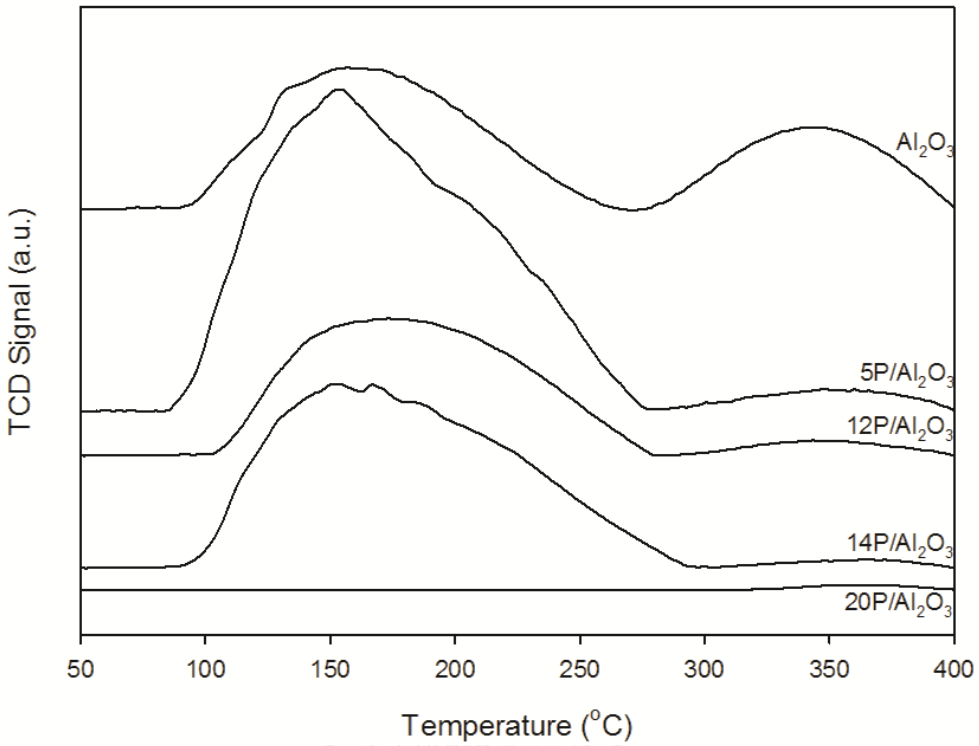

Figure 17 NH_3-TPD profiles of the phosphorus over alumina catalysts with various phosphorus loading

When considered the amount of acid sites of mixed γ- and χ-phase alumina supports modification with different loading of phosphorus, the total acidity of each catalyst was described in **Table 11** as follow;

Table 11 The amount of acidity of the phosphorus over alumina catalysts with various phosphorus loading

Catalysts	**NH_3 desorption total acidity (μmol/g cat.)**
Al_2O_3	1230
5P/Al_2O_3	2620
12P/Al_2O_3	1170
14P/Al_2O_3	1100
20P/Al_2O_3	-

The total acidity of all catalysts was in the range of 0-2620 μmol/g cat. The 5P/Al_2O_3 showed the highest amount of acid sites reaching 2620 μmol/g cat. It can be observed that when modification the alumina supports with phosphorus higher than 5 wt%, the acidity of the catalyst was decreased. This indicated that the phosphoric acid used as the modified agent may be eroded the catalysts surface and brought the catalyst to deactivated. Therefore, NH_3 cannot chemically bond with the acid species on catalyst surface and lead to detect the lower NH_3 desorption.

5.1.6 X-ray photoelectron spectroscopy (XPS)

The oxidation states of each element can be identified from X-ray photoelectron spectroscopy (XPS). In **Figure 18**, the binding energy of Al, O and P was analyzed from the fitting curves of Al 2p, O 1s and P 2p, respectively. The binding energy for Al 2p of alumina supports and P-modified alumina catalysts ordering from low to high phosphorus loading was 75.8, 75.4, 75.3 and 75.2 eV, respectively. For P 2p binding energy, the binding energy of the catalysts was 135.3, 135.0, 134.9 and 134.7 eV for 5, 10, 15 and 20 wt% P-modified alumina catalysts. When compared these values to standard of Al 2p in form of aluminum oxide and P 2p in form of phosphate which the binding energy was located at 74.6 eV [41] and 133 eV [42], respectively. It was found that all element curves shift to the higher core level with a decrease in phosphorus loading. This can be interpreted that the atoms of each catalyst loss their electrons, which brought the element to have a lower p-band. The lower p-band indicated that the molecule had a weaker bonding. Then, this could lead the catalysts to have higher catalytic activity [43].

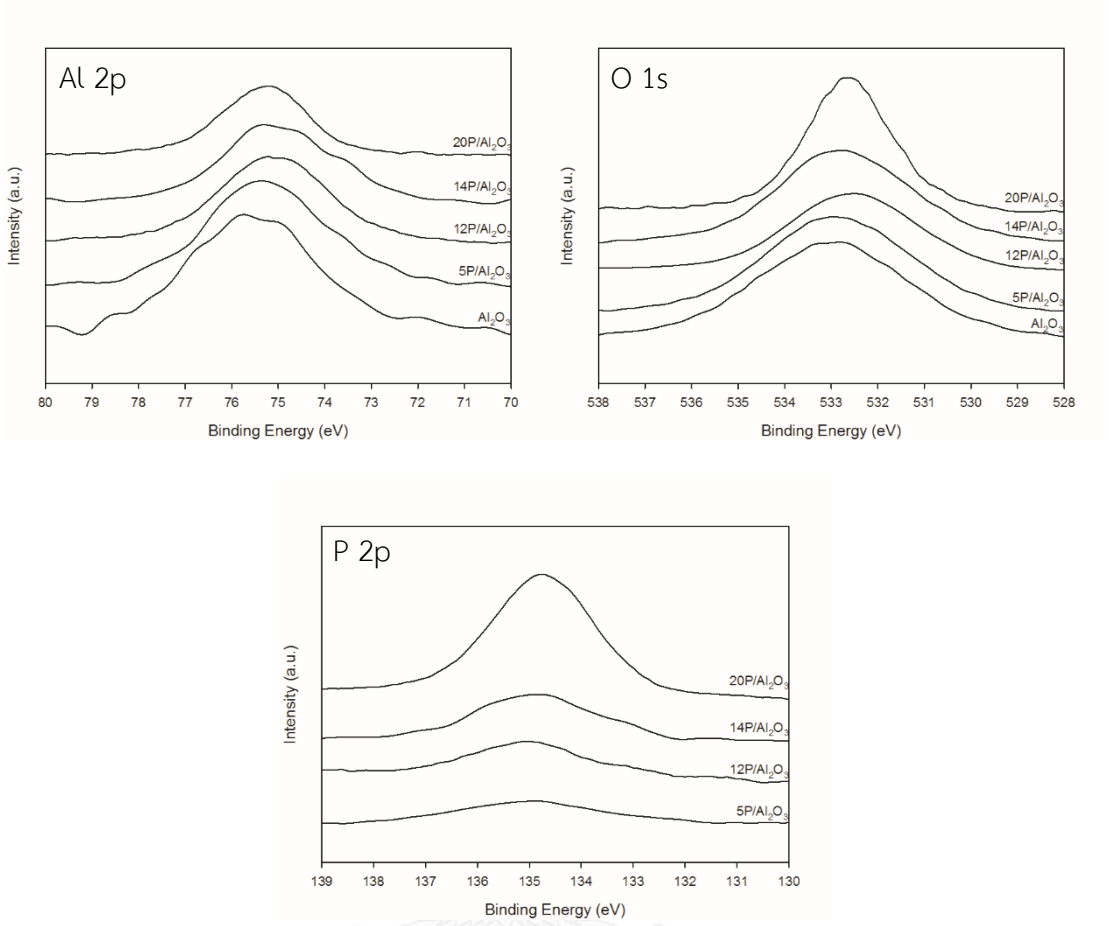

Figure 18 XPS spectra for alumina supports and P-modified alumina catalysts

Each element binding energy of all catalysts is described in **Table 12** as follows;

Table 12 Binding energy detected from alumina supports and P-modified alumina catalysts

Catalysts	Binding Energy (eV)		
	Al 2p	O 1s	P 2p
Al_2O_3	75.8	532.8	-
$5P/Al_2O_3$	75.4	533.0	135.3
$12P/Al_2O_3$	75.3	532.8	135.0
$14P/Al_2O_3$	75.3	532.8	134.9
$20P/Al_2O_3$	75.2	532.5	134.7

5.1.7 Reaction study

Beside of investigating the characteristics of each catalyst, the catalytic activity of alumina and P-modified alumina catalysts were examined through ethanol dehydration reaction at various reaction temperatures (200, 250, 300, 350 and 400°C). The considering terms of catalytic activity consist of ethanol conversion, selectivity towards interested products and products yield. The catalytic performance of each catalyst is presented in **Figure 19** to **Figure 23**. **Figure 19** represents the steady state ethanol conversion of P-modified alumina catalysts with different loading of phosphorus as follows;

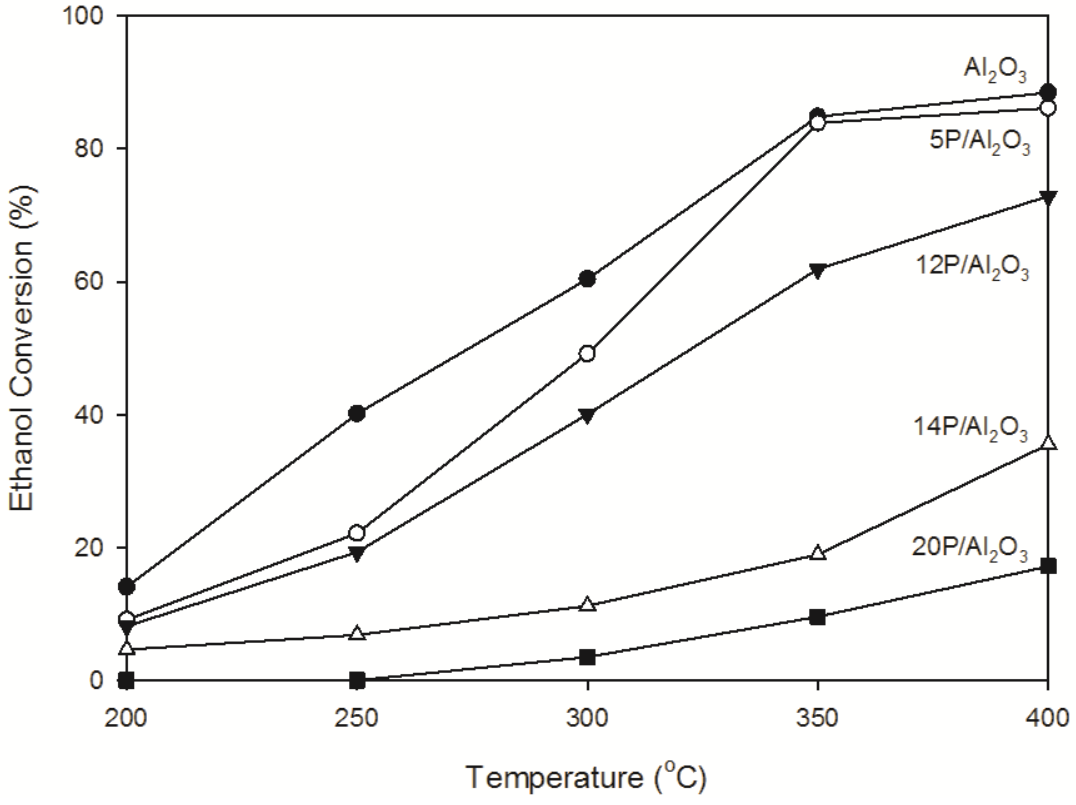

Figure 19 Ethanol conversion of Al_2O_3 and P-modified Al_2O_3 catalysts

The ethanol conversion is defined as the molar ratio of ethanol used in the reaction to the molar of ethanol feed. From the results display in **Figure 19**, it was found that ethanol conversion increased as the raising in reaction temperature. When considering all interested temperature, Al_2O_3 catalyst presented the highest ethanol conversion among other catalysts. The increasing of phosphorus amount tended to decrease conversion of ethanol or it can be said that the excessive amount of phosphorus had a negative effect on reactant conversion. In addition, when compared the ethanol conversion of Al_2O_3 and $5P/Al_2O_3$, the $5P/Al_2O_3$ was found to have slightly lower ethanol conversion than Al_2O_3 at high temperature (350-400°C). Consequently, $5P/Al_2O_3$ is an interesting catalyst which can be brought to examine in further study.

Rate of reaction is determined from the ratio of ethanol feed rate in mole/h multiply by ethanol conversion at the interested temperature to the universal gas constant (R = 0.0821 l.atm/mol.K) multiply with the interested temperature value and amount of catalyst used which the equation to determine the reaction rate is shown in **Eq.1** as follow;

$$\text{Rate of reaction (mole ethanol/g cat. h)} = \frac{\text{Ethanol feed rate (mole ethanol/h)} \times \text{Ethanol conversion at studied temperature (\%)}}{\text{0.0821 (l.atm/mol.K)} \times \text{Studied temperature (K)} \times \text{Amount of catalyst used (g)}}$$

Rate of reaction obtained from using catalysts in various temperatures are presented in **Table 13** as follows;

Table 13 Rate of reaction of Al_2O_3 and P-modified Al_2O_3 catalysts in various temperatures

Catalysts	Rate of Reaction $\times 10^2$ (mole ethanol reacted/g cat. h)				
	200°C	250°C	300°C	350°C	400°C
Al_2O_3	7.24	18.69	25.67	33.19	32.03
$5P/Al_2O_3$	4.70	10.30	20.90	32.81	31.17
$12P/Al_2O_3$	4.18	8.98	17.02	24.20	26.37
$14P/Al_2O_3$	2.38	3.18	4.76	7.39	12.85
$20P/Al_2O_3$	0.00	0.00	1.48	3.73	6.21

From the rate of reaction of the studied catalysts shown above, it was found that reaction rate of each catalyst was increased as the raising in temperature. Moreover, the reaction rate was found to be enhanced when decreasing phosphorus loading. It can be noticed that for Al_2O_3 and $5P/Al_2O_3$ catalysts at 350 and 400°C the rate of reaction was slightly decreased when raised the reaction temperature. Therefore, the temperature of 350°C was chosen as the most interesting temperature because of its highest rate of reaction.

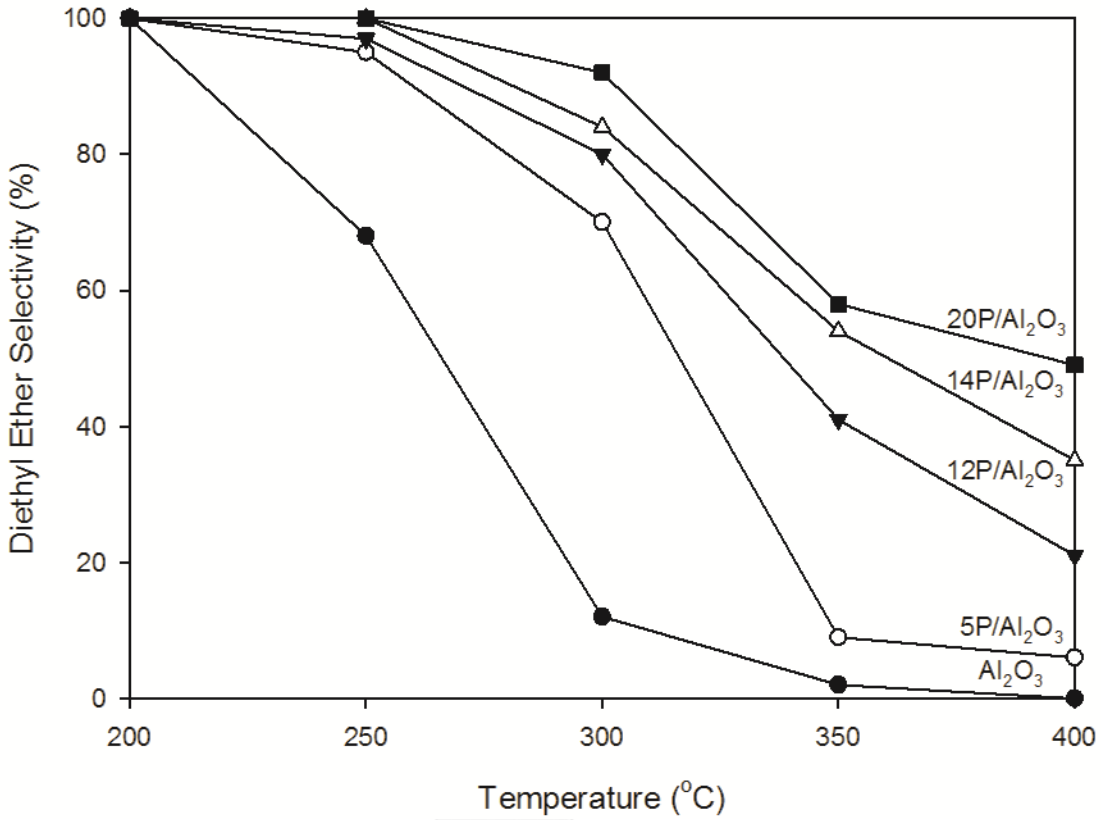

Figure 20 Diethyl ether selectivity of Al_2O_3 and P-modified Al_2O_3 catalysts

The selectivity towards the interested product is defined as the molar ratio of specific product to total products (diethyl ether, ethylene and acetaldehyde) formed. From **Figure 20** above, it shows the diethyl ether selectivity of all catalyst. The results represented that diethyl ether selectivity decreased as the increasing in reaction temperature. It was also found that the amount of phosphorus in the catalyst had a positive effect on the selectivity towards diethyl ether, noticed by its lower decrease in the diethyl ether selectivity and the diethyl ether selectivity of each catalyst obtained.

Yield of each specific product is defined as the ethanol conversion term in %mole multiply with the term of selectivity towards specific product in mole. The

diethyl ether yield of each catalyst was calculated and displayed in **Figure 21** as follows;

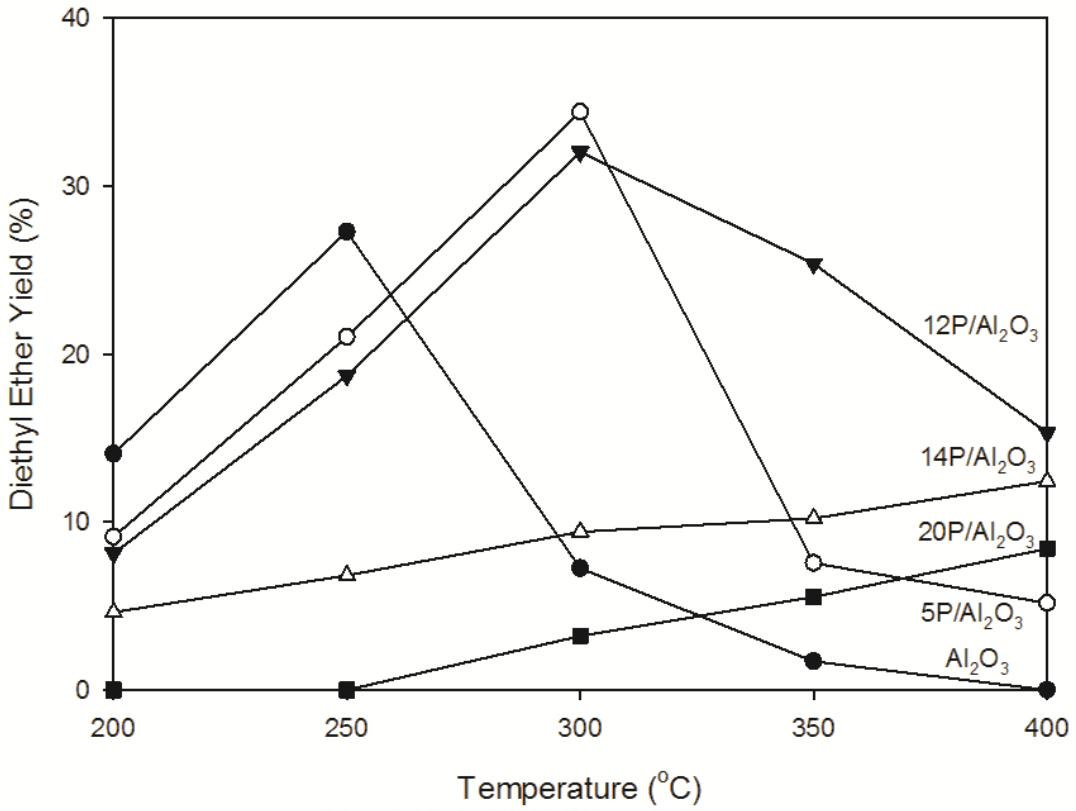

Figure 21 Diethyl ether yield of Al_2O_3 and P-modified Al_2O_3 catalysts

From **Figure 21**, it was observed that there were two factors including temperature and amount of phosphorus contained in the catalysts that played roles in changing diethyl ether yield. From these factor effects, it can be noticed that, for example, Al_2O_3 catalyst, which had no phosphorus contained had the highest diethyl ether yield in the temperature range of 200 to 250°C. In addition, it can be seen that at 300°C, $5P/Al_2O_3$ catalyst had the highest yield of diethyl ether among other studied temperature, which the diethyl ether yield was approximately 34.41%. While in the temperature range of 350 to 400°C, $12P/Al_2O_3$ had the highest diethyl ether yield. Consequently, it was found that the suitable amount of phosphorus in

appropriate reaction temperature led the reaction to exhibit its highest diethyl ether yield in that reaction condition.

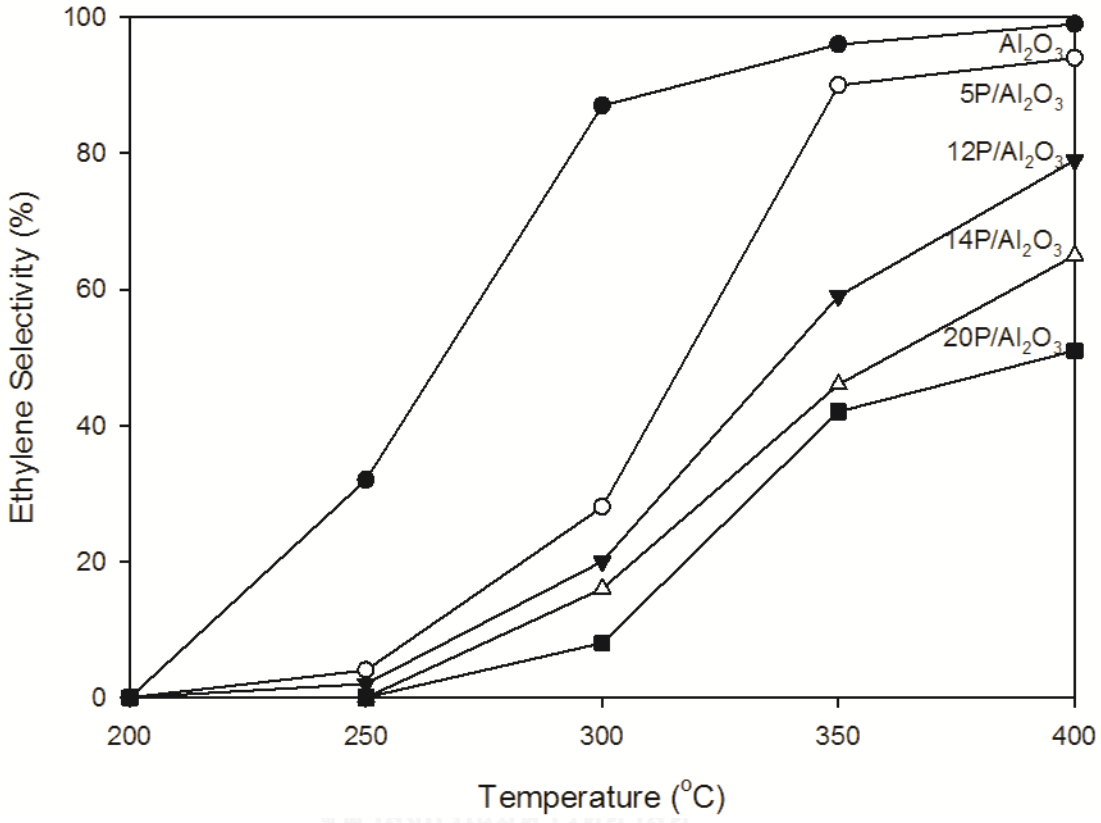

Figure 22 Ethylene selectivity of Al_2O_3 and P-modified Al_2O_3 catalysts

When consider other product formed such as ethylene, as shown in **Figure 22**, the result was found that the ethylene selectivity rose as the increasing in reaction temperature. While increasing the phosphorus contained in the catalyst tended to lower the ethylene selectivity. At low reaction temperature (200-300°C), the Al_2O_3 catalyst was observed to exhibit a significantly higher selectivity towards ethylene than P-modified Al_2O_3 catalysts.

The ethylene yields of all catalysts are presented in **Figure 23** as follows;

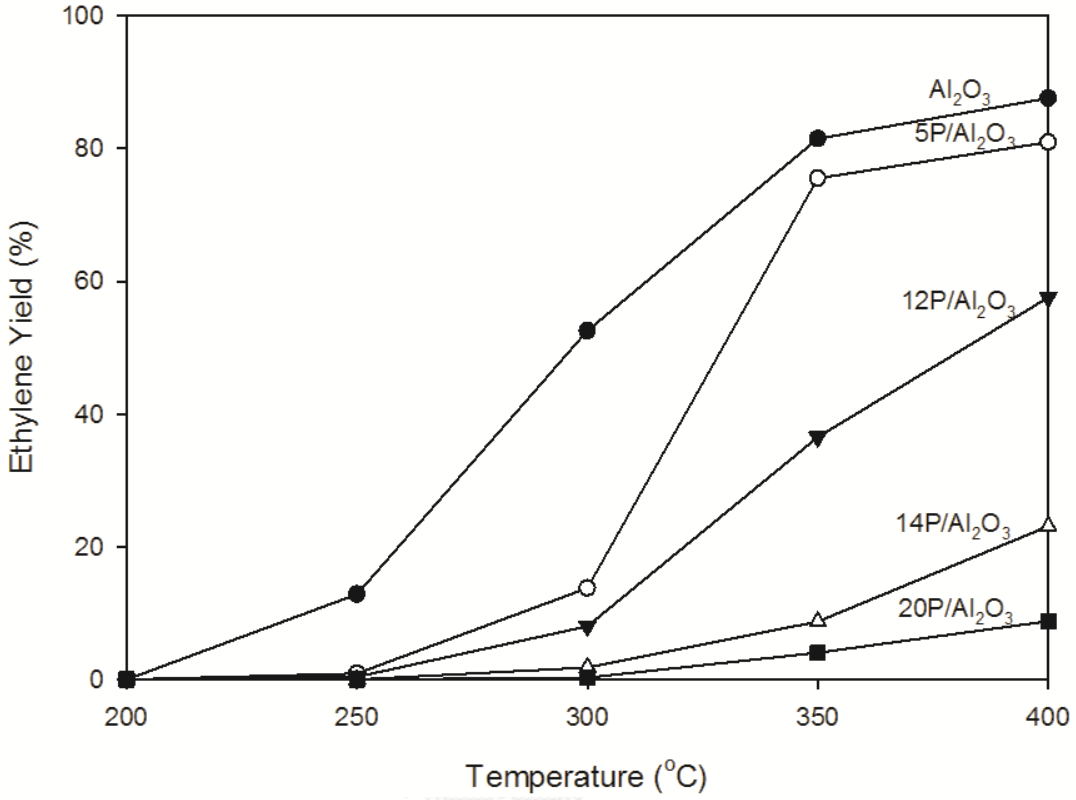

Figure 23 Ethylene yield of Al_2O_3 and P-modified Al_2O_3 catalysts

Because ethanol conversion and ethylene selectivity were both had a similar graph curve (the higher temperature gave the higher reactant conversion and ethylene selectivity). Therefore, yield of ethylene was also increased as the raising in reaction temperature. In other that, the higher amount of phosphorus in P-modified catalysts had brought the catalysts to have lower ethylene yield than the P-modified catalysts which had a smaller phosphorus amount.

When considered another product such as acetaldehyde, which the selectivity towards this product and its yield did not specified in this report. It may be presumed that the acetaldehyde selectivity and yield were not significantly affected by the amount of phosphorus in P-modified Al_2O_3 catalysts, because of its very low acetaldehyde selectivity (lower than 2%).

5.1.8 Thermal gravimetric and differential thermal analysis (TG/DTA)

The thermal decomposition of mixed γ- and χ-phase of alumina catalyst and mixed γ- and χ-phase of alumina catalyst modified with various loading of phosphorus both before and after using in ethanol dehydration reaction were observed by using TG/DTA technique under air atmosphere. The results of fresh catalyst decomposition are shown in **Figure 24**. From the results, it could be seen that all studied catalysts are detected the weight loss in two stages of temperature. The first stage was the weight loss at temperature below 200°C. The losing of catalysts weight are suggested that they would be from the water elimination. Another stage was the weight loss at temperature of 200 to 600°C. As the weight loss in this stage, it may be from an inorganic molecule volatilization. It was also observed that 20P/Al_2O_3 catalyst had the significantly decreasing in catalyst thermal decomposition at temperature range of 200 to 400°C. It can be suggested that there were the large amount of phosphorus species which did not make any chemical interact to the support. Therefore, these phosphorus species were volatized when increasing the temperature to higher than 200°C.

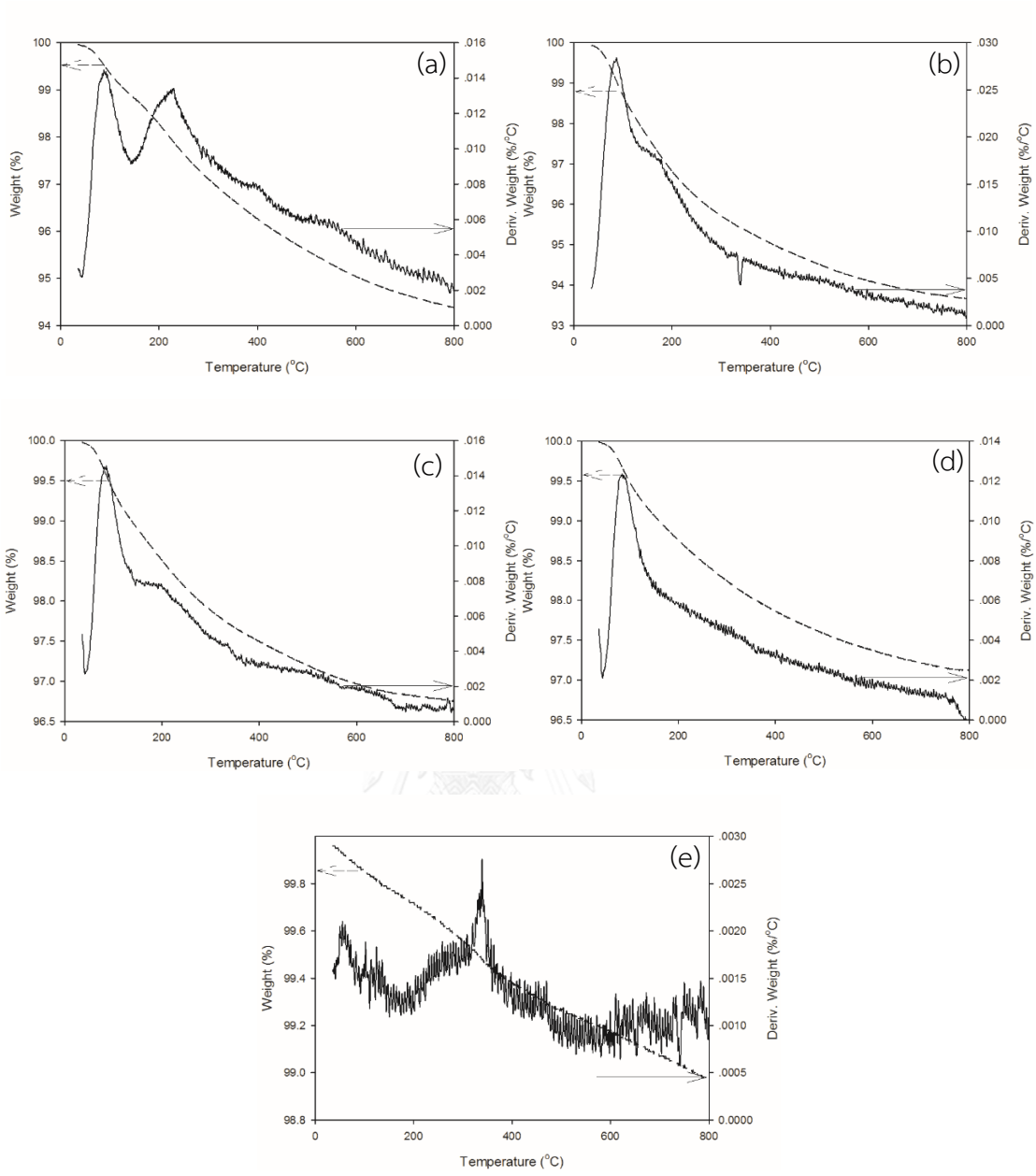

Figure 24 TG/DTA analysis of the fresh catalysts;
(a) Al_2O_3 (b) 5P/Al_2O_3 (c) 12P/Al_2O_3 (d) 14P/Al_2O_3 (e) 20P/Al_2O_3

The thermal decomposition of all spent catalyst was also brought to identify the amount of coke formation on the catalysts surface after using in the ethanol dehydration reaction. The decomposition of each catalyst is shown in **Figure 25** as follows;

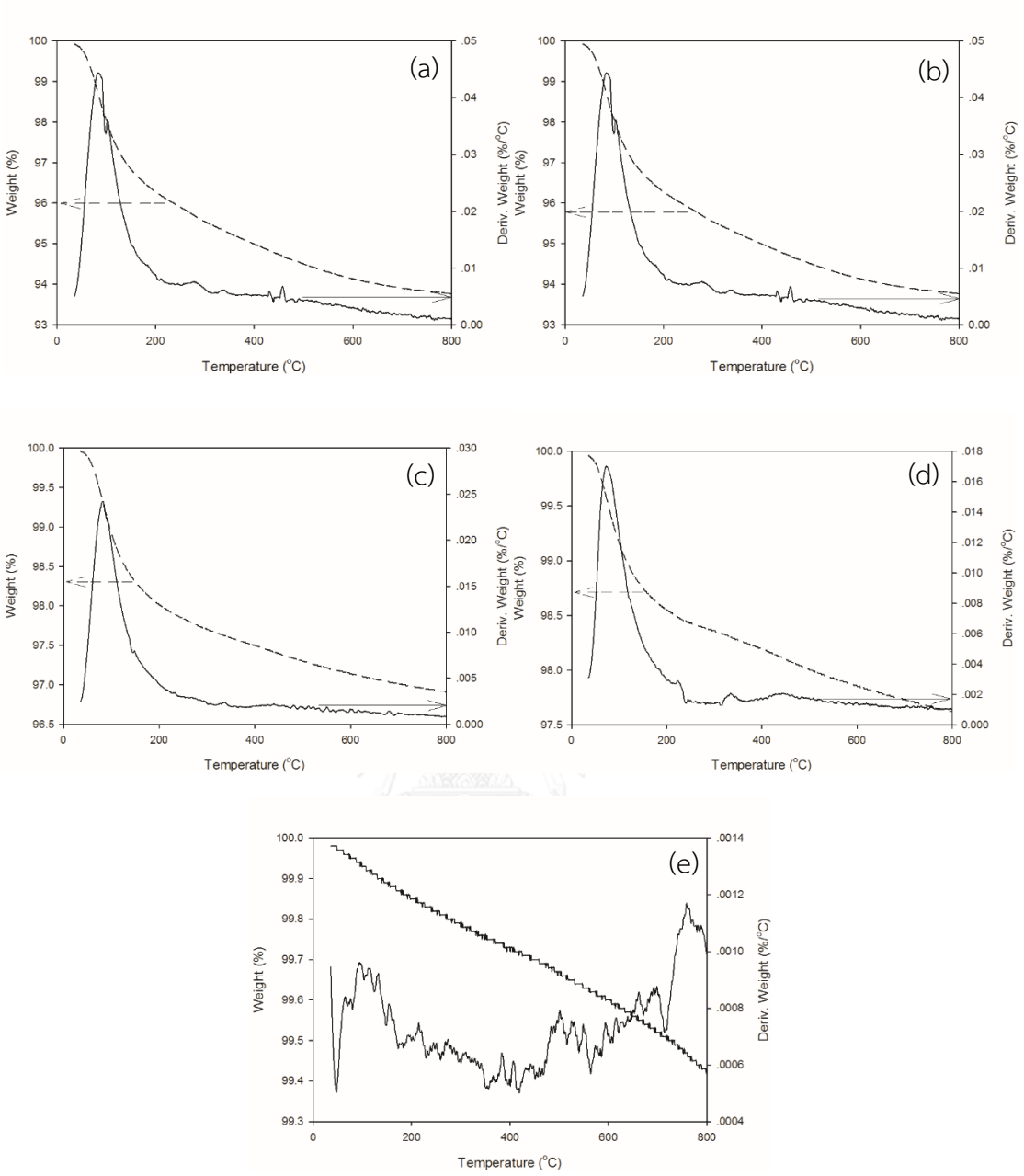

Figure 25 TG/DTA analysis of the spent catalysts;
(a) Al_2O_3 (b) $5P/Al_2O_3$ (c) $12P/Al_2O_3$ (d) $14P/Al_2O_3$ (e) $20P/Al_2O_3$

All catalysts were found to have moisture, which the TG/DTA analysis detected the decomposition in weight at temperature range below 200°C. At temperature range higher than 200°C, it was also found the small amount of species decomposition which was suggested to be the decomposition of coke formed on the

catalysts surface. The amount of coke formation in each catalyst was calculated (from 200 to 800°C) and shown in **Table 14** as follows;

Table 14 The amount of coke formation in the used catalysts

Catalysts	Temperature (°C)	Weight (%)	The amount of coke formation (%)
Al_2O_3	200	96.76	4.56
	800	92.20	
$5P/Al_2O_3$	200	96.28	2.51
	800	93.77	
$12P/Al_2O_3$	200	98.02	1.11
	800	96.91	
$14P/Al_2O_3$	200	98.55	0.93
	800	97.62	
$20P/Al_2O_3$	200	99.90	0.19
	800	99.71	

From **Table 14** which describes the amount of coke formation determining from the thermal decomposition of catalysts at 200 to 800°C, it was found that the higher amount of phosphorus modified on the catalysts caused the catalysts to have lower coke formation. These results were associated to NH_3-TPD results described in **Figure 17** and **Table 12** which demonstrated that the higher amount of phosphorus modified led the catalyst to have lower medium acid sites, then brought the catalyst to have lower amount of coke formation.

From the catalytic characterization and reaction study results, it was found that the phosphorus deposited on alumina supports in the form of phosphate. Therefore, the structure of P-modified alumina catalysts can be proposed and illustrated in **Scheme 1**.

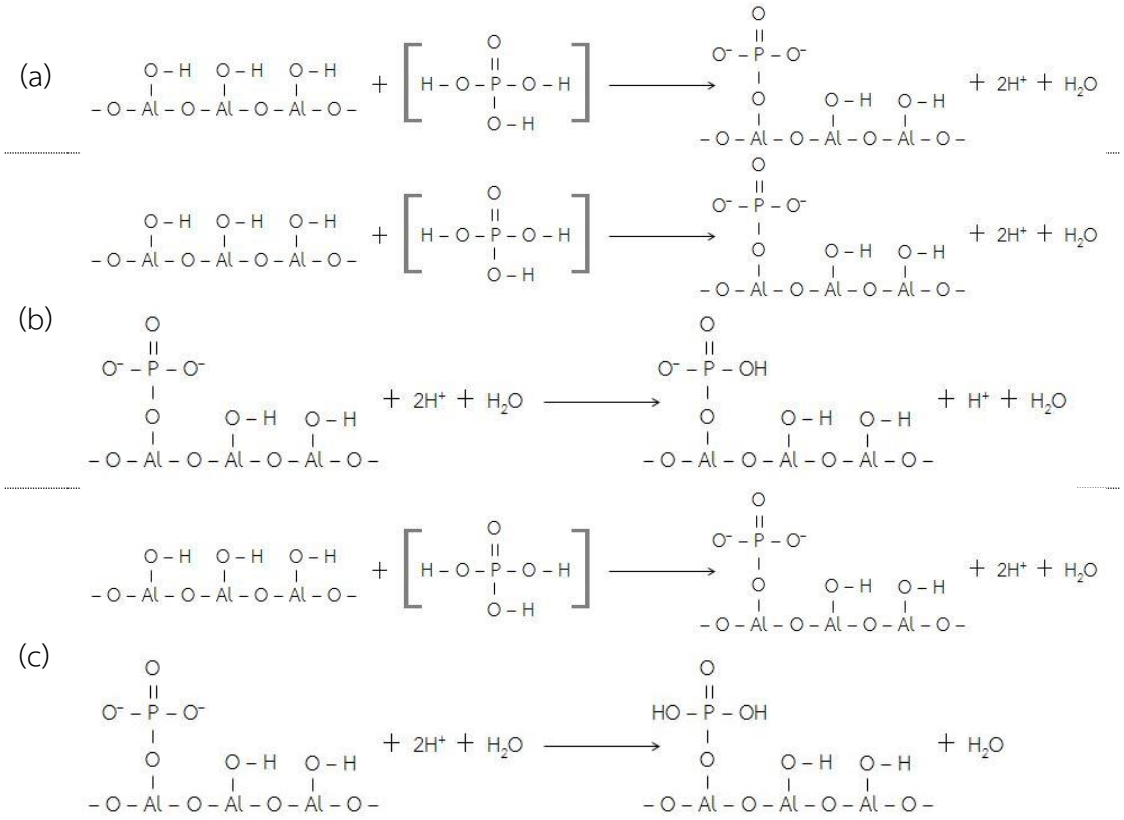

Scheme 1 Proposed structure of P-modified alumina catalysts

The proposed modification structure above showed the modification of 1 mole of phosphoric acid on alumina supports. The higher amount of phosphoric deposited is suggested to lead the structure of P-modified alumina catalysts to have lower amount of –OH group and increase the contained phosphate molecule. The deposition of phosphoric acid on alumina supports can be displayed into 3 pathways. In this research, the modification of phosphoric acid by acid activation technique is assumed to follow pathway (c). Because of the sufficient time in stirring the mixture between phosphoric acid and alumina supports and the higher acid sites

detected from NH_3-TPD, the proton seems to completely interacted with oxygen ion and formed 2 –OH groups.

The overall occurring mechanism in this research can be divided into 2 main steps as follows;

Step 1 : Removing water molecule from P-modified alumina catalyst [12]

When heat is added into the system, the water molecule could be removed by four pathways as shown in Scheme 2, one is removing from both –OH group on alumina supports (1st pathway) and second one is removing from both –OH on phosphate which incorporated with alumina supports (2nd pathway) and others are removing from –OH group on alumina supports and phosphate (3rd and 4th pathways). The proposed mechanisms are described as follows;

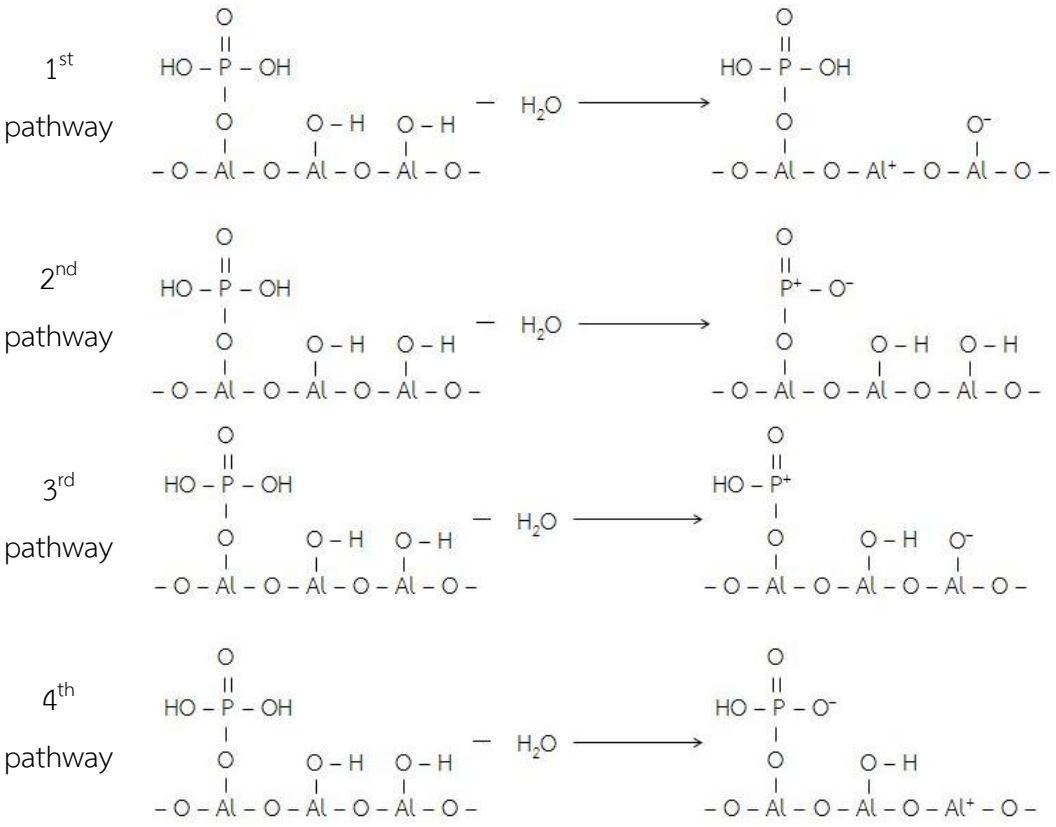

Scheme 2 Possible pathways of water removed from P-modified alumina catalysts

Step 2 : Production of the main product

The P-modified alumina catalysts which were already removed water molecule were brought to convert the ethanol (reactant) into a variety of products through ethanol dehydration reaction. In this context, 1st and 2nd pathway catalysts are raised as the represent catalysts, where the proposed mechanisms to each product are presented in **Scheme 3** and **Scheme 4** as follows;

1. Diethyl ether (Dehydration pathway)

1.1 Dissociative pathway

The proposed mechanism of dissociative pathway to produce diethyl ether starts when the Al^{+} attracts hydroxyl group in ethanol molecule to leave hydroxyl group. Then, the obtained carbonation molecule attacks with another ethanol molecule and leaves proton.

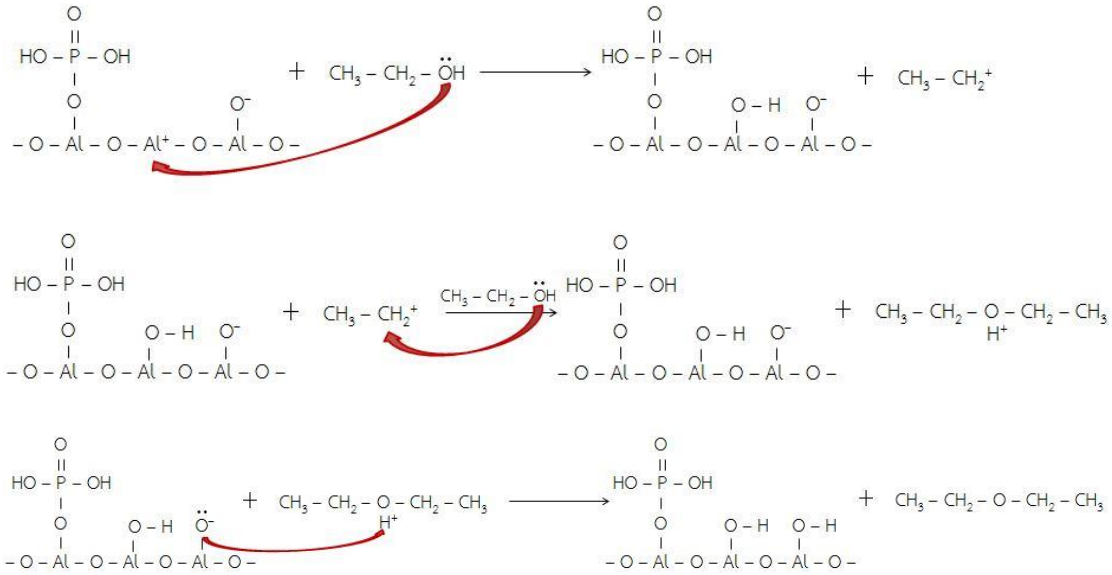

Scheme 3 Dissociative pathway (1st pathway)

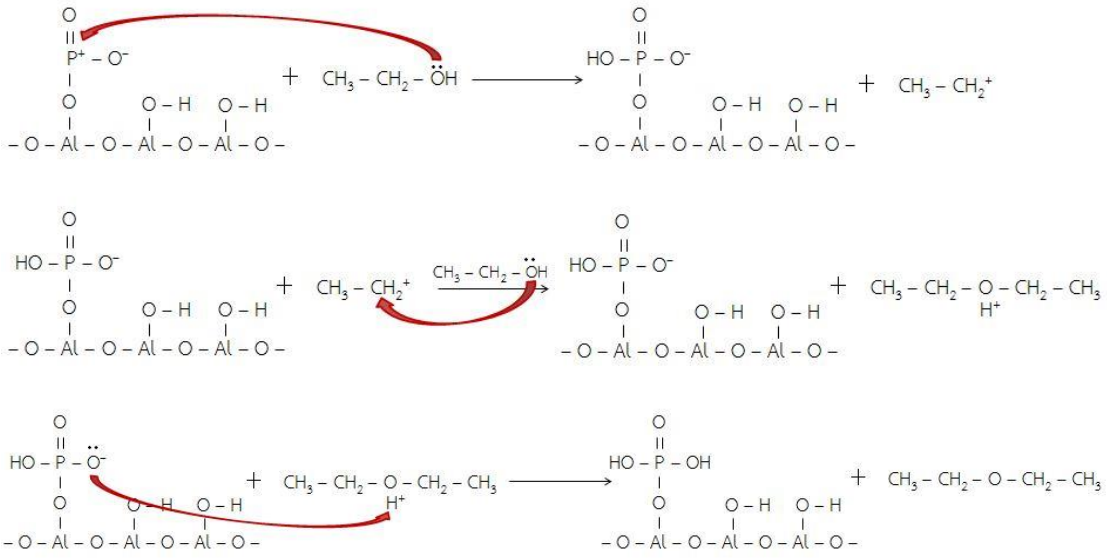

Scheme 4 Dissociative pathway (2nd pathway)

1.2 Associative pathway

The proposed mechanism in associative pathway starts when proton (Brønsted acid site) is attracted by hydroxyl group in ethanol molecule. After that, the resulting molecule attacks another ethanol molecule and leaves proton.

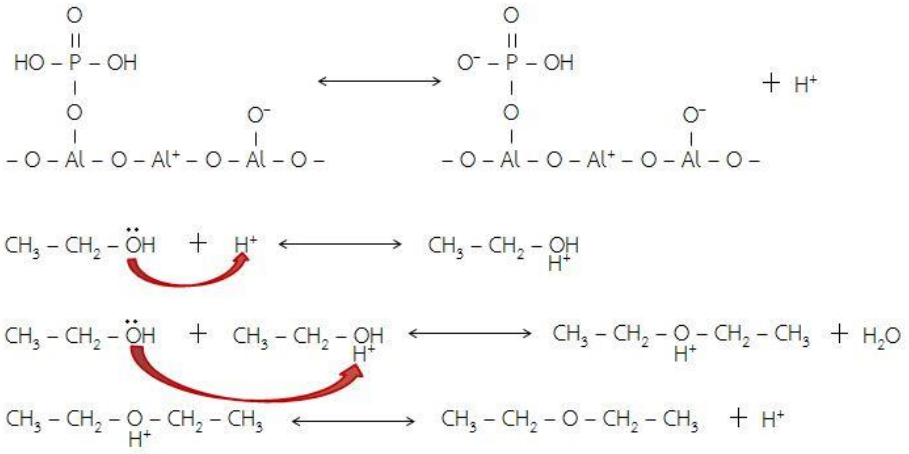

Scheme 5 Associative pathway (1st pathway)

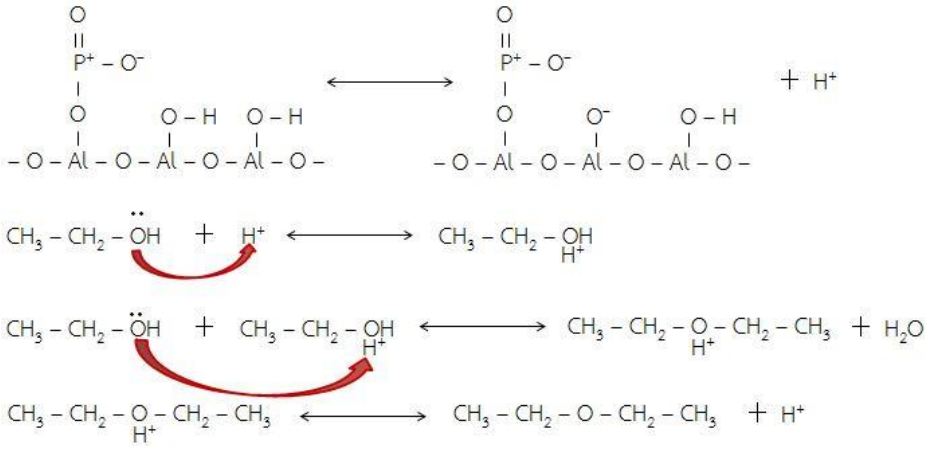

Scheme 6 Associative pathway (2nd pathway)

2. Ethylene (Dehydration pathway)

The proposed mechanism of ethanol to produce ethylene which is shown in **Scheme 7** and **Scheme 8** starts when hydroxyl group in ethanol molecule is protonated by proton (Brønsted acid site) and remove water molecule. The methyl group is then deprotonated by a conjugate base in the catalyst and releases ethylene.

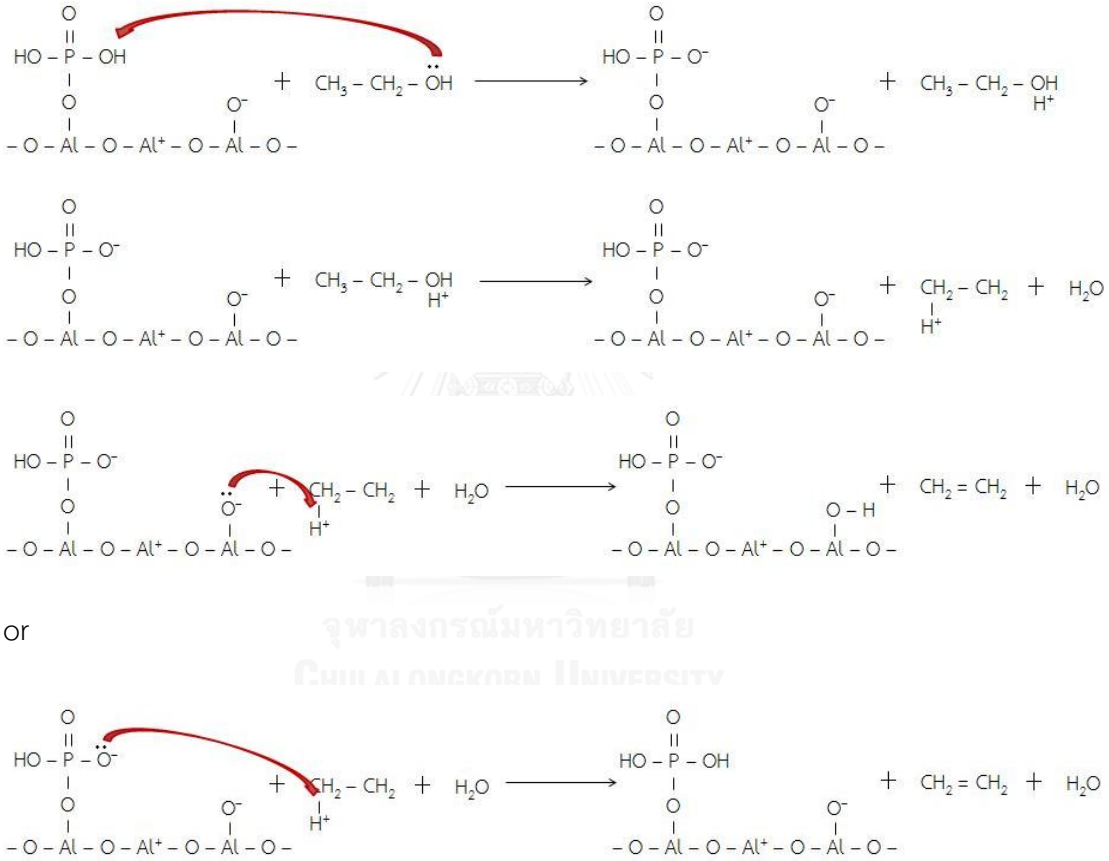

or

Scheme 7 Dehydration pathway of ethanol to ethylene (1st pathway)

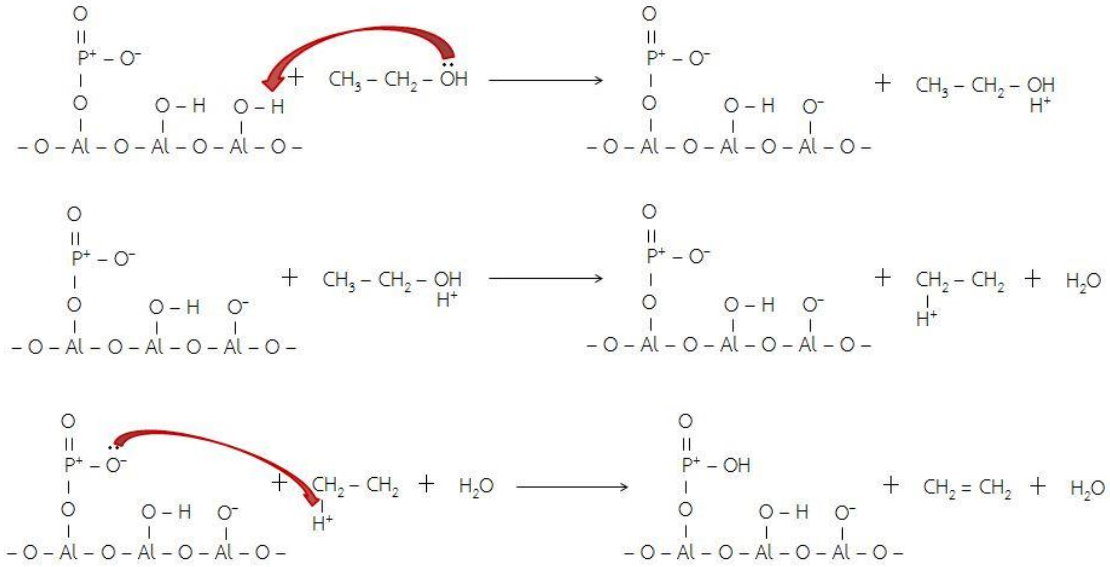

or

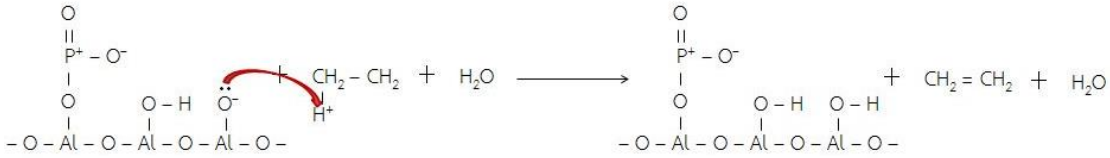

Scheme 8 Dehydration pathway of ethanol to ethylene (2nd pathway)

The proposed mechanism of diethyl ether to produce ethylene which is shown in **Scheme 9** and **Scheme 10** starts when oxygen atom in diethyl ether molecule is protonated by proton (Brønsted acid site) and remove water molecule. Then, the methyl group is deprotonated and releases ethylene.

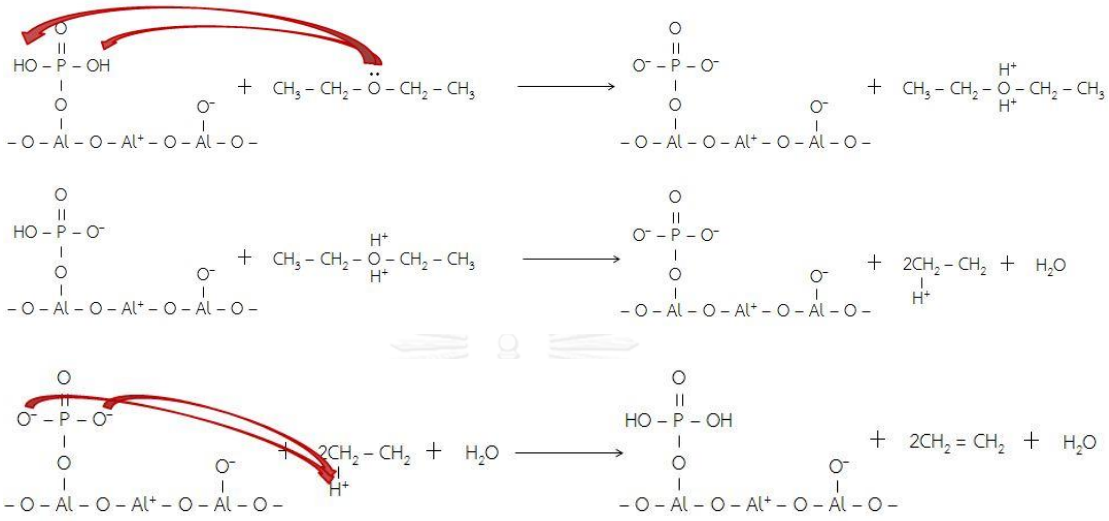

or

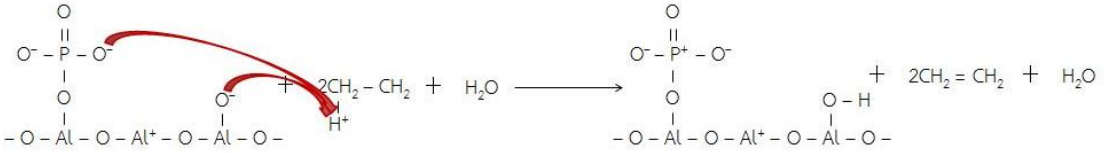

Scheme 9 Dehydration pathway of diethyl ether to ethylene (1st pathway)

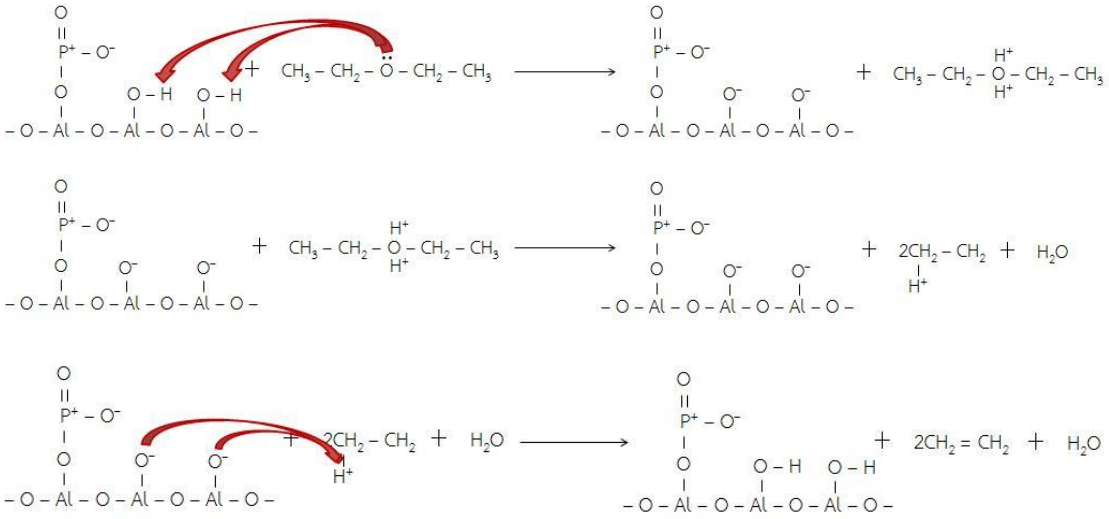

or

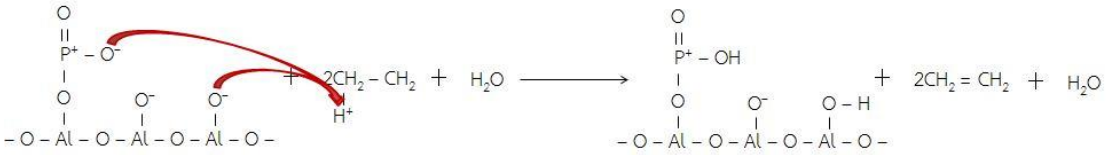

Scheme 10 Dehydration pathway of diethyl ether to ethylene (2nd pathway)

3. Acetaldehyde (Dehydrogenation pathway)

The proposed mechanism to produce acetaldehyde requires metal site to start the mechanism. Mechanism starts when oxygen molecule in catalyst attracts proton from hydroxyl group in ethanol molecule attracts metal site in catalyst. Then, an intermediate molecule is formed and leaves hydrogen molecule to produce acetaldehyde.

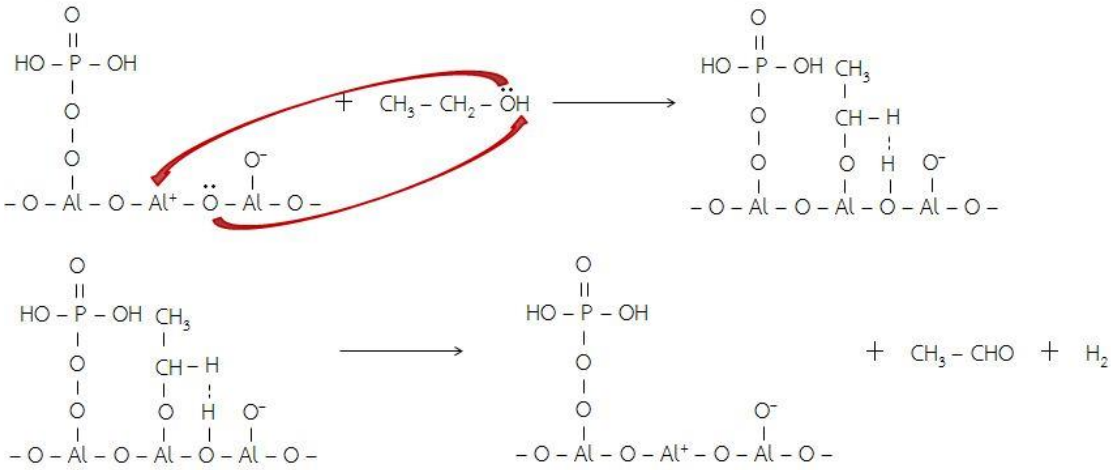

or

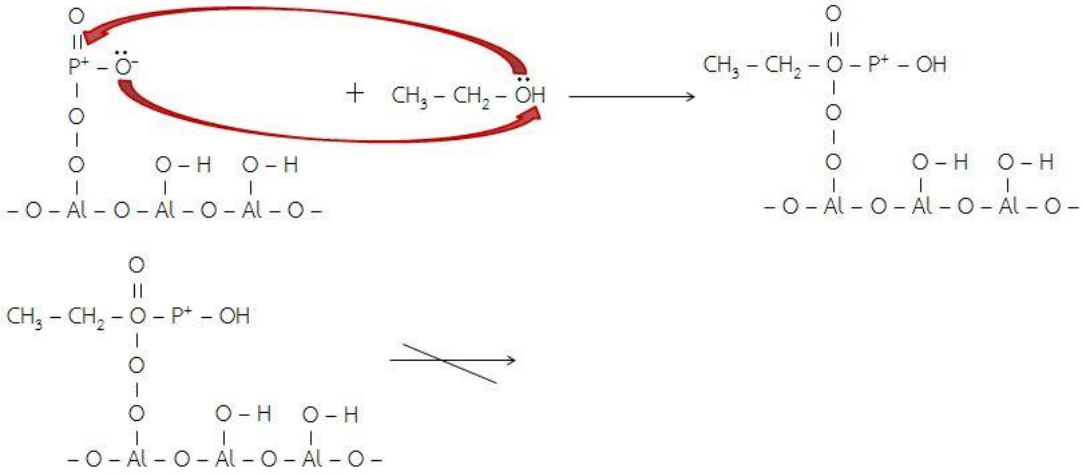

Scheme 11 Dehydrogenation pathway

5.1.9 Catalyst appearance

After modified mixed phase alumina supports with different loading of phosphorus (0-20 wt%), the prepared alumina catalysts were brought to study the catalyst appearance before and after being used in ethanol dehydration reaction. The image of each studied catalyst before and after being used (fresh and spent) in the reaction are displayed in **Figure 26** and **Figure 27**, respectively.

The appearance of fresh Al_2O_3 and P-modified Al_2O_3 catalysts which is illustrated in **Figure 26** showed that the amount of phosphorus loading led catalysts to have more gray color. These results indicated that phosphorus in excessive amounts might bring the catalyst structure to transform into the different one. These changes in structure were according to the previous results shown in N_2 physisorption, NH_3-TPD, reaction study, thermal gravimetric and differential thermal analysis.

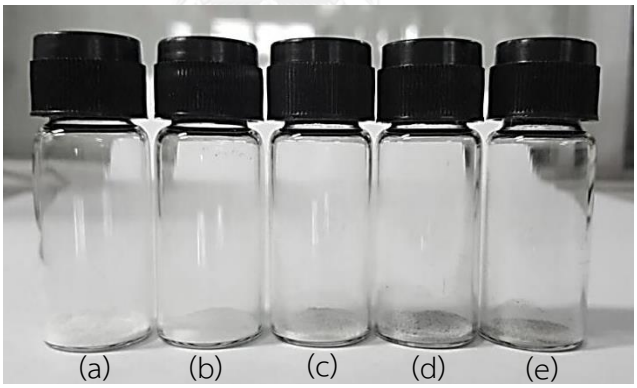

Figure 26 The appearance of fresh Al_2O_3 and P-modified Al_2O_3 catalysts;
(a) Al_2O_3 (b) 5P/Al_2O_3 (c) 12P/Al_2O_3 (d) 14P/Al_2O_3 (e) 20P/Al_2O_3

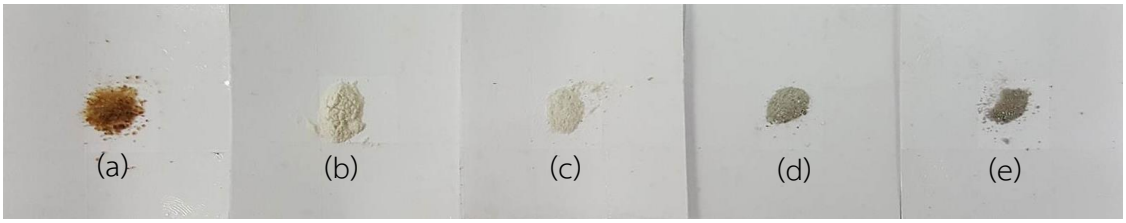

Figure 27 The appearance of spent Al_2O_3 and P-modified Al_2O_3 catalysts;
(a) Al_2O_3 (b) 5P/Al_2O_3 (c) 12P/Al_2O_3 (d) 14P/Al_2O_3 (e) 20P/Al_2O_3

Figure 27 displays the appearance of spent Al_2O_3 and P-modified Al_2O_3 catalysts. It can be suggested that color of Al_2O_3 catalyst was significantly change when compared to fresh catalyst. In other words, the color of P-modified Al_2O_3 catalysts was found to have slight change. Despite of their activities which decreased as the increasing in phosphorus amount, it can be concluded that the modification of catalyst with phosphorus can reduce the coke formation on catalysts surface as seen by a change of color.

Part II : The characteristic and catalytic activity of the P/Al_2O_3 catalysts modification with different noble metals (Ru, Pt and Pd)

Because the highest diethyl ether yield (34.41%) is obtained from using $5P/Al_2O_3$ as the catalyst in ethanol dehydration reaction at 300°C, the $5P/Al_2O_3$ catalyst is then chosen as the representative of P-modified alumina catalyst in order to modify with different type of noble metal in the further study. The study of noble metal modification on $5P/Al_2O_3$ catalyst including the characteristics and catalytic ability are all described in **Topic 5.2.1** to **5.2.9** as follows;

5.2.1 Inductively coupled plasma (ICP)

Noble metals including Ru, Pt and Pd were added to $5P/Al_2O_3$ catalyst by incipient wetness impregnation. Then the resulting catalysts were brought to estimate the contained amount of metal by inductively coupled plasma (for Pt and Pd) and X-ray fluorescence (for Ru). **Table 15** shows the amount of noble metal determined by ICP and XRF as follows;

Table 15 The amount of noble metal (Ru, Pt and Pd) contained in the catalysts bulk

Catalysts	Amount of Ru in catalysts bulk (wt%)	Amount of Pt in catalysts bulk (wt%)	Amount of Pd in catalysts bulk (wt%)
$Ru5P/Al_2O_3$	0.5*	-	-
$Pt5P/Al_2O_3$	-	0.3	-
$Pd5P/Al_2O_3$	-	-	0.2

*Determined form XRF

In this report, we then called the 5P/Al_2O_3 catalysts contained Ru, Pt and Pd in amount of 0.5, 0.3 and 0.2 wt% as Ru5P/Al_2O_3, Pt5P/Al_2O_3 and Pd5P/Al_2O_3, respectively.

5.2.2 X-ray diffraction (XRD)

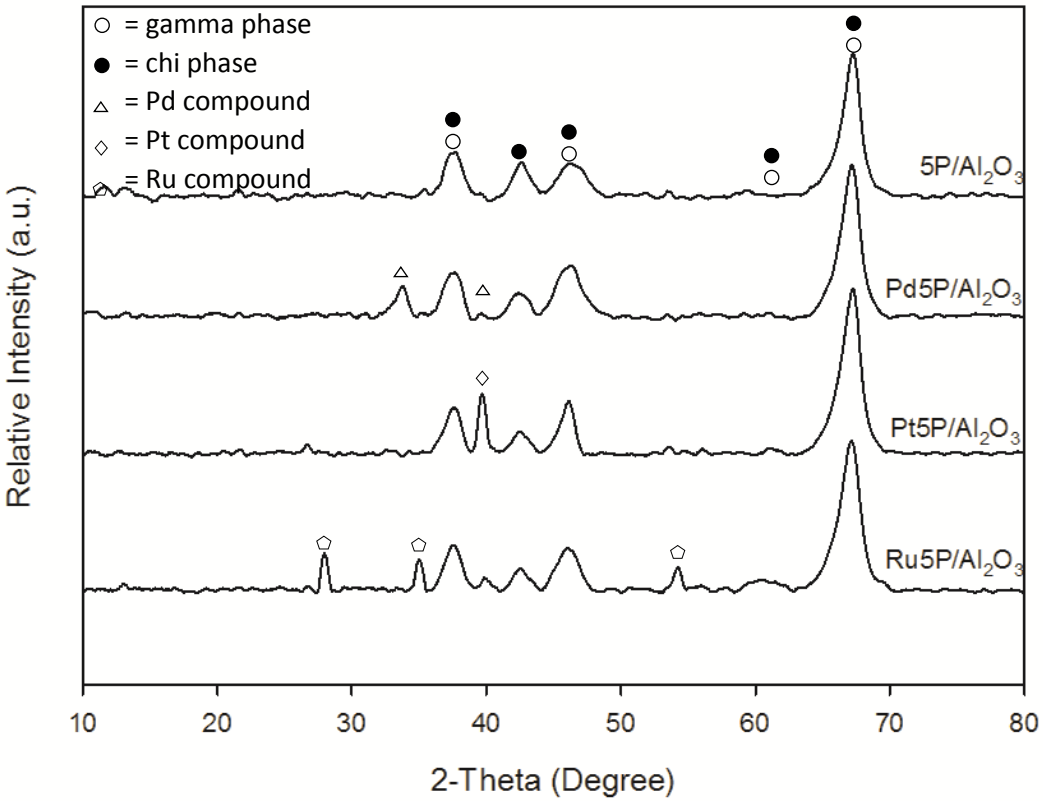

Figure 28 XRD patterns of 5P/Al_2O_3 and noble metal modified 5P/Al_2O_3 catalysts

Figure 28 illustrates XRD patterns of noble metal modified 5P/Al_2O_3 catalysts which the studied noble metals in this research are Ru, Pt and Pd. XRD patterns depicted above was observed both γ- and χ-phase of alumina supports as already described in **Part I**. When considered the noble metal which modified into 5P/Al_2O_3 catalyst, the ruthenium species were detected in XRD patterns at 2θ of 28°, 35° and 54° as E. J. Angueira et al. reported in Leading Edge Catalysis Research [44]. For the other noble metals, which are palladium and platinum, it was found that palladium

species were noticed in XRD patterns at 2θ of 33.5° and 40° as described in Lina Han et al. research [45] and platinum species were noticed in XRD patterns at 2θ of 40° where the XRD peak XRD peak showed in Tim Hyde report [46]. All of XRD patterns which were studied in this part did not detected the trace of phosphorus which can be presumed that phosphorus species had a very small crystalline size or dispersed thoroughly on alumina supports as the XRD result in **Part I**.

5.2.3 Scanning electron microscope (SEM) and energy dispersive X-ray spectroscopy (EDX)

The morphology of 5 wt% P-modified alumina catalyst after added noble metal including Ru, Pt and Pd was investigated by scanning electron microscope (SEM) and shown in **Figure 29**.

SEM images of noble metal modified 5P/Al_2O_3 catalysts showed that all of the studied catalysts had irregular shape. The noble metal modified 5P/Al_2O_3 catalysts presented the similar size with the size of P-modified Al_2O_3 catalysts. It can be noticed that there was the trace of particle dispersed throughout the samples. This could be suggested that the noble metal modification was both dispersed on the catalyst surface and agglomerated with itself in the smaller particle size form.

(a)

(b)

(c)

(d)

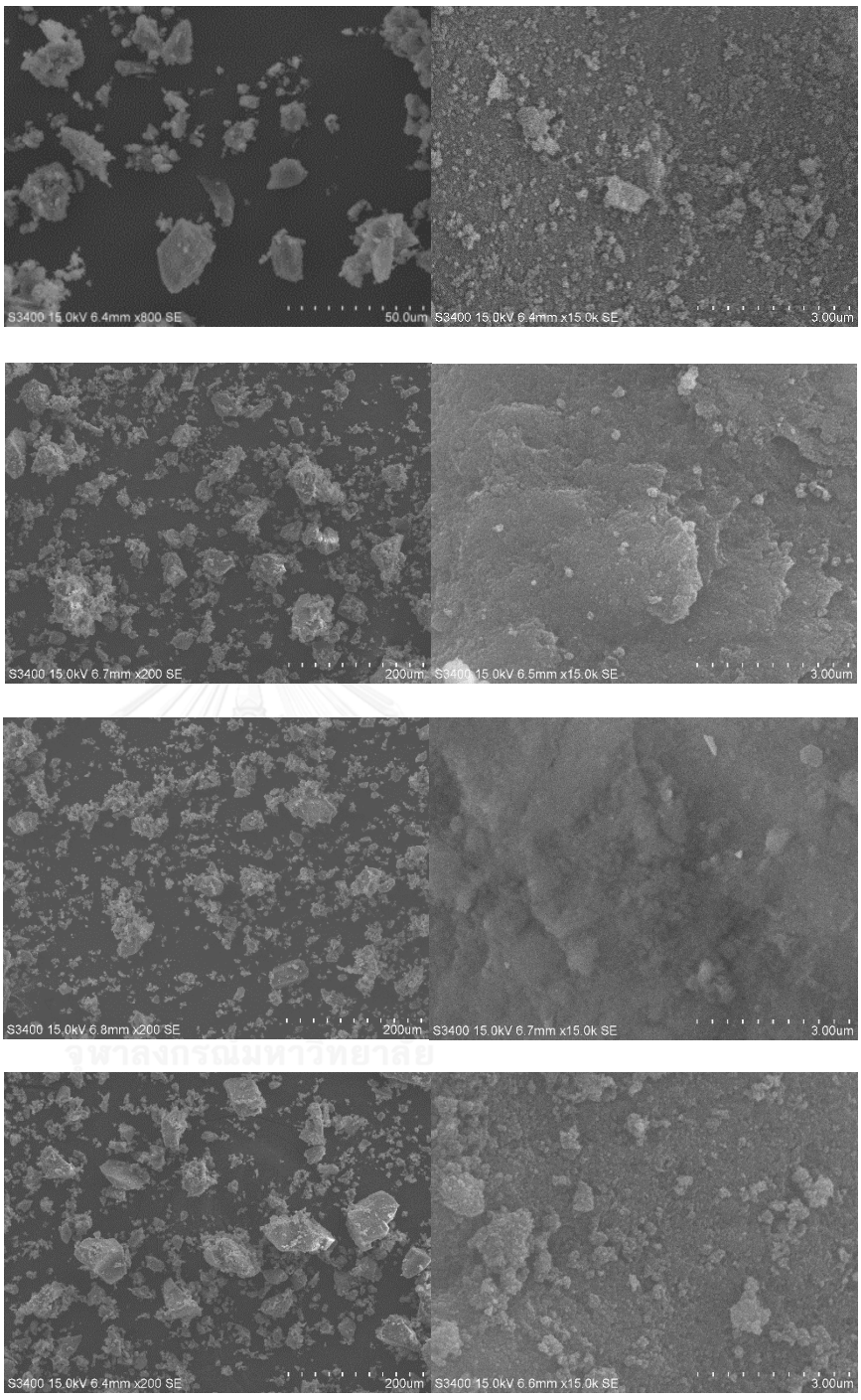

Figure 29 SEM micrograph of $5P/Al_2O_3$ and noble metal modified P/Al_2O_3 catalysts; (a) $5P/Al_2O_3$ (b) $Ru5P/Al_2O_3$ (c) $Pt5P/Al_2O_3$ (d) $Pd5P/Al_2O_3$

The noble metal modified $5P/Al_2O_3$ catalysts were also brought to study elemental dispersion including Al (green color), O (red color), P (blue color) and noble metal (yellow color) on the surface of the catalysts by energy dispersive X-ray

spectroscopy (EDX). The EDX mappings of studied catalyst are displayed in **Figure 30** to **Figure 33** as follows;

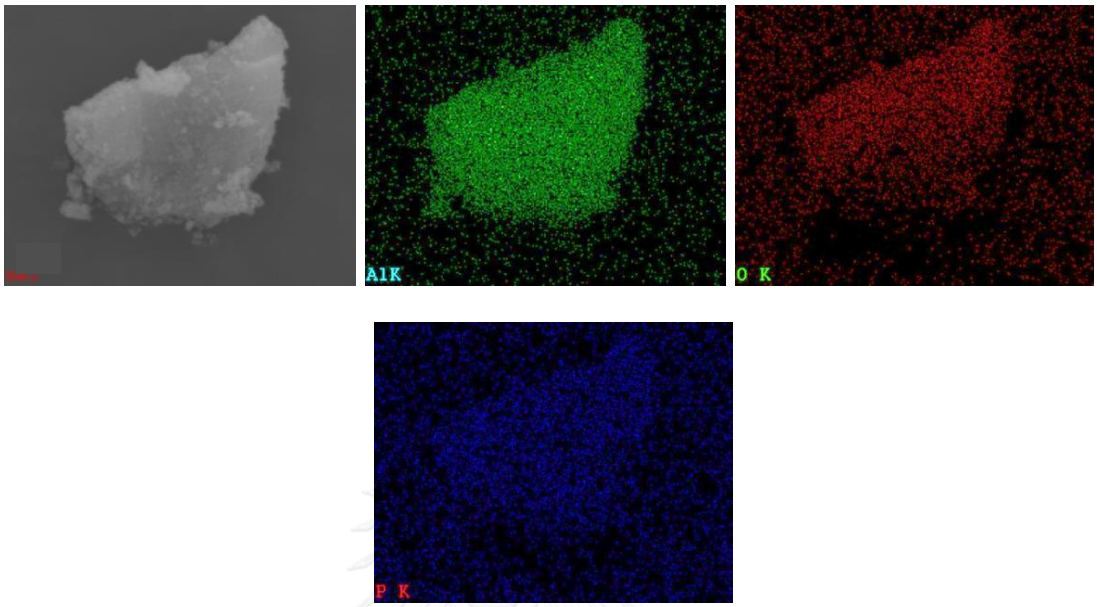

Figure 30 EDX mapping of 5P/Al_2O_3

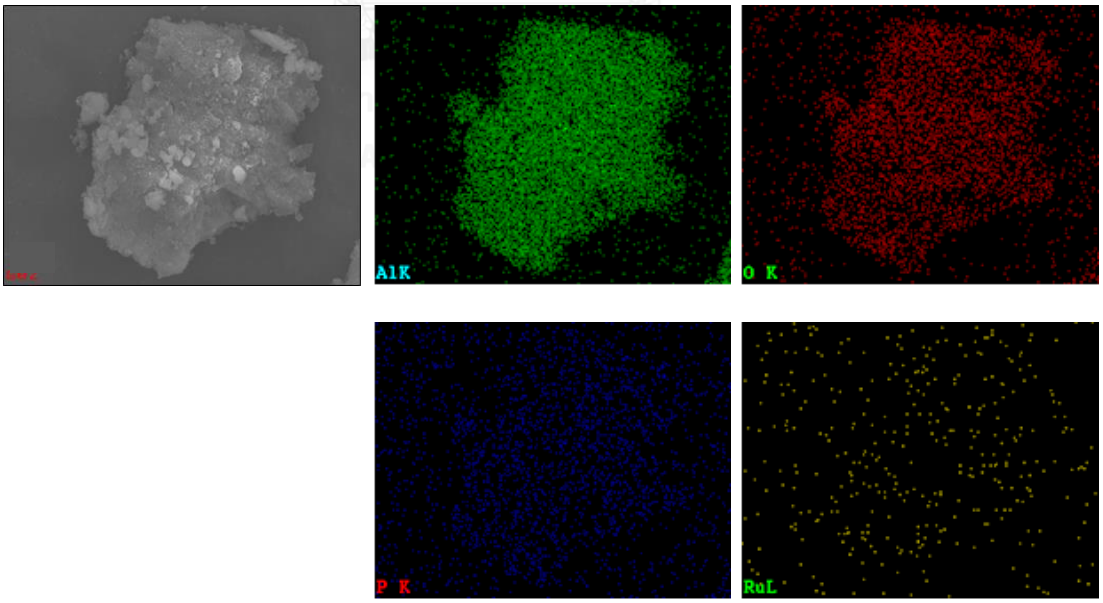

Figure 31 EDX mapping of Ru5P/Al_2O_3

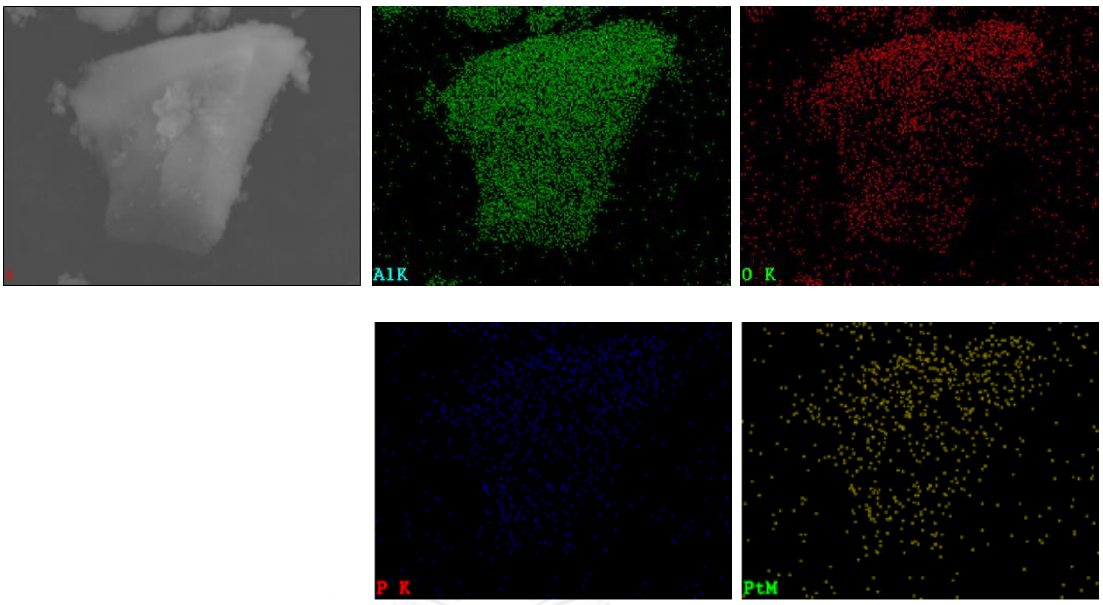

Figure 32 EDX mapping of Pt5P/Al_2O_3

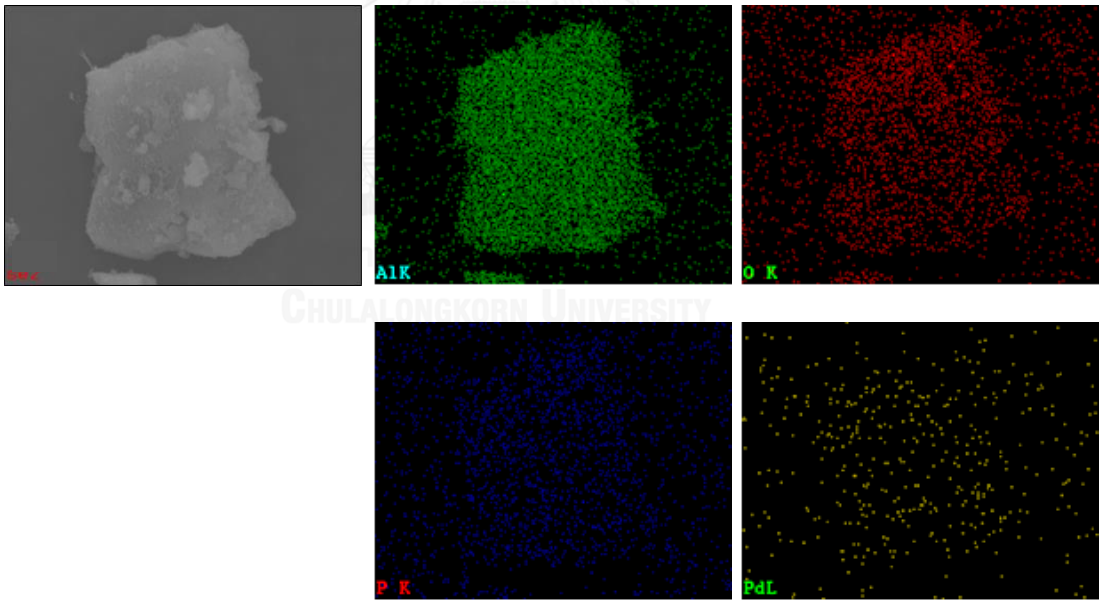

Figure 33 EDX mapping of Pd5P/Al_2O_3

The EDX mappings which are demonstrated in **Figure 30** to **Figure 33** investigated alumina, oxygen, phosphorus and noble metal (Ru, Pt and Pd) distribution on the catalysts granule. The elemental distribution results showed that all studied elements were well dispersed on catalysts. The amount of elemental

distribution (Al, O, P, Ru, Pt and Pd) in weight percent and atom percent over each catalyst surface are presented in **Table 16** and **Table 17**, respectively.

Table 16 The amount of elemental distribution on the catalysts (weight percent)

Catalysts	Amount of element on surface (wt%)						
	Al	O	P	Ru	Pt	Pd	Metal/Al
$5P/Al_2O_3$	55.43	31.11	13.46	-	-	-	-
$Ru5P/Al_2O_3$	48.15	37.63	13.08	1.14	-	-	0.024
$Pt5P/Al_2O_3$	54.69	39.18	5.40	-	0.73	-	0.013
$Pd5P/Al_2O_3$	46.06	37.47	14.08	-	-	2.39	0.052

Table 17 The amount of elemental distribution on the catalysts surface (atom percent)

Catalysts	Amount of element on surface (at%)						
	Al	O	P	Ru	Pt	Pd	Metal/Al
$5P/Al_2O_3$	46.33	43.87	9.80	-	-	-	-
$Ru5P/Al_2O_3$	39.05	51.47	9.24	0.25	-	-	0.006
$Pt5P/Al_2O_3$	43.55	52.62	3.75	-	0.08	-	0.002
$Pd5P/Al_2O_3$	37.72	51.74	10.04	-	-	0.50	0.013

As the results in **Part I**, the amount of each element on samples (investigated by EDX) was brought to compare with the amount of each element in bulk samples (investigated by ICP and XRF) as concluded in **Table 18** as follow;

Table 18 The amount of noble metal comparing between catalysts surface and bulk catalysts

Catalyst	Amount of noble metal on catalysts surface identified by EDX (wt%)	Amount of noble metal in bulk catalysts identified by ICP or XRF (wt%)
Ru5P/Al_2O_3	1.14	0.50
Pt5P/Al_2O_3	0.73	0.26
Pd5P/Al_2O_3	2.39	0.19

*EDX is measured at the depth around 2 μm from surface.

From the amount of noble metal detected by EDX and ICP shown in **Table 18**, it was found that most of platinum, palladium and ruthenium species had larger size than the pore of catalyst. Thus, the amount of all noble metals identified on catalyst surface was found to be higher than the amount identified in bulk catalyst.

5.2.4 N_2 physisorption

The surface area, pore volume, pore size, N_2 adsorption-desorption isotherm and pore size distribution of noble metal modified 5P/Al_2O_3 catalysts were also brought to investigate and report in this research. The summary of catalysts surface area, pore volume and pore size are displayed in **Table 19** as follows;

Table 19 The surface area, pore volume and pore size of noble metal modified 5P/Al_2O_3 catalysts;

Catalysts	Surface Area[a] (m^2/g)	Pore Volume[b] (cm^3/g)	Pore Size[c] (Å)
5P/Al_2O_3	151	0.486	114.9
Ru5P/Al_2O_3	138	0.517	131.0
Pt5P/Al_2O_3	142	0.549	131.7
Pd5P/Al_2O_3	149	0.564	132.3

[a] Determined from BET method

[b,c] Determined from BJH adsorption method

Porous properties of noble metal modified 5P/Al_2O_3 catalysts which is shown in **Table 19** were found to have similar porous properties which all catalysts had surface area, pore volume and pore size in range of 138 to 149 m^2/g. 0.486 to 0.564 cm^3/g and 114.9 to 132.3 Å, respectively. When compared these results with porous properties in **Part I**, it was observed that the modification with noble metal tended to slightly decrease catalysts surface area, but increase pore volume and pore size of the catalysts.

Considering the N_2 adsorption-desorption isotherms of noble metal modified 5P/Al_2O_3 catalysts displayed in **Figure 34**, the results showed that all studied catalysts had similar isotherm, which were type-IV isotherms as the **Part I** results. However, the noble metal modified 5P/Al_2O_3 catalysts exhibited lower amount of N_2 adsorption than non-noble metal modified 5P/Al_2O_3 catalysts. The results were corresponding to the results of catalysts pore volume that noble metal modified catalysts had lower pore volume than non-noble metal modified catalyst.

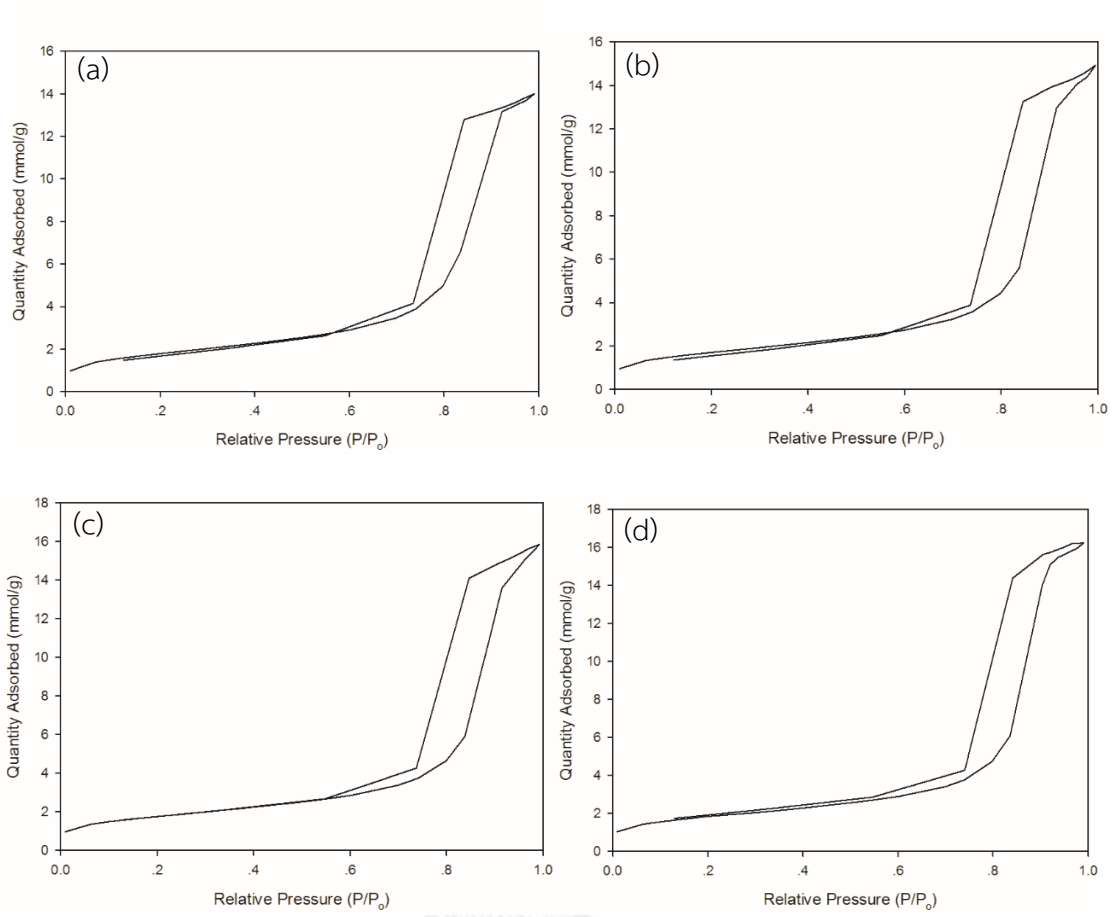

Figure 34 The N_2 adsorption-desorption isotherms at –196°C of catalysts; (a) $5P/Al_2O_3$ (b) $Ru5P/Al_2O_3$ (c) $Pt5P/Al_2O_3$ (d) $Pd5P/Al_2O_3$

The pore size distribution of noble metal modified $5P/Al_2O_3$ catalysts are depicted in **Figure 35**. All of catalyst pore size demonstrated unimodal distribution. This distribution was the same as the result of $5P/Al_2O_3$ catalyst in **Part I**.

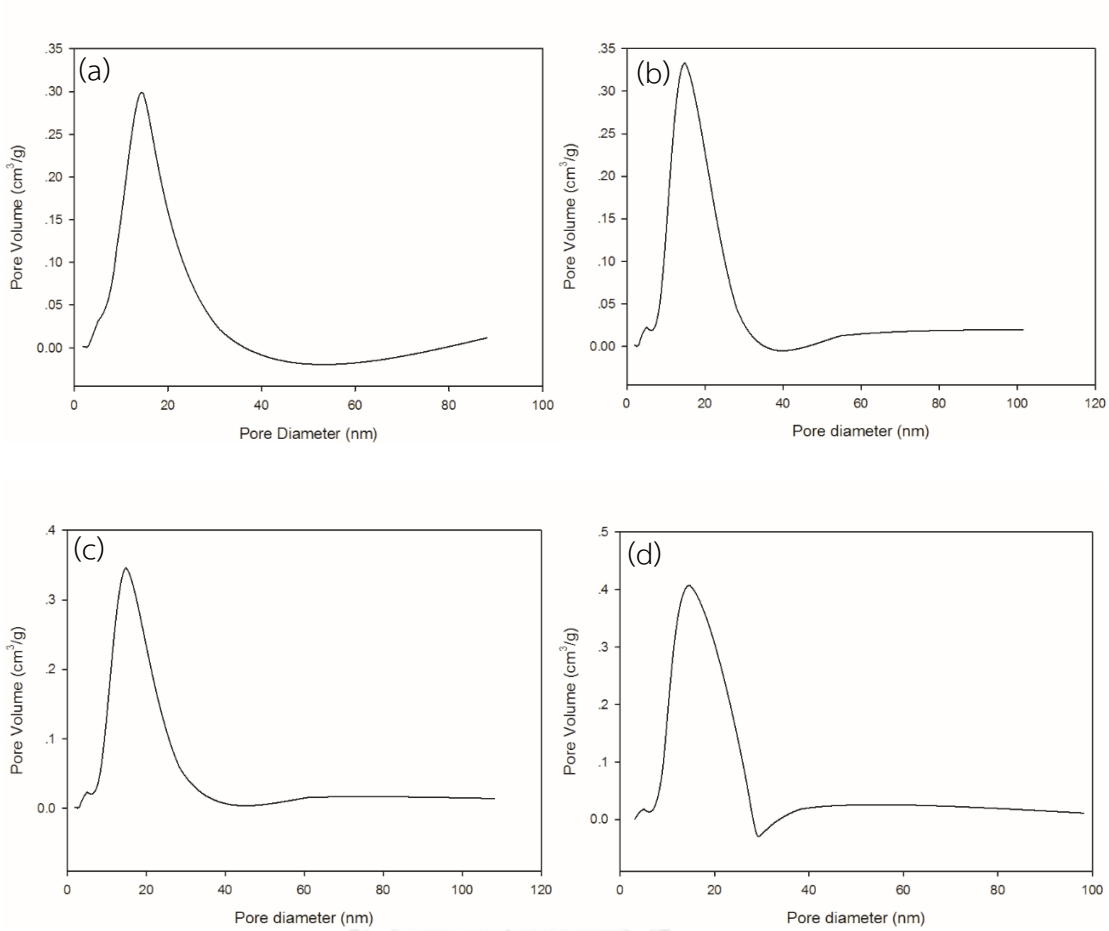

Figure 35 The pore size distribution of catalysts**;**

(a) 5P/Al_2O_3 (b) Ru5P/Al_2O_3 (c) Pt5P/Al_2O_3 (d) Pd5P/Al_2O_3

5.2.5 Ammonia temperature-programmed desorption (NH_3-TPD)

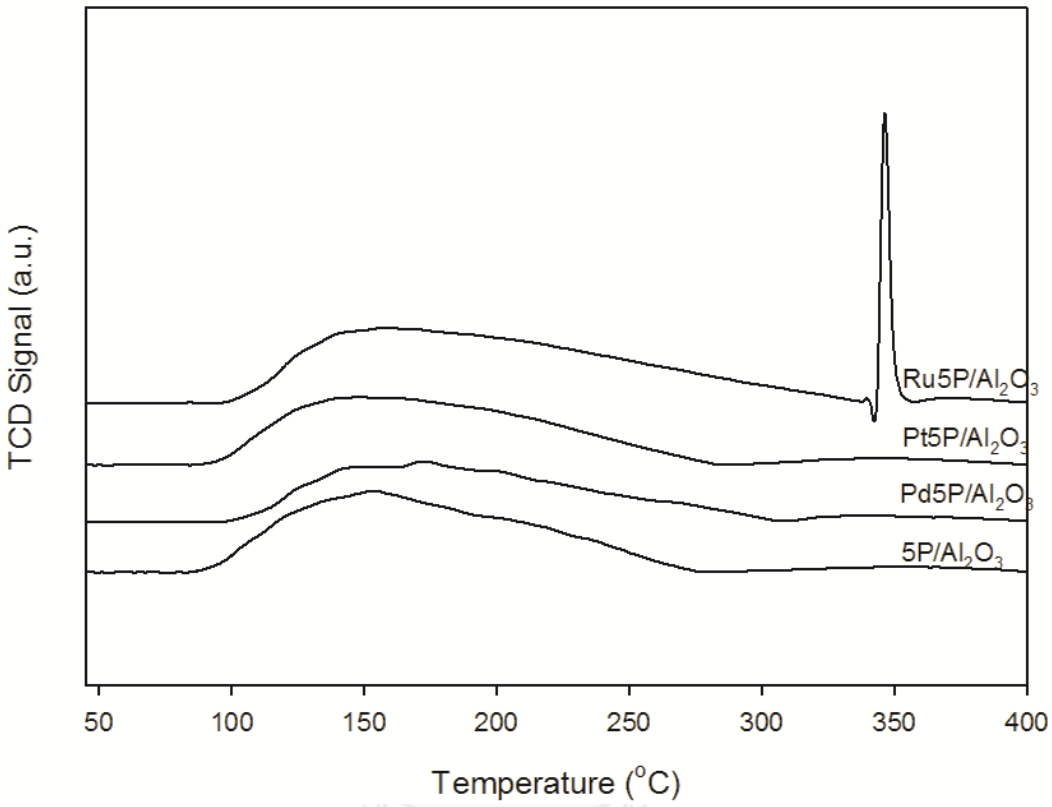

Figure 36 NH_3-TPD profiles of the $5P/Al_2O_3$ and noble metal modified $5P/Al_2O_3$ catalysts with various types of noble metal

The acid strength of the studied catalysts was identified and shown in **Figure 36** above. The NH_3-TPD profiles of $5P/Al_2O_3$ and different types of noble metal modified $5P/Al_2O_3$ catalysts were found to have two desorption peaks. It was noticed that the NH_3-TPD profiles of $Ru5P/Al_2O_3$ catalyst showed a non-characteristic peak at the temperature around 350°C. This sharp non-characteristic peak may be occurred due to the spark of electric generated from the impurities in the catalysts. In order to calculate catalyst acidity, the area under sharp the non-characteristic peak was not included in the computation. It was also observed that the weak and medium to strong acid sites of each catalyst did not have a significant difference in

the quantity as shown in **Part I**. The quantity of total acid in studied catalysts was all determined in **Table 20** as follows;

Table 20 The amount of acidity of the noble metal modified 5P/Al_2O_3 catalysts with various types of noble metal

Catalysts	**NH_3 desorption total acidity (μmol/g cat.)**
5P/Al_2O_3	2620
Ru5P/Al_2O_3	2680
Pt5P/Al_2O_3	2270
Pd5P/Al_2O_3	2060

The results of total acid amounts in all catalysts were not found the significant change when modified the 5P/Al_2O_3 catalyst with different types of noble metal. Most of noble metal modified 5P/Al_2O_3 catalysts including Pt5P/Al_2O_3 and Pd5P/Al_2O_3 showed the lower amount of total acidity, while Ru5P/Al_2O_3 catalyst exhibited the slightly higher amount of total acidity than non-noble metal modified 5P/Al_2O_3 catalysts.

5.2.6 X-ray photoelectron spectroscopy (XPS)

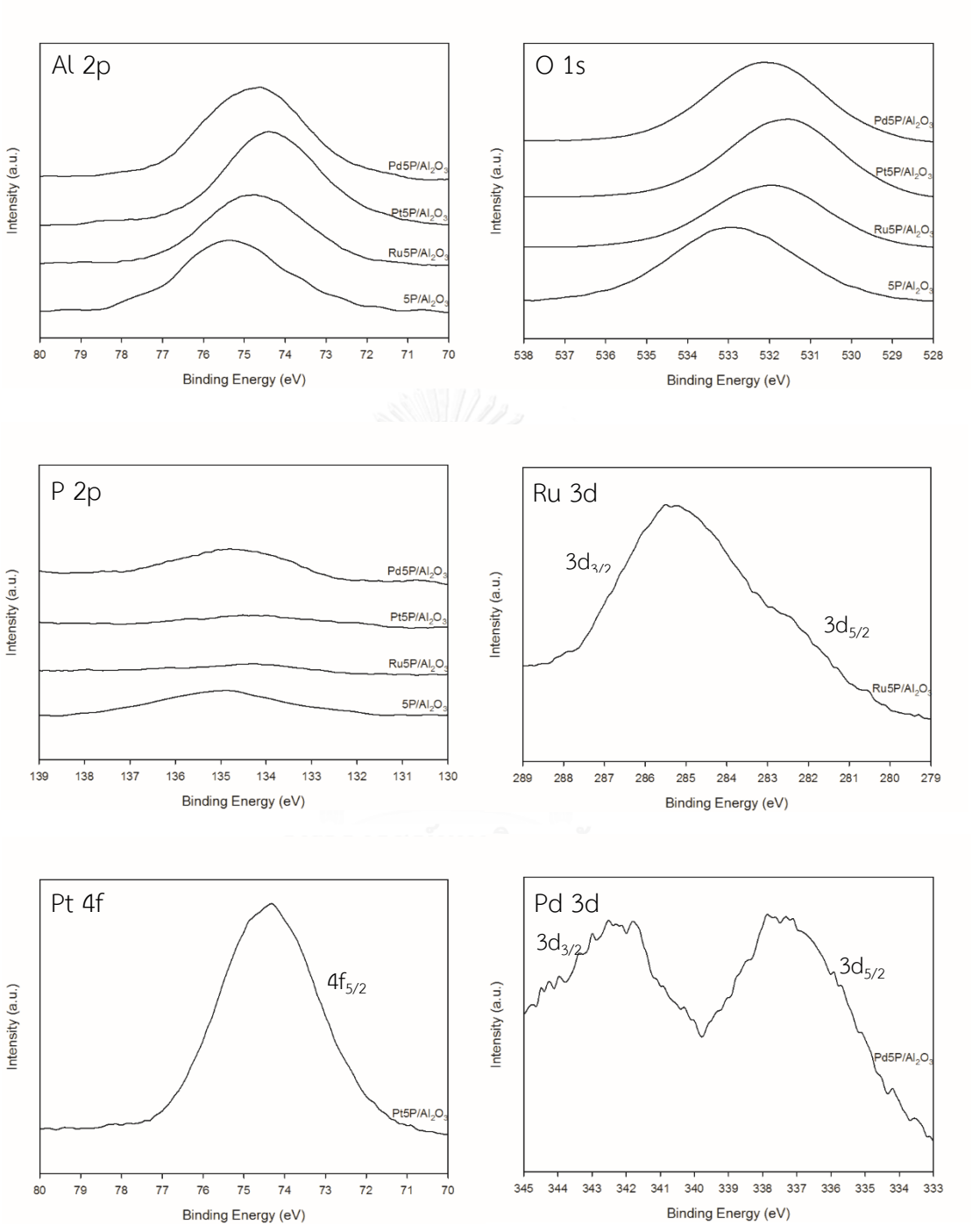

Figure 37 XPS spectra for $5P/Al_2O_3$ and noble metal modified alumina catalysts

Figure 37 presents the XPS spectra of the studied catalysts. In **Figure 37**, the binding energy for Al 2p of $5P/Al_2O_3$, $Ru5P/Al_2O_3$, $Pt5P/Al_2O_3$ and $Pd5P/Al_2O_3$ was 75.4,

75.3. 74.5 and 74.9, respectively. Considering binding energy for P 2p of all catalysts, it was located at 135.3, 134.3, 134.5 and 134.5, respectively. The binding energy of Al 2p and P 2p, which is shown above was found to step up from Al 2p and P 2p standard. Therefore, the XPS spectra of all catalysts was presumed to upshift in all studied elements. XPS spectra of noble metal modified alumina catalysts were specified peak of $3d_{3/2}$ and $3d_{5/2}$ for both Ru and Pd and $4f_{5/2}$ for Pt. The binding energy of noble metals including Ru, Pt and Pd specified from XPS spectra is located at 285.3 and 282.6 eV (for Ru $3d_{3/2}$ and Ru $3d_{5/2}$, respectively), 74.2 eV (for Pt $4f_{5/2}$), 343.3 and 338.6 (for Pd $3d_{3/2}$ and Ru $3d_{5/2}$, respectively). Consequently, it was found that the noble metals deposited on $5P/Al_2O_3$ catalysts were formed oxide structures when the binding energy of each noble metal standard including RuO_2, PtO and PdO was known to upshift from standard and located at 280.7, 72.4 and 336.7 eV, respectively [47-49]. Therefore, when the binding energy of Al 2p and P 2p was considered, it can be summarized that the modified noble metal did not change the structure of the catalysts.

The binding energy for all elements of studied catalysts is shown in **Table 21** as follows;

Table 21 Binding energy detected from $5P/Al_2O_3$ and noble metal modified alumina catalyst

	Binding Energy (eV)					
Catalysts	**Al 2p**	**O 1s**	**P 2p**	**Ru 3d**	**Pt 4f**	**Pd 3d**
$5P/Al_2O_3$	75.4	533.0	135.3	-	-	-
$Ru5P/Al_2O_3$	75.3	531.6	134.3	285.3.282.6	-	-
$Pt5P/Al_2O_3$	74.5	531.6	134.5	-	74.2	-
$Pd5P/Al_2O_3$	74.9	532	134.5	-	-	342.3,338.6

5.2.7 Reaction study

The noble metal modified on $5P/Al_2O_3$ catalysts were also brought to investigate the catalytic performance in ethanol dehydration reaction at specific reaction temperature of 200, 250, 300, 350 and 400°C. In this reaction study, the catalytic performance terms including ethanol conversion, selectivity towards interested products and products yield were all examined and described in **Figure 38** to **Figure 44**, respectively.

The ethanol conversion of noble metal modified $5P/Al_2O_3$ catalysts (noble metal including Ru, Pt and Pd) is illustrated in **Figure 38** as follows;

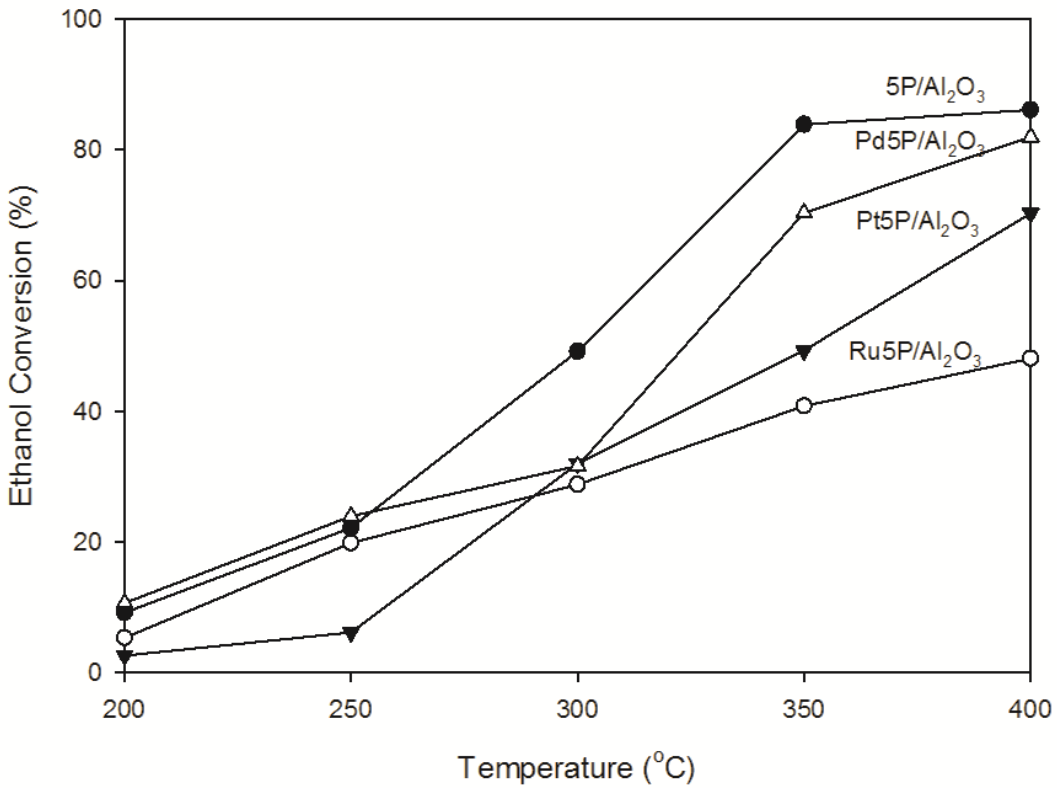

Figure 38 Ethanol conversion of $5P/Al_2O_3$ and noble metal modified $5P/Al_2O_3$ catalysts

From the ethanol conversion result shown in **Figure 38**, conversion of ethanol increased as the raising in temperature. At interested temperature, palladium modified catalyst tended to have the highest ethanol conversion among all studied catalysts. The highest ethanol conversion of Pd5P/Al_2O_3 catalyst reached 81.97% at 400°C. Considering at temperature of 300°C, it was found that all noble metal modified 5P/Al_2O_3 catalyst had a similar amount of ethanol conversion. When compared this ethanol conversion result with the result in **Part I**, the addition of 5P/Al_2O_3 catalysts with noble metal led the reaction to have lower conversion of ethanol. Nevertheless, it can be summarized that palladium modified on 5P/Al_2O_3 catalyst (Pd5P/Al_2O_3) which had the highest ethanol conversion at all studied reaction temperature was interesting enough to examine in further study.

Rate of reaction of all catalysts were also identified and displayed in **Table 22**. The reaction rate of noble metal modified 5P/Al_2O_3 catalysts showed the similar trend as depicted in **Part I** or it could be said that the rate of reaction was all increased when increasing reaction temperature. From all of studied catalysts, Pd5P/Al_2O_3 catalyst was found to have the highest rate of reaction among other catalysts reaching 0.2967 mole of ethanol/g cat. h. When compared these reaction rate results with the reaction rate of 5P/Al_2O_3 or unmodified noble metal catalyst in **Part I**, it was found that Pd5P/Al_2O_3 catalyst was observed to have higher reaction rate than 5P/Al_2O_3 catalyst at low studied temperature (200-250°C). However, when increased the reaction temperature above 300°C, 5P/Al_2O_3 catalyst showed the higher reaction rate than Pd5P/Al_2O_3 catalyst and reaching the highest reaction temperature at 350°C in the reaction rate of 0.3281 mole of ethanol/g cat.h.

Table 22 Rate of reaction of noble metal modified 5P/Al_2O_3 catalysts (noble metal including Ru, Pt and Pd)

Catalysts	Rate of Reaction ×10^2 (mole ethanol/g cat. h)				
	200°C	250°C	300°C	350°C	400°C
5P/Al_2O_3	4.70	10.30	20.90	32.81	31.17
Ru5P/Al_2O_3	2.71	9.23	12.22	15.94	17.39
Pt5P/Al_2O_3	1.31	2.84	13.58	19.27	25.44
Pd5P/Al_2O_3	5..46	11.12	13.44	27.50	29.67

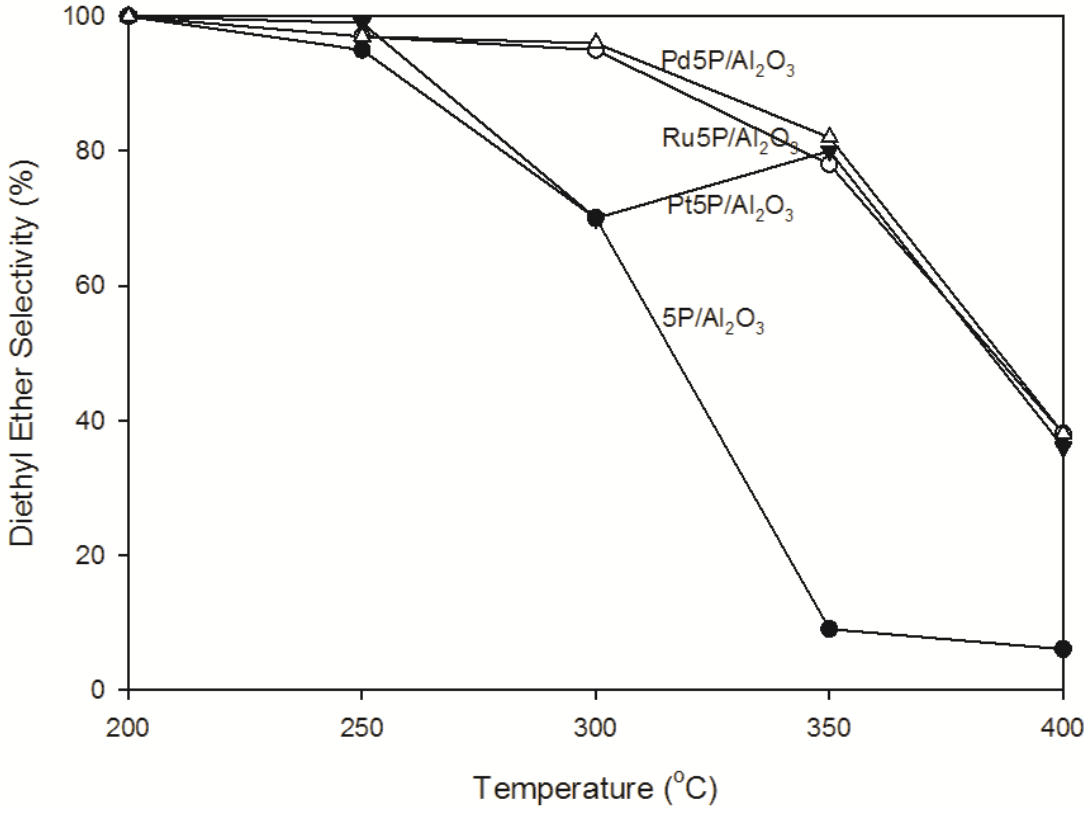

Figure 39 Diethyl ether selectivity of 5P/Al_2O_3 and noble metal modified 5P/Al_2O_3 catalysts

Figure 39 shows diethyl ether selectivity among all studied catalysts. According to the diethyl ether selectivity results, the selectivity towards diethyl ether of all catalysts found to be decreased as the raising in temperature. The diethyl

ether selectivity of all catalysts seemed to have a similar amount at all studied temperature, despite of Pt5P/Al_2O_3 catalyst which had significantly lower diethyl ether selectivity than other catalysts at 300°C. From the comparison of diethyl ether selectivity between noble metal modified and non-modified on 5P/Al_2O_3 catalysts, it can be summarized that the addition of noble metal could escalate the selectivity towards diethyl ether, significantly at high temperature (350 to 400°C).

Yield of diethyl ether was also calculated and shown in **Figure 40** as follows;

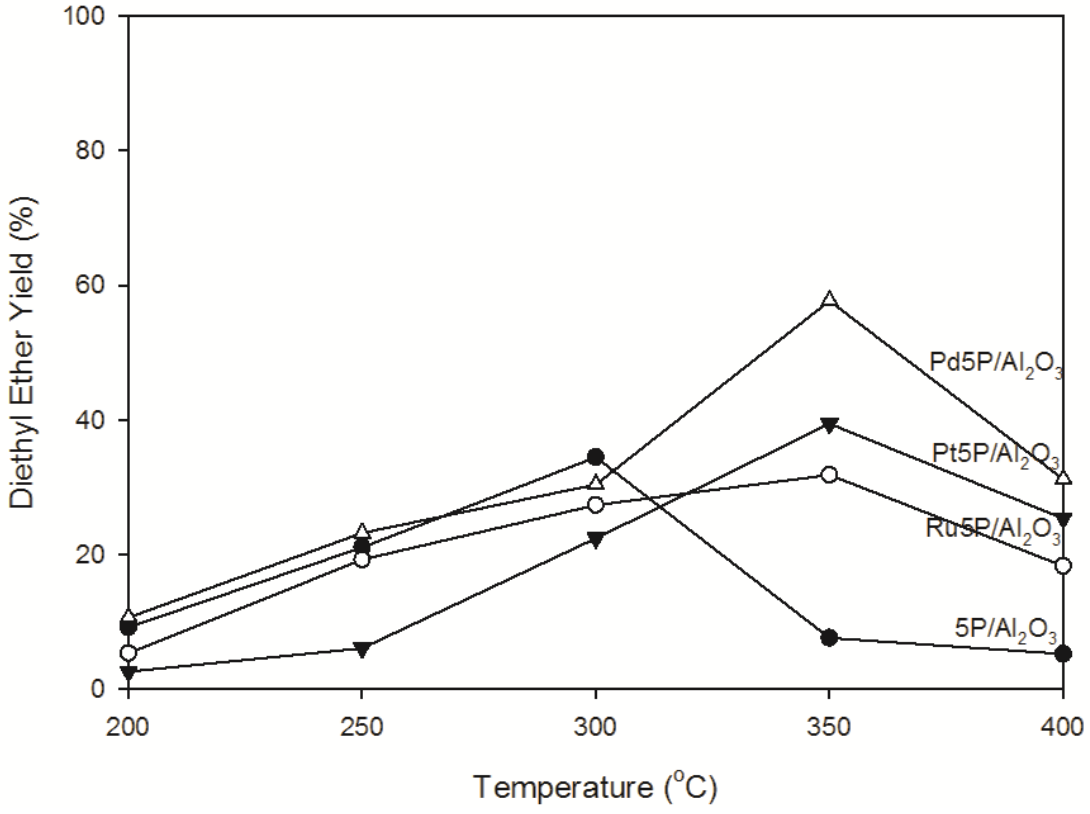

Figure 40 Diethyl ether yield of 5P/Al_2O_3 and noble metal modified 5P/Al_2O_3 catalysts

From diethyl ether yield specified in **Figure 40**, it can be noticed that at temperature of 350°C all of studied catalyst had the highest diethyl ether yield when compared to other studied temperatures. These occurred phenomena were because

diethyl ether yields were calculated from the multiplied terms between ethanol conversion and diethyl ether selectivity. Consequently, at 350°C, which had not much low diethyl ether selectivity compared to the temperature of 200-300°C and had slightly less ethanol conversion than the temperature of 400°C, would had the highest diethyl ether yield among other temperatures. While the noble metal modified 5P/Al_2O_3 catalysts had diethyl ether yield of 57.68% at high temperature (350 to 400°C), the 5P/Al_2O_3 catalyst had the diethyl ether yield of 34.41% when examined in low temperature (200 to 300°C). While the performance noble metal modified on diethyl ether yield was considered, it was found that palladium modified had the highest yield though all catalyst which its diethyl ether yield was 57.68% at 350°C.

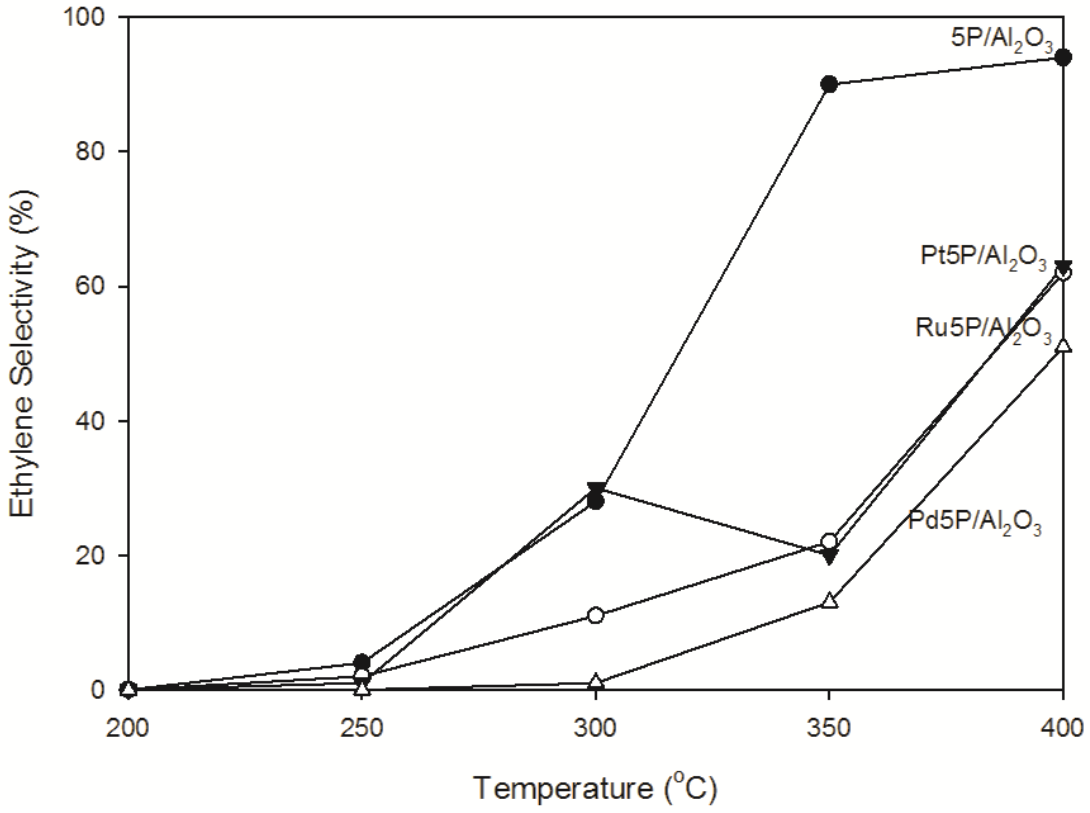

Figure 41 Ethylene selectivity of 5P/Al_2O_3 and noble metal modified 5P/Al_2O_3 catalysts

Figure 41 displays the selectivity towards ethylene of noble metal modified 5P/Al_2O_3 catalysts. It was found that the trend of ethylene selectivity was contrast with diethyl ether selectivity or it can be said that when increased the reaction temperature, ethylene selectivity was increased. At all studied temperature, Pd5P/Al_2O_3 catalyst tended to show lower ethylene selectivity than other catalysts. While Pt5P/Al_2O_3 and Ru5P/Al_2O_3 catalysts seemed to have similar amount of ethylene selectivity, despite of the ethylene selectivity of Pt5P/Al_2O_3 catalyst at 300°C had the highest specific selectivity among other catalysts at its specified temperature. In other words, the ethylene selectivity of 5P/Al_2O_3 catalyst tended to have higher ethylene selectivity than that of all noble metal modified 5P/Al_2O_3 catalysts in every studied temperature.

The ethylene yield of all noble metal modified 5P/Al_2O_3 catalysts is described in **Figure 42** as follows;

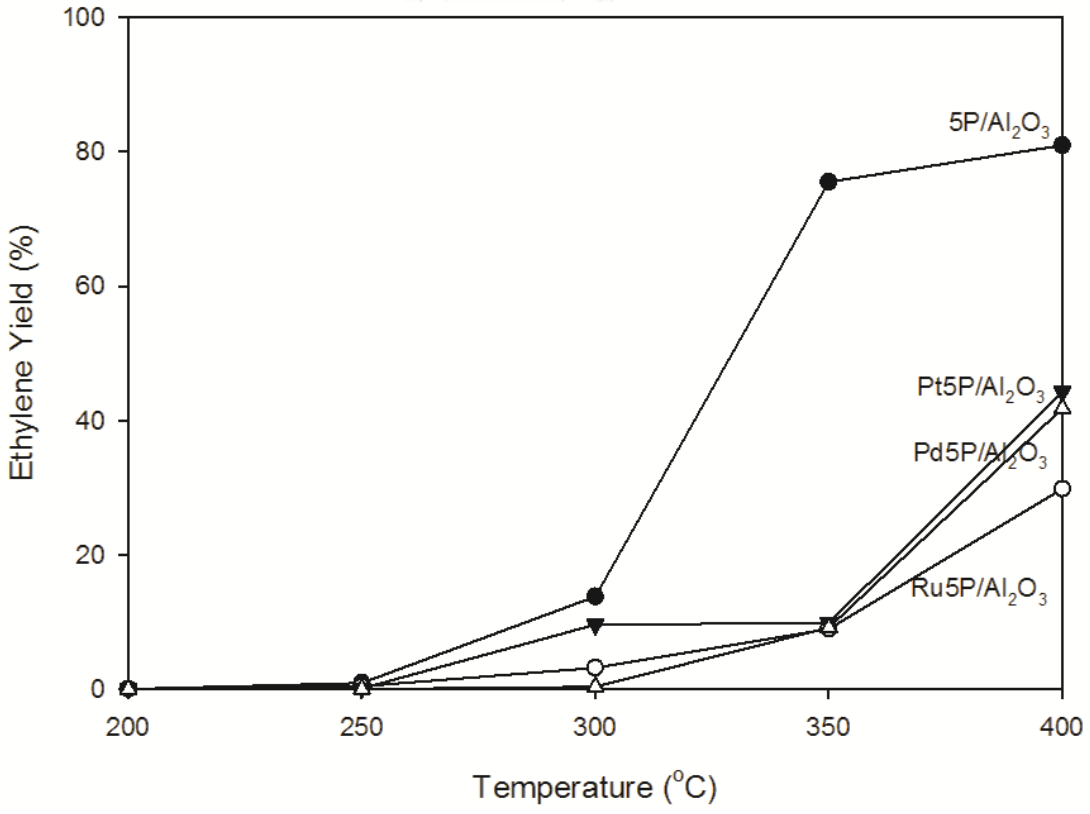

Figure 42 Ethylene yield of 5P/Al_2O_3 and noble metal modified 5P/Al_2O_3 catalysts

From the calculated ethylene yield of all catalysts which is illustrated in **Figure 42**, the overview of ethylene yield at all interested temperature including **Part I** result can be ordered as follows: $5P/Al_2O_3$>$Pt5P/Al_2O_3$>$Pd5P/Al_2O_3$>$Ru5P/Al_2O_3$. In this part, it was found that when considered about noble metal modified on $5P/Al_2O_3$ catalysts, the temperature of 400°C is the most suitable temperature to use $Pt5P/Al_2O_3$ as the catalyst to produce ethylene from ethanol dehydration reaction. At 300°C, the ethylene yield of $Pt5P/Al_2O_3$ catalysts found to be significantly higher than using other noble metal modified on $5P/Al_2O_3$ catalysts.

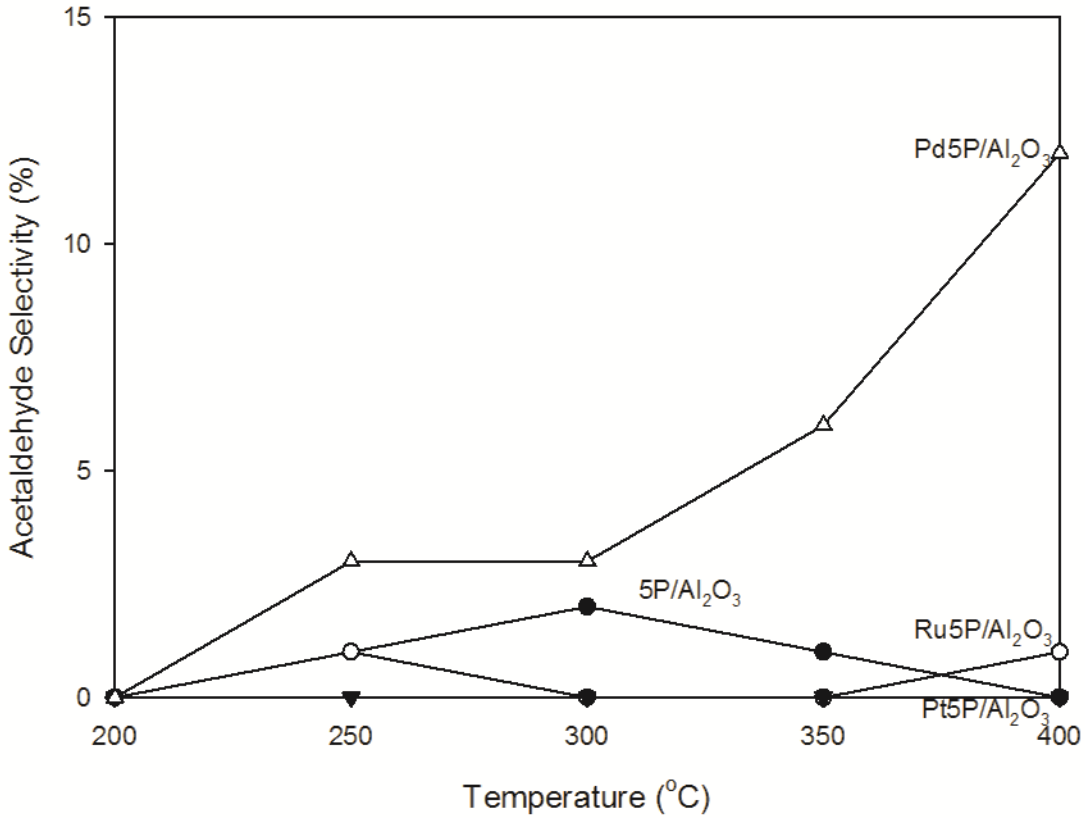

Figure 43 Acetaldehyde selectivity of $5P/Al_2O_3$ and noble metal modified $5P/Al_2O_3$ catalysts

When considered acetaldehyde selectivity of all catalysts presented in **Figure 43**, it was observed that platinum modified catalyst had the lowest selectivity

towards acetaldehyde. However, palladium modified catalyst tended to have higher acetaldehyde selectivity than other studied catalysts. The acetaldehyde selectivity trend of $Pd5P/Al_2O_3$ was increased as an increasing in reaction temperature. Furthermore, $Pd5P/Al_2O_3$ was increased reach 11% of acetaldehyde selectivity at 400°C.

Both acetaldehyde selectivity and ethanol conversion were brought to determine acetaldehyde yield which is shown in **Figure 44** as follows;

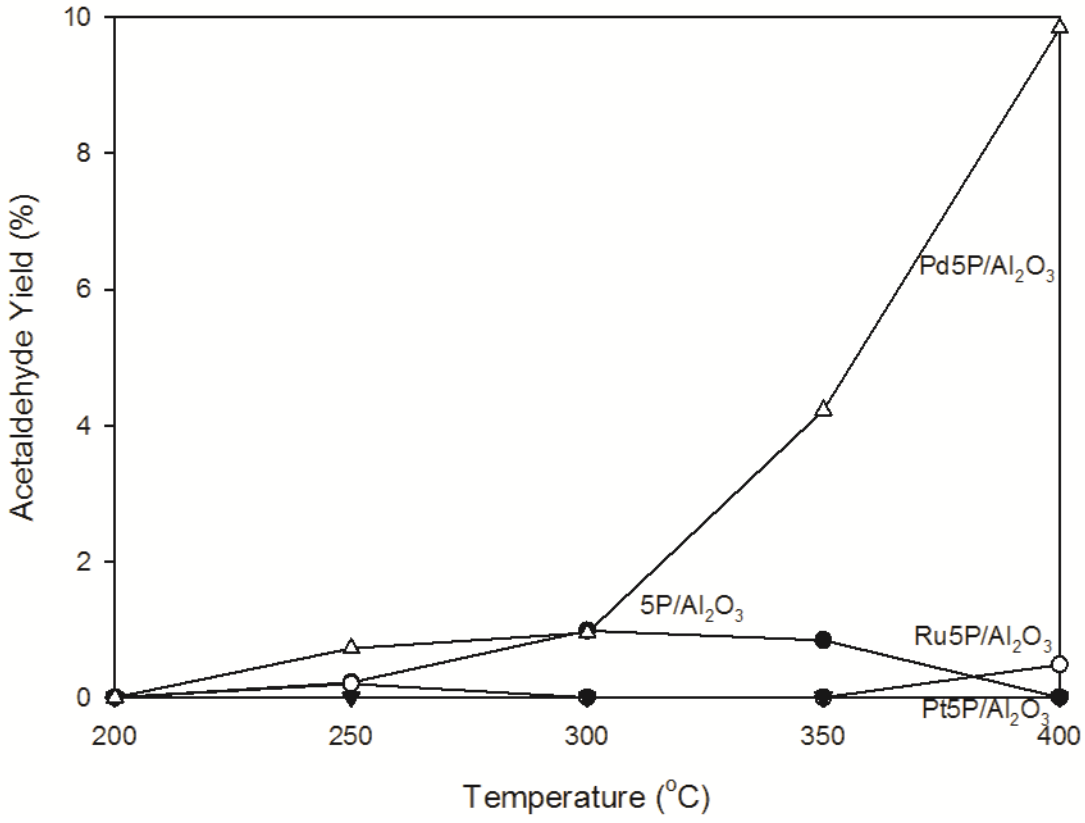

Figure 44 Acetaldehyde yield of $5P/Al_2O_3$ and noble metal modified $5P/Al_2O_3$ catalysts

From acetaldehyde yield results, it was found that the modification of $5P/Al_2O_3$ catalysts with ruthenium and platinum cannot increase the acetaldehyde yield from **Part II** results. However, when modified palladium on $5P/Al_2O_3$, the

acetaldehyde yield was improved reaching 9.02% at 400°C. Therefore, it can be concluding that Pd5P/Al_2O_3 not only suitable to produce diethyl ether, but also can use to produce acetaldehyde.

5.2.8 Thermal gravimetric and differential thermal analysis (TG/DTA)

The noble metals including Ru, Pt and Pd, which were added into 5P/Al_2O_3 catalyst as the promoter were all brought to investigate the decomposition of catalysts by increasing the temperature of the samples under air atmosphere. Both fresh and spent catalysts through the dehydration of ethanol were brought to analyze and show in **Figure 45** and **Figure 46** as follows;

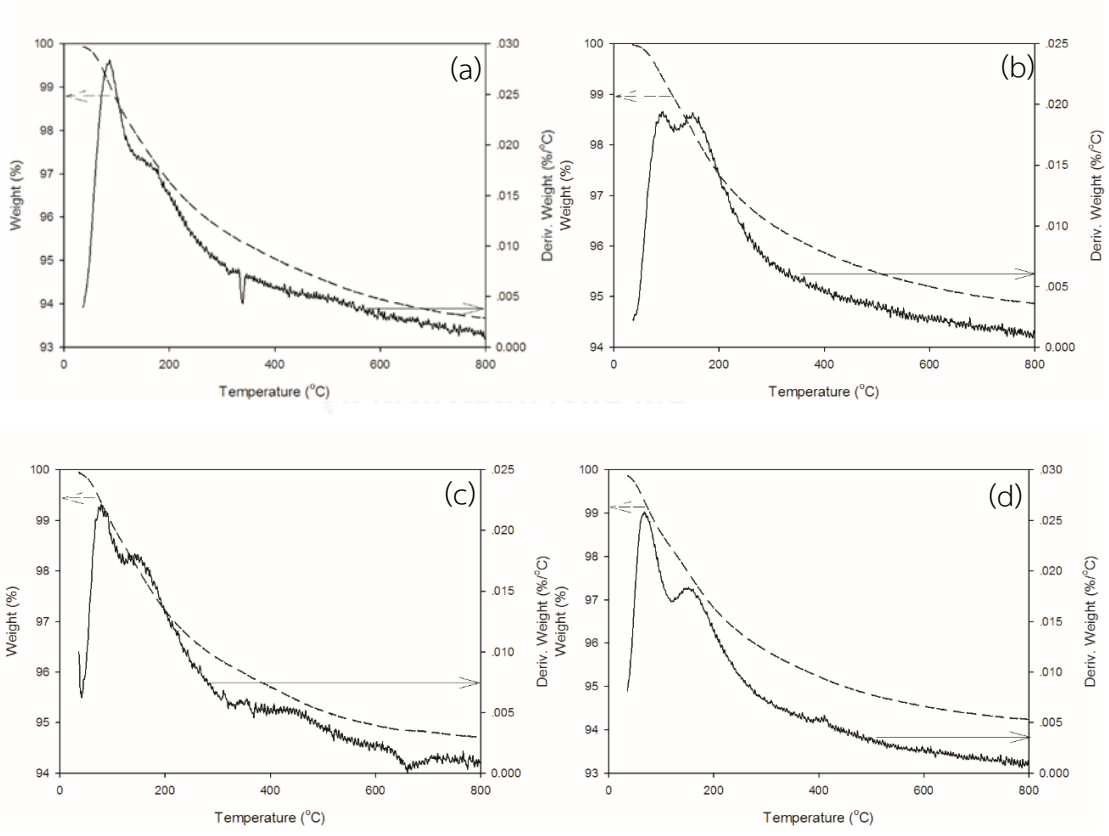

Figure 45 TG/DTA analysis of the fresh catalysts;
(a) 5P/Al_2O_3 (b) Ru5P/Al_2O_3 (c) Pt5P/Al_2O_3 (d) Pd5P/Al_2O_3

The results of all fresh catalysts were observed two main losing weight stages which were at temperature below 200°C and temperature above 200°C. At the temperature lower than 200°C, the results exhibited the moisture peak in all catalysts. While at the temperature above 200°C, it was found that there was the decomposition of volatile species in the catalyst.

The spent catalysts results which are all shown in **Figure 46** describe the characteristics of catalyst including amount of coke formation through thermal decomposition technique as follows;

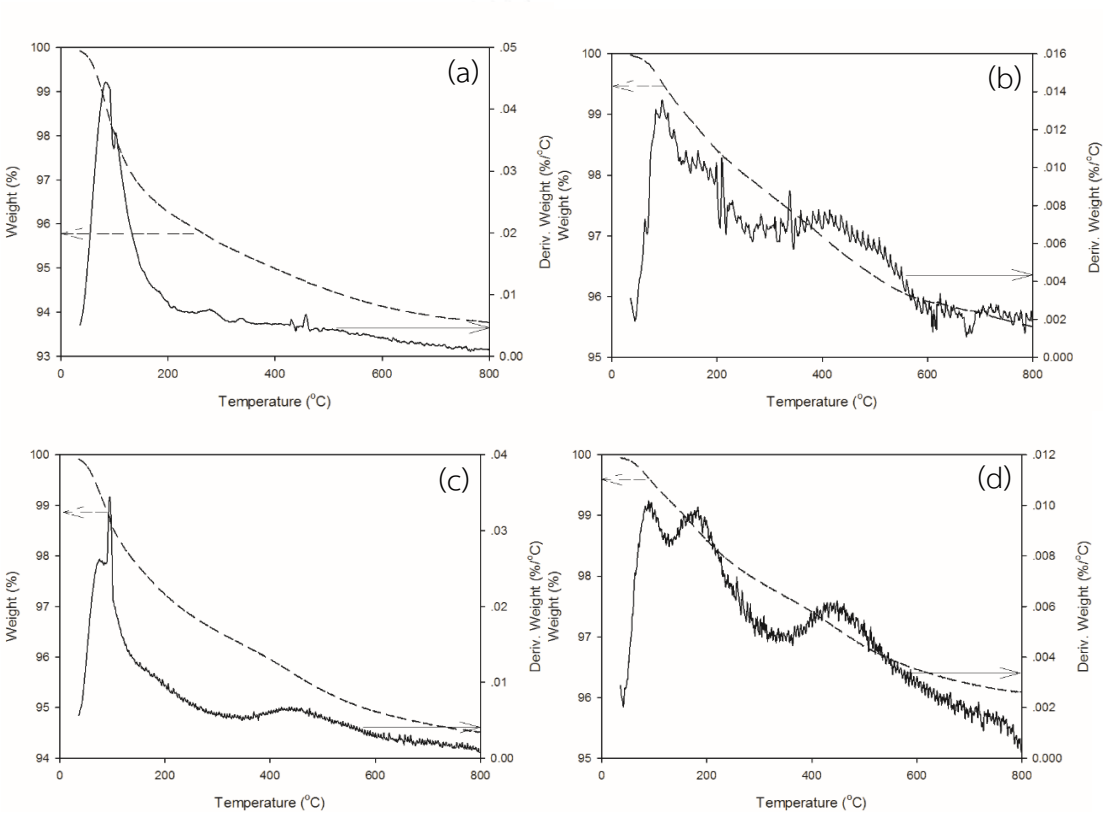

Figure 46 TG/DTA analysis of the spent catalysts;
(a) 5P/Al_2O_3 (b) Ru5P/Al_2O_3 (c) Pt5P/Al_2O_3 (d) Pd5P/Al_2O_3

The thermal decomposition of spent catalyst showed the higher decomposition in the temperature range of higher than 200°C, which indicated that the coke formation on the catalyst surface can be removed in this temperature range. Therefore, in order to regenerate the spent catalyst, the catalyst would be

brought to burn in air atmosphere in the temperature range higher than 200°C. The estimation of coke formation amount on the catalysts surface was investigated and displayed in **Table 23** as follows;

Table 23 The amount of coke formation in the used catalysts

Catalysts	Temperature (°C)	Weight (%)	The amount of coke formation (%)
5P/Al_2O_3	200	96.28	2.51
	800	93.77	
Ru5P/Al_2O_3	200	98.41	2.91
	800	95.50	
Pt5P/Al_2O_3	200	97.23	2.72
	800	94.51	
Pd5P/Al_2O_3	200	98.58	2.50
	800	96.08	

5.2.9 Catalyst appearance

The 5P/Al_2O_3 catalyst which exhibited the best catalytic performance in **Part I** was brought to modify by adding the noble metal including Ru, Pt and Pd using incipient wetness impregnation. After finished catalyst preparation, the resulting catalysts were brought to observe the appearance of catalysts. The appearances of each catalyst in forms fresh and spent catalysts in the reaction are shown in **Figure 47** and **Figure 48**, respectively.

Considering the fresh 5P/Al_2O_3 catalysts modified with different types of noble metal (Ru, Pt and Pd) shown in **Figure 46**, all catalysts including Ru5P/Al_2O_3, Pt5P/Al_2O_3 and Pd5P/Al_2O_3 were observed to have dark gray, light gray and yellow-brown color, respectively.

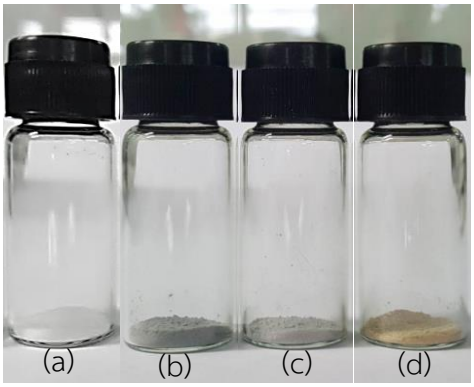

Figure 47 The fresh appearance of noble metal modified 5P/Al_2O_3 catalysts; (a) 5P/Al_2O_3 (b) Ru5P/Al_2O_3 (c) Pt5P/Al_2O_3 (d) Pd5P/Al_2O_3

When using the studied catalysts in the reaction, the appearance of spent catalysts was changed into other colors, where these catalyst appearances are all illustrated in **Figure 47** as follows;

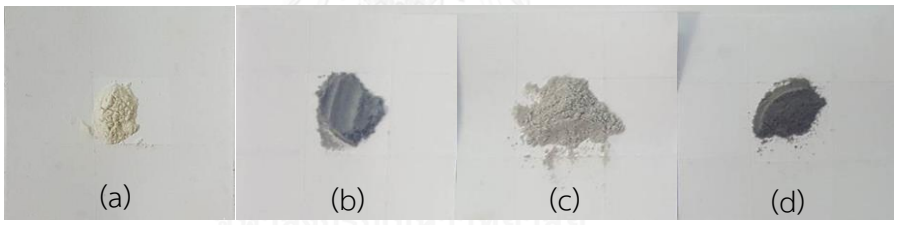

Figure 48 The appearance of spent noble metal modified 5P/Al_2O_3 catalysts; (a) 5P/Al_2O_3 (b) Ru5P/Al_2O_3 (c) Pt5P/Al_2O_3 (d) Pd5P/Al_2O_3

From the appearance of spent catalysts depict in **Figure 48**, it was found that colors of Ru5P/Al_2O_3 and Pt5P/Al_2O_3 catalysts were slightly changed into the darker color. Nevertheless, Pd5P/Al_2O_3 was found to have a significantly changed in color by changing the color of yellow-brown into dark gray color. However, the lowest coke formation amount was obtained from DG/TGA result, it can be suggested that using Pd as the noble metal to modify the catalyst could brought about the change in catalyst structure. Therefore, the spent Pd5P/Al_2O_3 catalyst had the color change.

Part III : The comparison of the catalytic post-reaction properties and catalytic performance in time on stream system between Al_2O_3 supports, P-modified Al_2O_3 catalyst and the noble metal modified P/Al_2O_3 catalyst which was observed the highest diethyl ether yield.

The $5P/Al_2O_3$ and $Pd5P/Al_2O_3$ catalysts were chosen as the representative catalysts having the highest diethyl ether yield in **Part I** and **Part II**, respectively. Therefore, these two catalysts were brought to compare the characteristics and catalytic activities with Al_2O_3 supports in time on stream system for 10 h. The studies of spent catalysts characteristic described in **Part III** are including X-ray diffraction and thermal gravimetric and differential thermal analysis.

5.3.1 Reaction study in time on stream system

The Al_2O_3 supports, $5P/Al_2O_3$ and $Pd5P/Al_2O_3$ catalysts were all studied via time on stream system at their most suitable condition as described in **Figure 49** and **Figure 50**.

In **Figure 49**, the ethanol conversion of these three catalysts was investigated through ethanol dehydration reaction for 10 h. The results were found that at the beginning of the reaction study, the ethanol conversion of all catalysts had a similar value. As an increase of reaction time, $Pd5P/Al_2O_3$ showed the significant enhancement in ethanol conversion. While both Al_2O_3 supports and $5P/Al_2O_3$ showed less ethanol conversion enhancement. In addition, it could be observed that both Al_2O_3 supports and $5P/Al_2O_3$ catalyst demonstrated the similar ethanol conversion throughout 10 h of reaction study.

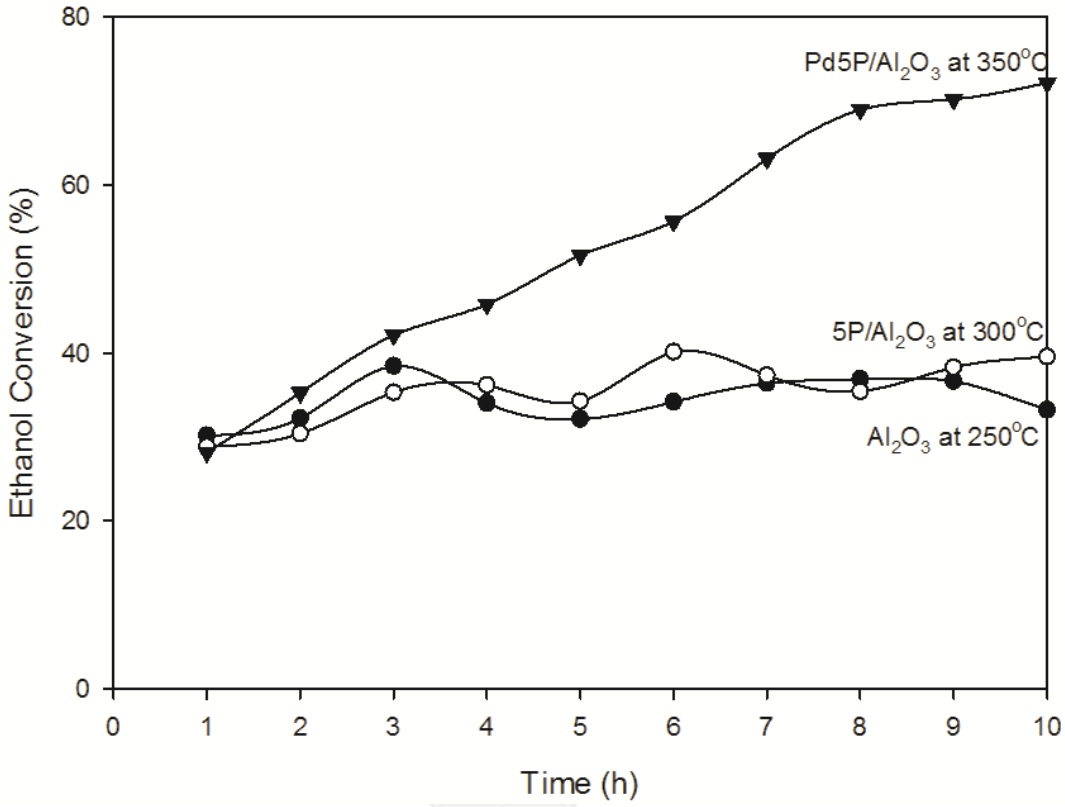

Figure 49 Ethanol conversion of Al_2O_3 used at 250°C, 5P/Al_2O_3 used at 300°C and Pd5P/Al_2O_3 used at 350°C

The diethyl ether yield of each catalyst through time on stream system was picked up as the most interesting consideration, which is illustrated in **Figure 50** as follows;

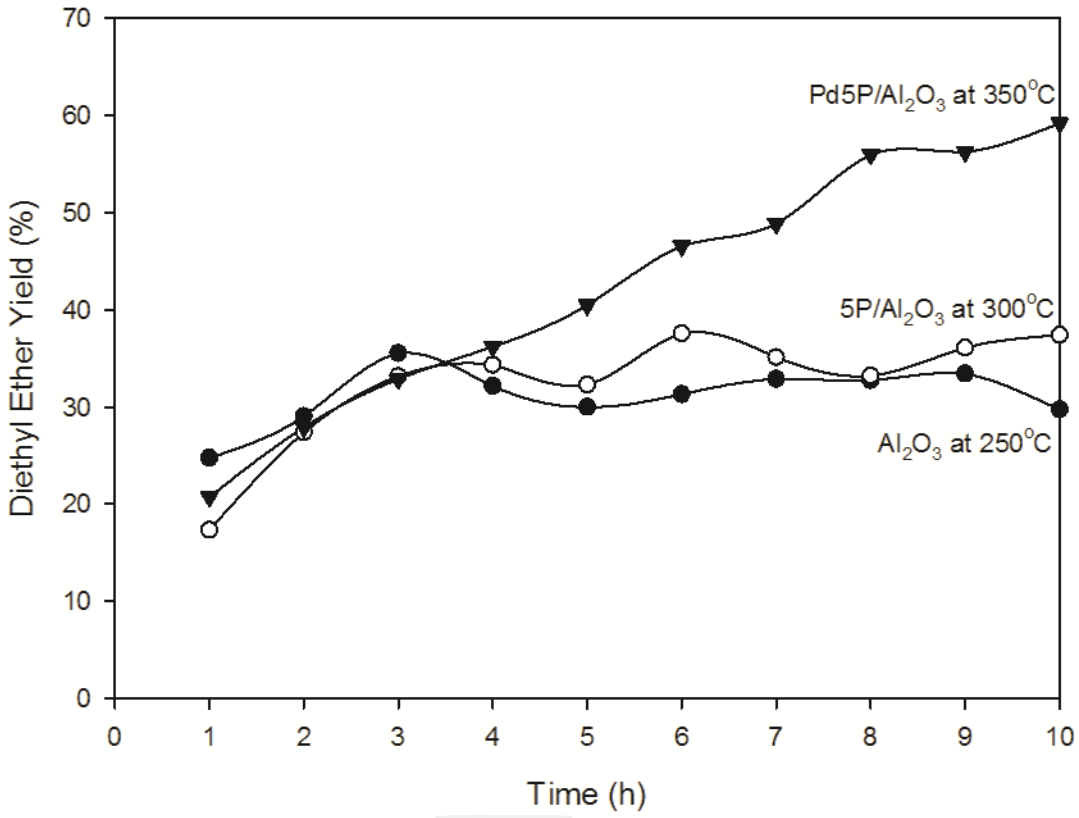

Figure 50 Diethyl ether yield of Al_2O_3 used at 250°C, 5P/Al_2O_3 used at 300°C and Pd5P/Al_2O_3 used at 350°C

Diethyl ether yield of all studied catalysts at its suitable temperature was reported as the function of time. The results were found to have the similar trend as ethanol conversion depicted in **Figure 50**. From the results, it was found that Pd5P/Al_2O_3 catalyst, which was studied at 350°C exhibited the highest diethyl ether yield since using through the reaction for 4 h and reached 59.20% of diethyl ether yield when it was used for 10 h. The average of diethyl ether yield through 10 h of the reaction study of each catalyst is reported in **Table 24** as follows;

Table 24 Average diethyl ether yield obtained from Al_2O_3 used at 250°C, 5P/Al_2O_3 used at 300°C and Pd5P/Al_2O_3 used at 350°C (10 h)

Catalysts	Average Diethyl Ether Yield in 10 h (%)
Al_2O_3 used at 250°C	31.17
5P/Al_2O_3 used at 300°C	32.40
Pd5P/Al_2O_3 used at 350°C	42.50

5.3.2 X-ray diffraction (XRD)

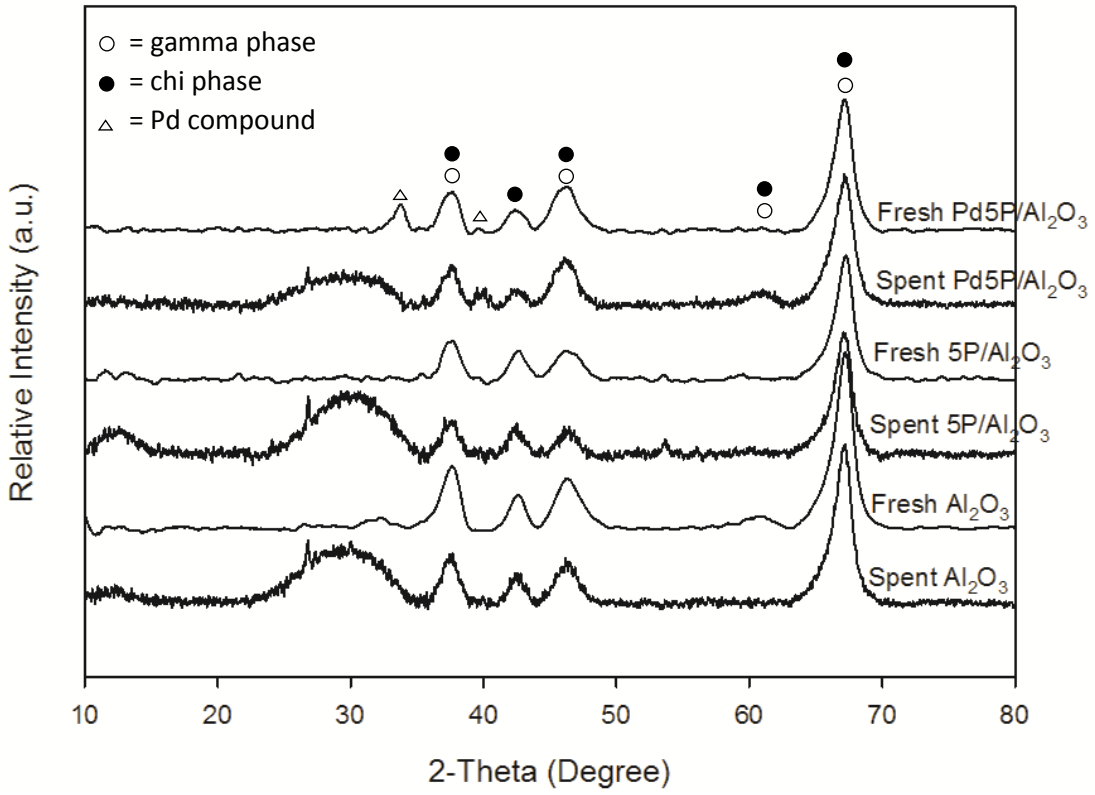

Figure 51 XRD patterns of fresh and spent catalyst including Al_2O_3 (using at 250°C), 5P/Al_2O_3 (using at 300°C) and Pd5P/Al_2O_3 (using at 350°C)

Figure 51 displays XRD patterns of fresh and spent catalysts where the spent Al_2O_3 catalyst was used at 250°C, spent 5P/Al_2O_3 was used at 300°C and spent

Pd5P/Al_2O_3 catalyst was used at 350°C. XRD patterns of all catalysts were detected both γ- and χ-phase of alumina supports as already described in **Part I**. The XRD patterns of P-modified catalysts were not observed the phosphorus species in the catalyst. This can be ascribed that phosphorus species had small crystalline size or well dispersed thoroughly on alumina supports. When considered the palladium modified on 5P/Al_2O_3 catalyst, the palladium species were detected in XRD patterns at 2θ of 33.5° and 40° [44]. In other words, when considered the difference between XRD patterns of each fresh and spent catalyst, it was found that broad XRD patterns of carbon at 2θ of 27° was observed, which is according to Lina Han et al. research [44]. This is confirmed that there is the formation of coke on the surface of all spent catalysts.

5.3.3 Thermal gravimetric and differential thermal analysis (TG/DTA)

The decomposition of chosen catalysts after spent in the reaction had been studied through thermal gravimetric and differential thermal analysis (TG/DTA). The thermal decomposition trend of each catalyst is presented in **Figure 52** as follows;

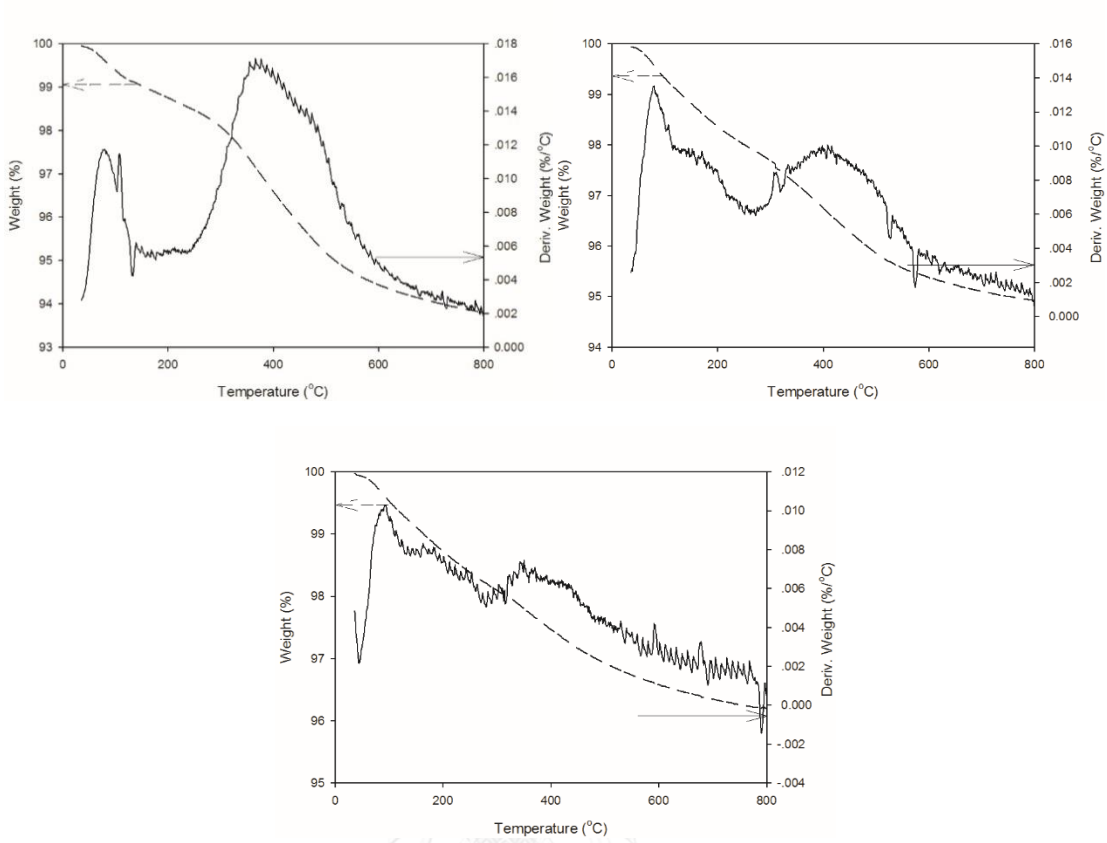

Figure 52 TG/DTA analysis of the post-reaction catalysts;
(a) Al_2O_3 used at 250°C (b) 5P/Al_2O_3 used at 300°C (c) Pd5P/Al_2O_3 used at 350°C

From all of the catalysts results, there were two stages of thermal decomposition, which are at temperature range lower than 200°C and temperature range higher than 200°C. Considering at temperature below 200°C, the decomposition of all catalysts was found due to from water elimination. However, at temperature range above 200°C, the decomposition was found due to coke disposition. Furthermore, it was found that when ordering the amount of coke found on catalyst surface from high to low amount, the Al_2O_3 supports had the highest amount of coke followed by 5P/Al_2O_3 and Pd5P/Al_2O_3 catalyst, respectively. The amount of coke formation in the temperature of 200 to 800°C was all described in **Table 25** as follows;

Table 25 The amount of coke formation in the spent catalysts

Catalysts	Temperature (°C)	Weight (%)	The amount of coke formation (%)
Al_2O_3 used in temperature programmed	200	96.76	4.56
	800	92.20	
Al_2O_3 used at 250°C	200	98.75	4.95
	800	93.80	
5P/Al_2O_3 used in temperature programmed	200	96.28	2.51
	800	93.77	
5P/Al_2O_3 used at 300°C	200	98.36	3.43
	800	94.93	
Pd5P/Al_2O_3 used in temperature programmed	200	98.58	2.50
	800	96.08	
Pd5P/Al_2O_3 used at 350°C	200	98.72	2.52
	800	96.20	

Part IV : Comparison of the characteristics and catalytic activity between the chosen noble metal modified Al_2O_3 catalyst and the chosen noble metal modified P/Al_2O_3 catalyst.

From the results in **Part I** and **Part II**, $Pd5P/Al_2O_3$ catalyst exhibited the highest diethyl ether yield among all of the studied catalysts. Thus, the palladium modified on alumina catalyst was synthesized as the reference in order to compare the catalyst properties and its activities with $Pd5P/Al_2O_3$ catalyst. The characteristics and catalytic performance of both Pd/Al_2O_3 and $Pd5P/Al_2O_3$ catalysts are reported in **Topic 5.4.1** to **5.4.5** as follows;

5.4.1 Inductively coupled plasma (ICP)

The studied catalysts including Pd/Al_2O_3 and $Pd5P/Al_2O_3$ were brought to estimate the palladium contained in the catalyst bulk by inductively coupled plasma (ICP). The amount of palladium contained in each sample is shown in **Table 26** as follows;

Table 26 The amount of palladium contained in the catalysts bulk

Catalysts	Amount of Pd in catalyst bulk (wt%)
Pd/Al_2O_3	0.3
$Pd5P/Al_2O_3$	0.2

5.4.2 X-ray diffraction (XRD)

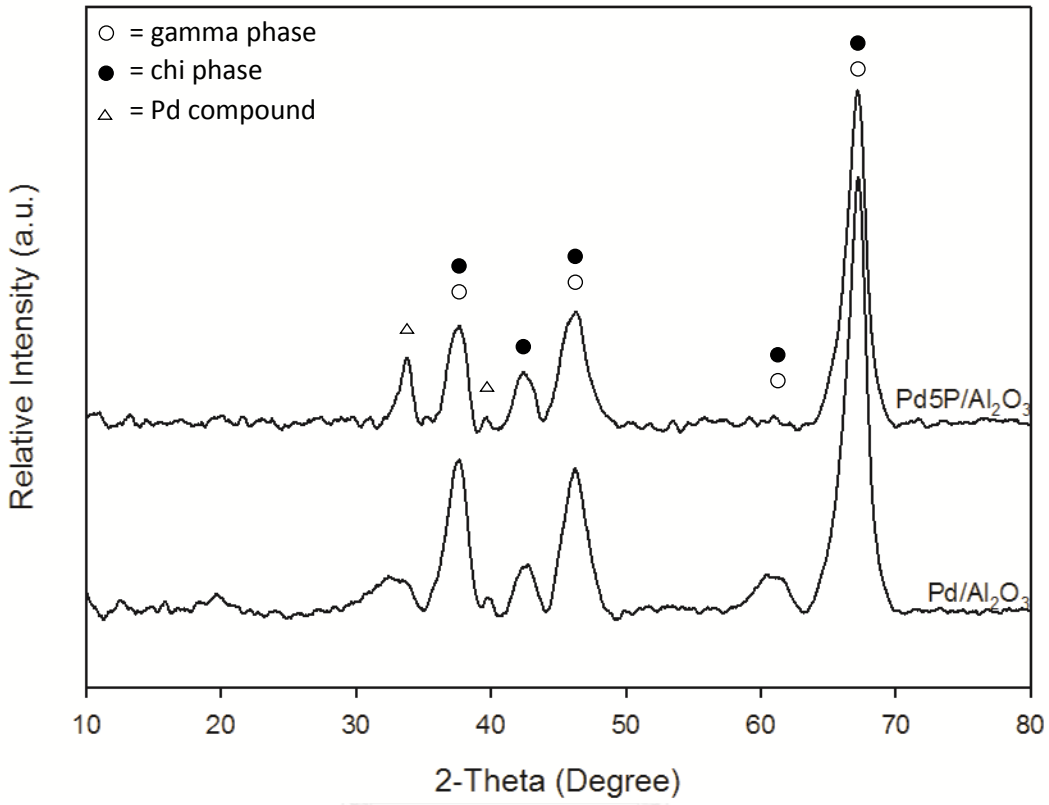

Figure 53 XRD patterns of Pd/Al_2O_3 and $Pd5P/Al_2O_3$ catalysts

XRD patterns of the investigating catalysts, which are Pd/Al_2O_3 and $Pd5P/Al_2O_3$ are all depicted in **Figure 53**. The results showed similar XRD patterns with the results in **Part I** and **Part II**. XRD patterns of two catalysts were specified for both γ- and χ-phase of alumina supports as described in **Part I** and also detected palladium in XRD patterns at the same 2θ as **Part II**. Furthermore, it was not detected any phosphorus species in $Pd5P/Al_2O_3$ catalyst; however, there were 5 wt% of phosphorus contained in bulk $Pd5P/Al_2O_3$ as shown in **Topic 5.4.1**. This can be suggested that the phosphorus species were dispersed well on $Pd5P/Al_2O_3$ catalyst or had a small size of crystalline phase.

5.4.3 Ammonia temperature-programmed desorption (NH_3-TPD)

The acid strength of all studied catalysts was investigated through NH_3-TPD technique. The NH_3-TPD profiles of Pd/Al_2O_3 and $Pd5P/Al_2O_3$ catalysts were found to have two desorption peaks. Moreover, it was noticed that the existence of phosphorus in Pd/Al_2O_3 catalyst tended to increase the acid strength of the catalyst by raising both medium to strong acid site and weak acid site of the catalyst.

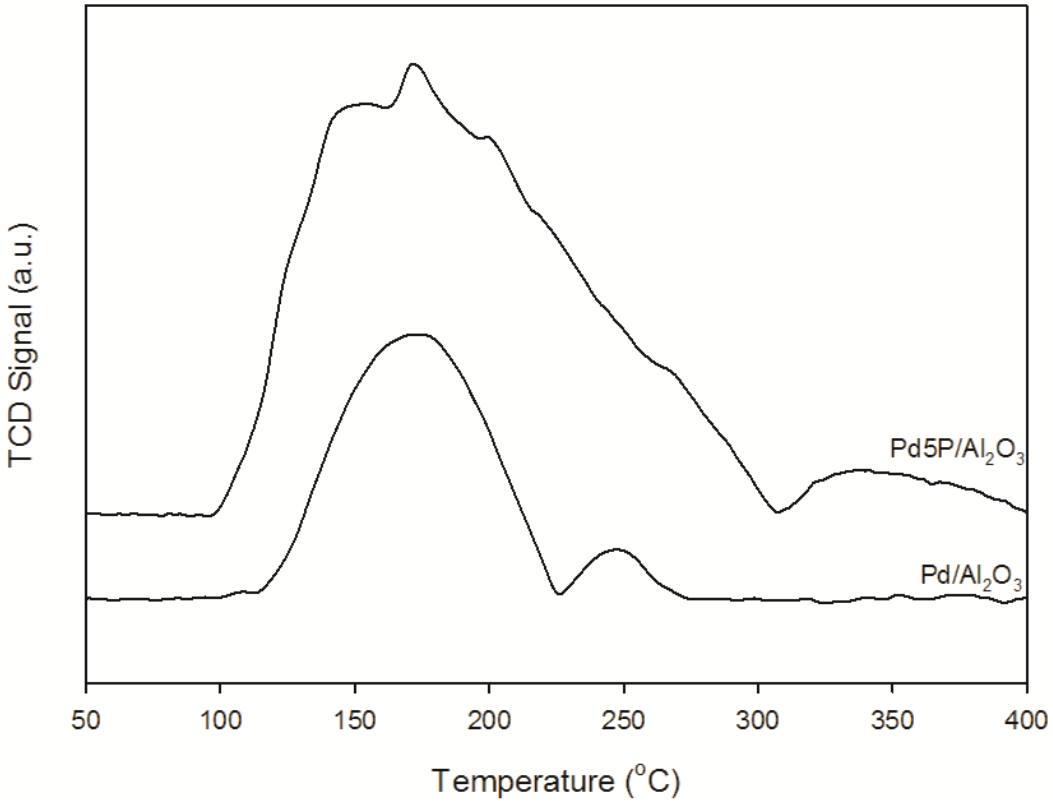

Figure 54 NH_3-TPD profiles of the Pd/Al_2O_3 and $Pd5P/Al_2O_3$ catalysts

The amount of total acid site of catalysts is all reported in **Table 27** as follows;

Table 27 The amount of acidity of Pd/Al_2O_3 and $Pd5P/Al_2O_3$ catalysts

Catalysts	NH_3 desorption total acidity (μmol/g cat.)
Pd/Al_2O_3	1310
$Pd5P/Al_2O_3$	2060

From the acidity results of all catalysts, the total acidity of phosphorus contained catalyst was higher than the non-phosphorus contained one. Therefore, it can be concluded and confirms the results of **Part I**, which was described that the modification of phosphorus could enhance the acidity of the catalyst.

5.4.4 Reaction study

The catalytic performance of both Pd/Al_2O_3 and $Pd5P/Al_2O_3$ catalysts were also determined via ethanol dehydration reaction at reaction temperature of 200, 250, 300, 350 and 400°C. Terms of catalytic activity including ethanol conversion, selectivity towards interested products and products yield were investigated in this part and depicted in **Figure 55** to **Figure 61**.

The steady state ethanol conversion of these two catalysts is displayed in **Figure 55** as follows;

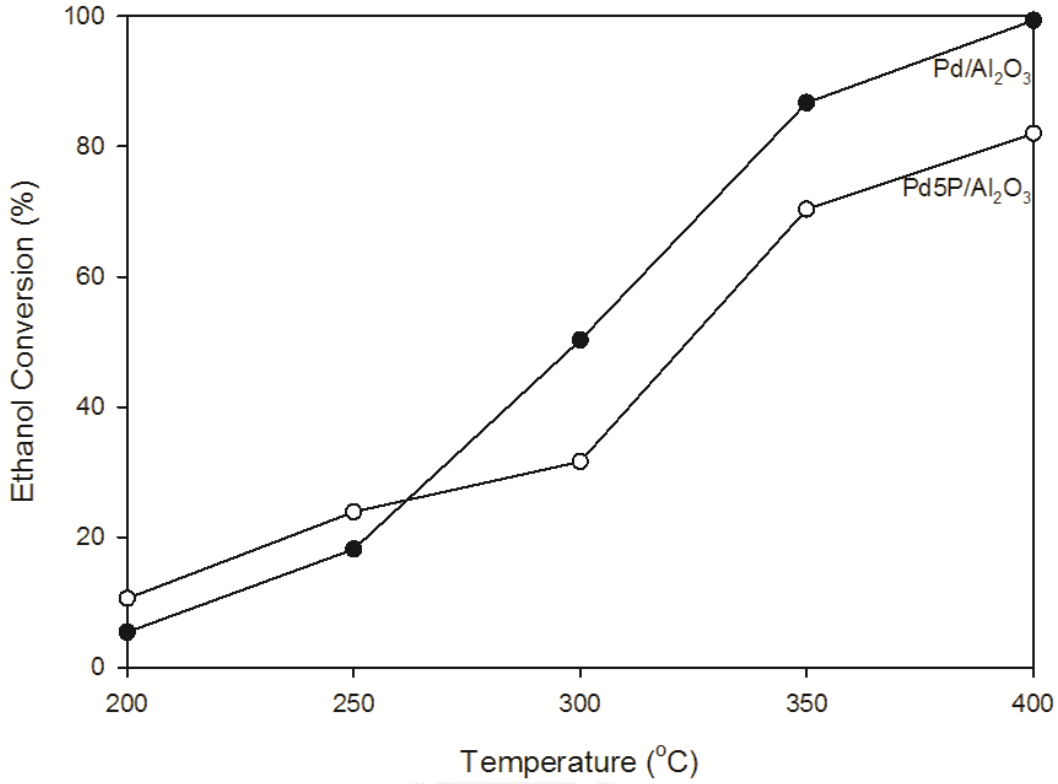

Figure 55 Ethanol conversion of Pd/Al_2O_3 and $Pd5P/Al_2O_3$ catalysts

From the ethanol conversion result above, it was found that the conversion of ethanol of these two catalysts was escalated when increased reaction temperature. At low reaction temperature of 200 to 250°C, Pd/Al_2O_3 catalyst tended to have slightly lower ethanol conversion than $Pd5P/Al_2O_3$ catalyst. On the other hand, the Pd/Al_2O_3 catalyst showed higher ethanol conversion than $Pd5P/Al_2O_3$ catalyst when used at high reaction temperature (300 to 400°C) and reached 99.35% of ethanol conversion at 400°C, while the Pd/Al_2O_3 catalyst gave the highest ethanol conversion of 81.97% at the same reaction temperature. This result was corresponding to the conversion of ethanol in **Part I**, which was found that the addition of phosphorus tended to have a negative effect on the ethanol conversion.

Reaction rate of the studied catalysts was calculated, and then is described in **Table 28** as follows;

Table 28 Rate of reaction of Pd/Al_2O_3 and $Pd5P/Al_2O_3$ catalysts

Catalysts	Rate of Reaction $\times 10^2$ (mole ethanol/g cat. h)				
	200°C	250°C	300°C	350°C	400°C
Pd/Al_2O_3	2.80	8.46	21.36	33.89	35.96
$Pd5P/Al_2O_3$	5.46	11.12	13.44	27.50	29.67

The result of studied catalysts reaction rate exhibited the similar trend as the results in **Part I** and **Part II** where the rate of reaction of all catalysts was found to increase as increasing reaction temperature. Moreover, because of a significant increase in ethanol conversion of Pd/Al_2O_3 catalyst, the Pd/Al_2O_3 catalyst was found to have higher rate of reaction than the $Pd5P/Al_2O_3$ catalyst especially at high reaction temperature (300 to 400°C).

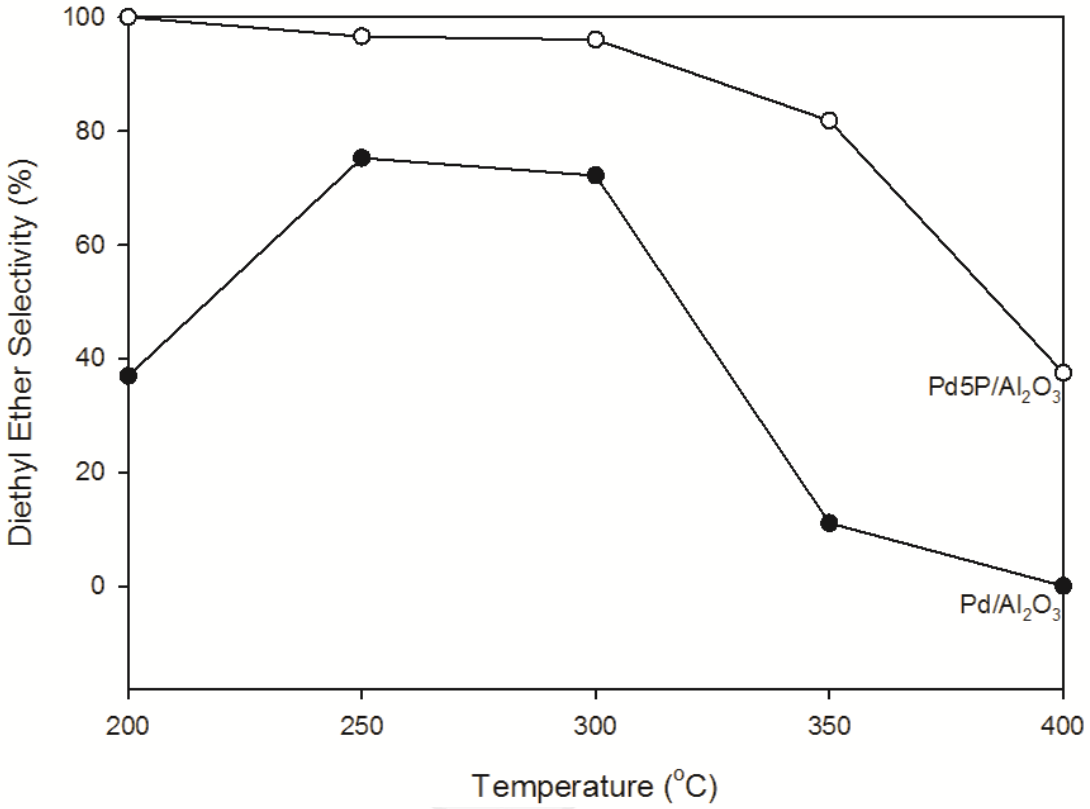

Figure 56 Diethyl ether selectivity of Pd/Al_2O_3 and $Pd5P/Al_2O_3$ catalysts

Figure 56 represents the diethyl ether selectivity of all studied catalysts. The result found that the modification of phosphorus could lead the catalyst to exhibit higher selectivity towards diethyl ether. The diethyl ether curve of all catalysts were decreased as raising in reaction temperature, excepting for the diethyl ether selectivity of Pd/Al_2O_3 catalyst at temperature of 200°C, which was lower at temperature of 250 to 300°C. This can be suggested that the reaction path way of Pd/Al_2O_3 catalyst at temperature of 200°C was shifted to generate acetaldehyde instead of diethyl ether.

Diethyl ether yield of each catalyst was calculated and specified in **Figure 57** as follows;

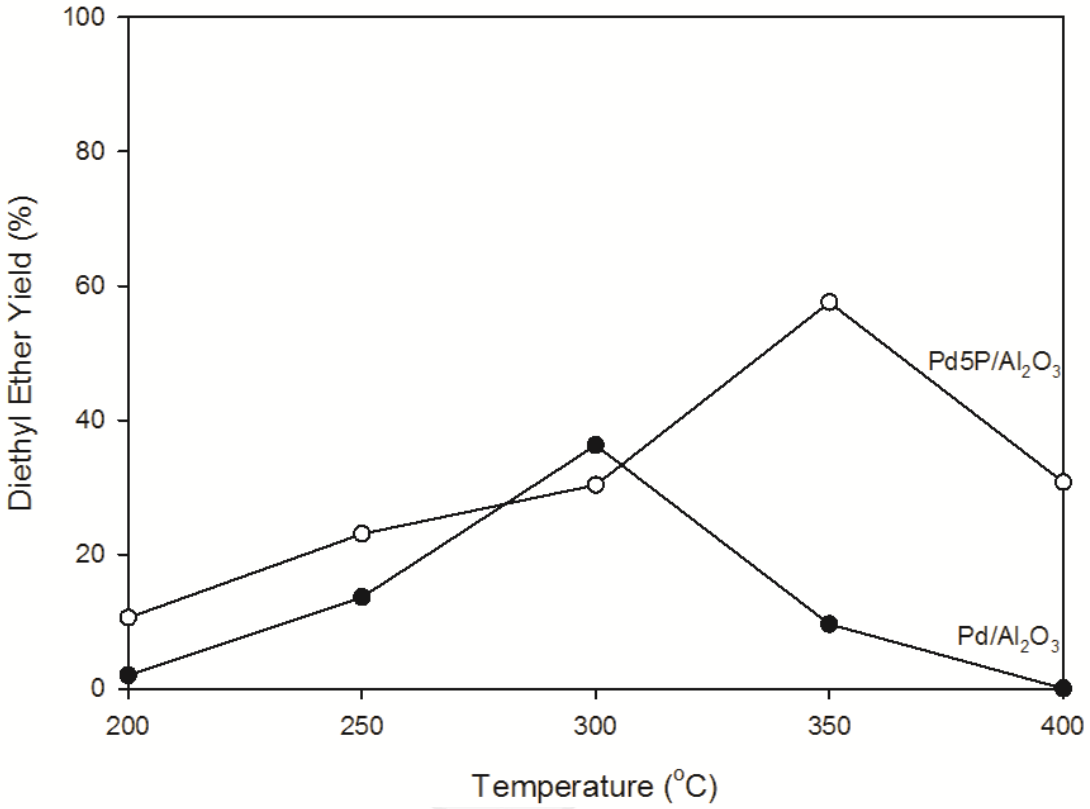

Figure 57 Diethyl ether yield of Pd/Al_2O_3 and $Pd5P/Al_2O_3$ catalysts

According to the diethyl ether yield results, which is shown in **Figure 57**, it was observed that the addition of phosphorus could enhance the diethyl ether yield obtained from ethanol dehydration reaction by increasing the diethyl ether yield from 36.18% at 300°C into 57.68% at 350°C when added 5 wt% of phosphorus into alumina.

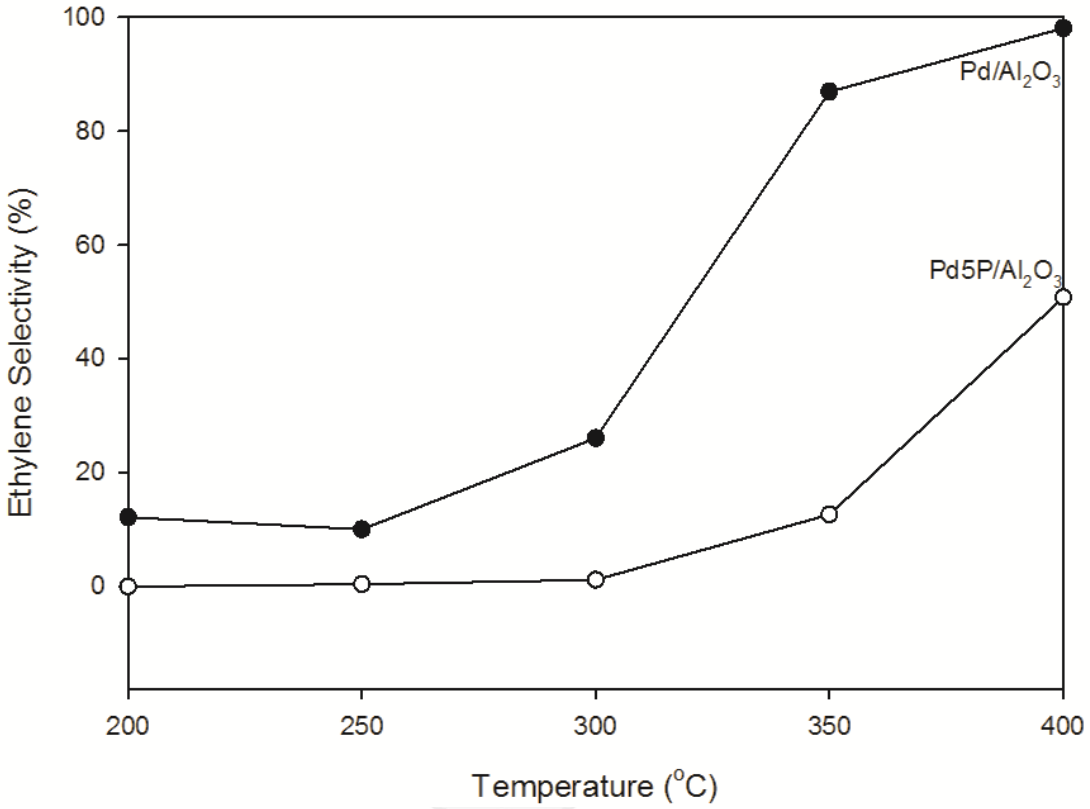

Figure 58 Ethylene selectivity of Pd/Al_2O_3 and $Pd5P/Al_2O_3$ catalysts

Figure 58 illustrates the selectivity towards ethylene obtained from Pd/Al_2O_3 and $Pd5P/Al_2O_3$ catalysts. The result demonstrated the higher ethylene selectivity when increasing reaction temperature. In addition, the modification of phosphorus into catalyst tended to decrease selectivity towards ethylene. This can be suggested that phosphorus addition played role in shifted the reaction pathway into the diethyl ether instead of ethylene.

The ethylene yield of all catalysts, which was calculated from both ethanol conversion and ethylene selectivity and shown in **Figure 59** was also specified the similar curve as the selectivity towards ethylene results. The Pd/Al_2O_3 catalyst was expected to have the highest ethylene yield among the studied catalyst in **Part I** and **Part II** which it exhibited the specific yield of 97.36% at 400°C, while $Pd5P/Al_2O_3$

catalyst showed the lower ethylene yield of 41.80% at the same reaction temperature. Therefore, the non-phosphorus modified Pd/Al_2O_3 catalyst is more appropriate for produce ethylene than the phosphorus modified catalyst.

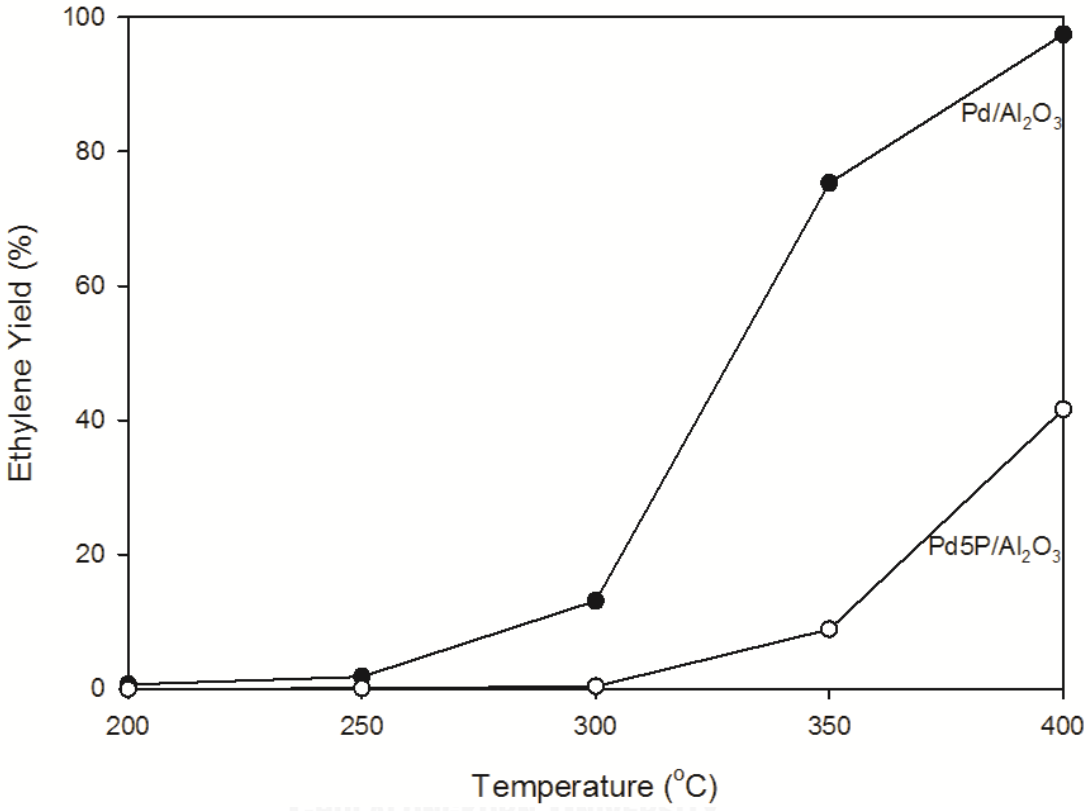

Figure 59 Ethylene yield of Pd/Al_2O_3 and $Pd5P/Al_2O_3$ catalysts

Another interested product, acetaldehyde, was brought to determine for both selectivity and yield, where the selectivity towards acetaldehyde and acetaldehyde yield are shown in **Figure 60** and **Figure 61** as follows;

The selectivity towards acetaldehyde of studied catalysts is displayed in **Figure 60**. It was found that Pd/Al_2O_3 and $Pd5P/Al_2O_3$ catalysts had the adversative trend. This could be said that as the increasing in reaction temperature, $Pd5P/Al_2O_3$ catalyst showed the higher amount of acetaldehyde selectivity, while Pd/Al_2O_3 catalyst tended to have the lower acetaldehyde selectivity. At 200°C, Pd/Al_2O_3

catalyst exhibited the highest selectivity towards acetaldehyde among all of the studied catalysts in **Part I** and **Part II**. The acetaldehyde selectivity of 51% was obtained from using Pd/Al_2O_3 catalyst in ethanol dehydration reaction at 200°C.

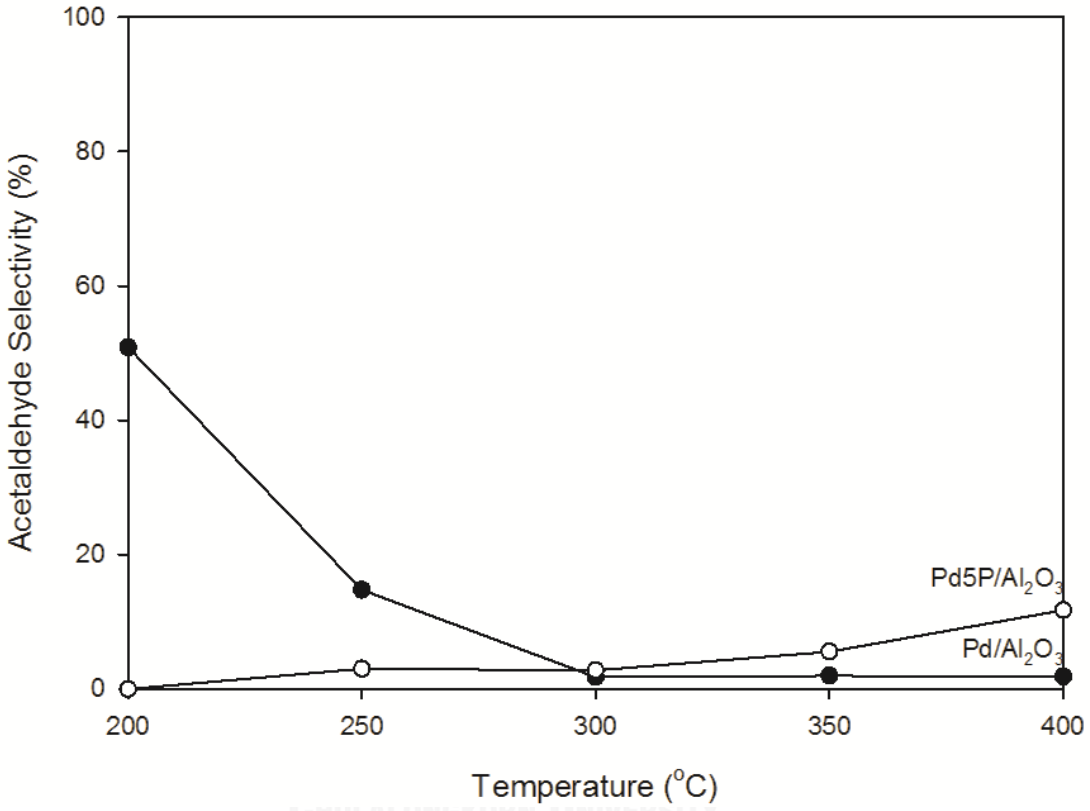

Figure 60 Acetaldehyde selectivity of Pd/Al_2O_3 and $Pd5P/Al_2O_3$ catalysts

Yield of acetaldehyde is specified from multiple ethanol conversion terms with acetaldehyde selectivity and depicted in **Figure 61** as follows;

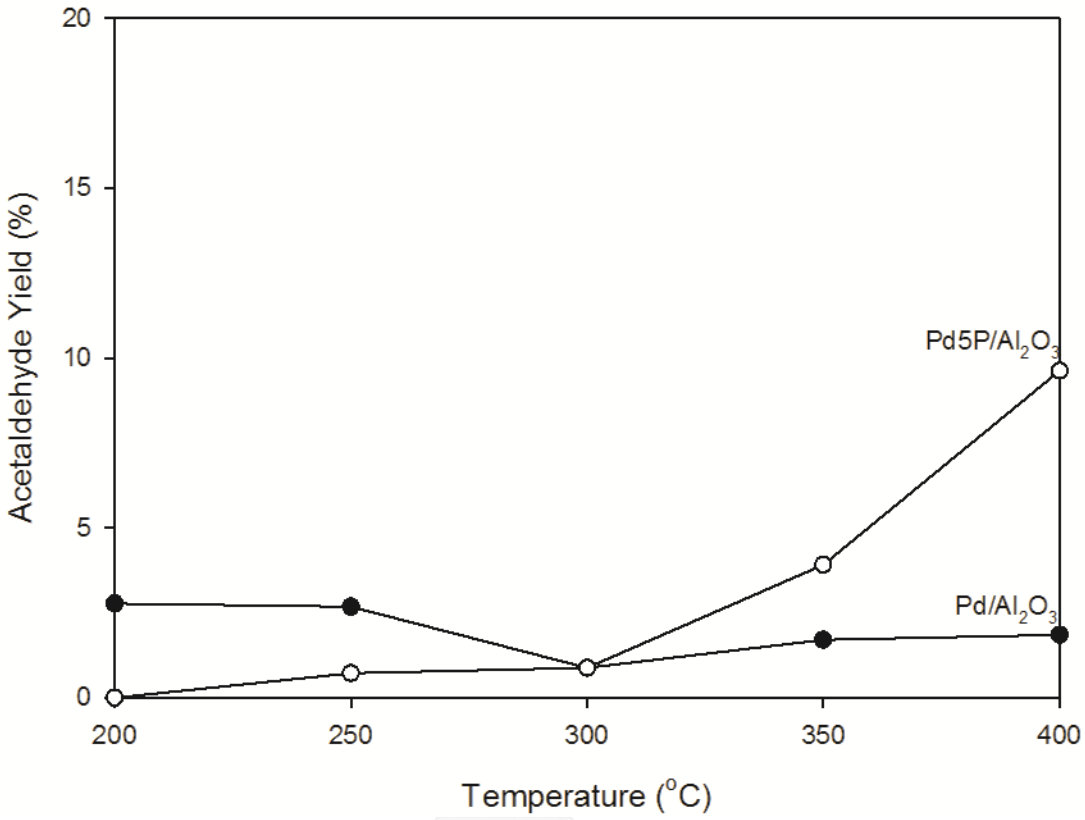

Figure 61 Acetaldehyde yield of Pd/Al_2O_3 and $Pd5P/Al_2O_3$ catalysts

The result of acetaldehyde yield through each studied catalyst was found to have the similar trend as acetaldehyde selectivity. The acetaldehyde yield of $Pd5P/Al_2O_3$ catalyst was raised with the rising in reaction temperature, while the Pd/Al_2O_3 catalyst showed the decreasing in acetaldehyde yield when increasing the reaction temperature. Furthermore, the $Pd5P/Al_2O_3$ catalyst exhibited the highest acetaldehyde yield of 9.02% at temperature of 400°C. Then, it can be concluded that at high temperature, $Pd5P/Al_2O_3$ catalyst is not only suitable for producing significant amount of diethyl ether, but can also use to produce some amount of acetaldehyde.

5.4.5 Catalyst appearance

Pd/Al_2O_3 and $Pd5P/Al_2O_3$ catalysts were brought to study and compared the catalyst appearance for both before and after used in the ethanol dehydration, reaction which are shown in **Figure 62** as follows;

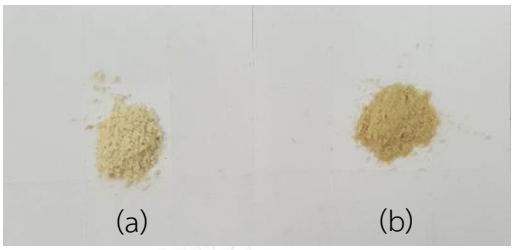

Figure 62 The appearance of the fresh catalysts;
(a) Pd/Al_2O_3 (b) $Pd5P/Al_2O_3$

It was found that both fresh catalysts displayed yellow-brown color. The modified phosphorus showed the darker color of yellow-brown. After used the catalysts in the reaction at 200 to 400°C, the appearance of catalysts were changed into grey to black color shown in **Figure 63** as follows;

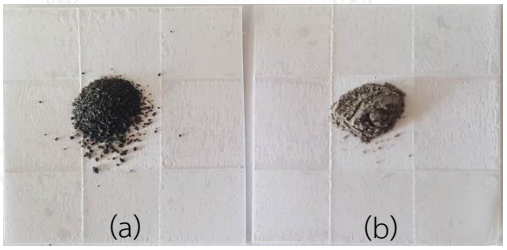

Figure 63 The appearance of the spent catalysts;
(a) Pd/Al_2O_3 (b) $Pd5P/Al_2O_3$

From the catalyst color, which is illustrated in **Figure 63**, it was found that the color of spent Pd/Al_2O_3 catalyst was observed to change into black color. On the other hand, $Pd5P/Al_2O_3$ catalyst, which had the phosphorus in the catalyst demonstrated only a slight change of its color into the darker color. This indicated that phosphorus performed the significant effect in order to inhibit the formation of coke on catalyst surface. In the other words, there were the reports, which was

found that the usage of palladium catalyst is suitable for air-included system. Therefore, in this system which did not have air flow, the palladium catalyst would bring the rapid deactivation.

CHAPTER 6
CONCLUSIONS AND RECOMMENDATIONS

This chapter summarized the experimental results of the mixed γ- and χ-phase alumina catalysts which are considered in the effect of phosphorus loading and noble metal types to characteristics and catalytic performance through ethanol dehydration reaction and the recommendations of the research. Therefore, the research conclusions are all described in section 6.1 and the recommendations are described in section 6.2 as follows;

6.1 Conclusions

1) The phosphorus species on the catalyst surface are the active sites, which promote the dehydration pathway.
2) The 5P/Al_2O_3 catalyst exhibits the highest catalytic performance among the P-modified alumina catalysts due to its highest total acidity, which gives the highest diethyl ether yield of 34.41% at 300°C.
3) The phosphorus loading has the effect on the characteristics, which is described as follows;
    - The surface area and pore volume of catalysts decrease with the increasing in phosphorus loading.
    - The weak acid sites of catalyst increase, whereas medium to strong acid sites decrease as rising in phosphorus loading.
    - The higher phosphorus loading tends to reduce the amount of coke formation on the catalyst surface.

4) The addition of noble metals on P-modified alumina catalyst can increase diethyl ether yield of the catalysts through ethanol dehydration reaction.
5) The Pd5P/Al_2O_3 catalyst demonstrates the highest catalytic performance when compared to other noble metals modified 5P/Al_2O_3 catalysts by increasing the diethyl ether yield to 57.68% at 350°C.
6) The different types of noble metal modification have the effect on the characteristics which are all described as follows;
    - The noble metal addition tends to decrease surface area of the catalysts, but enhances the studied catalysts pore volume and pore size.
    - The acid site of catalysts does not have a significant change when changed the types of noble metal.
7) The noble metal modification does not affect the formation of coke on the catalyst when using through ethanol dehydration reaction.
8) The modification of phosphorus and noble metals does not affect the morphology of the catalysts.
9) The elemental distribution of phosphorus and noble metals on alumina supports is uniform and well dispersed.
10) The noble metal in non-modified phosphorus catalyst promotes the dehydrogenation pathway.
11) The results of catalysts, which were brought to identify characteristic and catalytic performance through 10 h of ethanol dehydration reaction can be concluded into 2 points as follows;
    - At 350°C, Pd5P/Al_2O_3 catalyst exhibits the highest diethyl ether yield since 4 h of reaction time and reaches 59.20% of diethyl ether yield when it was used for 10 h.
    - The time on stream of catalysts shows the slightly higher amount of coke formation than temperature-program (200 to 400°C) of catalysts despite

of the higher amount of coke detection found in XRD patterns of time on stream.

6.2 Recommendations

1) The pyridine adsorption analysis should be used to indicate types of acid site including Brønsted acid site and Lewis acid site.
2) The back titration technique should also be investigated to confirm NH_3-TPD results.
3) The catalytic stability of the Pd5P/Al_2O_3 catalyst should be further studied.
4) In order to apply this research to industry, the different sources of ethanol should be studied via ethanol dehydration reaction.
5) The other noble metal modified on alumina supports including Ru/Al_2O_3 and Pt/Al_2O_3 should be needed the further study in both their characteristics and catalytic activity in order to use as the reference catalyst of Ru5P/Al_2O_3 and Pt5P/Al_2O_3, respectively.
6) The modification of noble metals on alumina supports and P-modified alumina catalysts in various loading should be further investigated
7) In the study which investigated the effect of noble metal types to their characteristics and catalytic activity through ethanol dehydration reaction, XRF technique should be analyzed in all studied catalysts in order to reduce the error between XRF and ICP techniques.

REFERENCES

1. Davison, J., *Performance and costs of power plants with capture and storage of CO2.* Energy, 2007. **32**(7): p. 1163-1176.
2. (IPCC), I.P.o.C.C., *Climate change 2001, third assessment report of the Intergovernmental Panel on Climate Change.* Cambridge, UK: Cambridge University Press, 2001.
3. Riittonen, T., et al., *One-Pot Liquid-Phase Catalytic Conversion of Ethanol to 1-Butanol over Aluminium Oxide—The Effect of the Active Metal on the Selectivity.* Catalysts, 2012. **2**(4): p. 68-84.
4. Miller Jothi, N.K., G. Nagarajan, and S. Renganarayanan, *Experimental studies on homogeneous charge CI engine fueled with LPG using DEE as an ignition enhancer.* Renewable Energy, 2007. **32**(9): p. 1581-1593.
5. Khom-in, J., et al., *Dehydration of methanol to dimethyl ether over nanocrystalline Al2O3 with mixed γ- and χ-crystalline phases.* Catalysis Communications, 2008. **9**(10): p. 1955-1958.
6. Ramesh, K.J., C.; Han, Y.; and Borgna, A., *Synthesis, characterization, and catalytic activity of phosphorus modified H-ZSM-5 catalysts in selective ethanol dehydration.* Ind. Eng. Chem. Res., 2010. **49**: p. 4080-4090.
7. Golay, S.M., L.; Doepper, R.; and Renken, A., *Influence of the catalyst acid/base properties on the catalytic ethanol dehydration under steady state and dynamic conditions. In situ surface and gas phase analysis.* Chemical Engineering Science, 1999. **54**: p. 3593-3598.
8. Zaki, T., *Catalytic dehydration of ethanol using transition metal oxide catalysts.* J Colloid Interface Sci, 2005. **284**(2): p. 606-13.
9. Matori, K.A., et al., *Phase transformations of alpha-alumina made from waste aluminum via a precipitation technique.* Int J Mol Sci, 2012. **13**(12): p. 16812-21.
10. Santos, P.e.a., *Standard Transition Aluminas. Electron Microscope Studies.* Materials Research, 2000. **3**(4): p. 104-114.

11. Ros, S.D., et al., *Modeling the effects of calcination conditions on the physical and chemical properties of transition alumina catalysts.* Materials Characterization, 2013. **80**: p. 50-61.
12. Santacesaria, E.e.a., *Basic Behavior of Alumina in the Presence of Strong Acids.* Ind. Eng. Chem., Prod. Res. Dev., 1977. **16**(1): p. 45-46.
13. Perego, C.a.V., P., *Catalyst preparation methods.* Catalysis Today, 1997. **34**: p. 281-305.
14. *Manual of Symbols and Terminology.* Pure Appl. Chem., 1976. **46**: p. 71.
15. Setterfield, C., *Practical Course of Heterogeneous Catalysis (in Russian)*. 1984, Moscow: Mir. 520.
16. Krylov, O.V., *Heterogeneous Catalysis (in Russian)*. 2004, Moscow: IKC <Akademkniga>. 679.
17. Fan, D., D.-J. Dai, and H.-S. Wu, *Ethylene Formation by Catalytic Dehydration of Ethanol with Industrial Considerations.* Materials, 2012. **6**(1): p. 101-115.
18. Phung, T.K. and G. Busca, *Diethyl ether cracking and ethanol dehydration: Acid catalysis and reaction paths.* Chemical Engineering Journal, 2015. **272**: p. 92-101.
19. Alharbi, W., et al., *Dehydration of ethanol over heteropoly acid catalysts in the gas phase.* Journal of Catalysis, 2014. **319**: p. 174-181.
20. Domok, M., et al., *Adsorption and reactions of ethanol and ethanol–water mixture on alumina-supported Pt catalysts.* Applied Catalysis B: Environmental, 2007. **69**(3-4): p. 262-272.
21. Rajakumar, B.e.a., *Thermal decomposition of 2-fluoroethanol: single pulse tube and ab initio studies.* J. Phys. Chem. A., 2003. **107**(46): p. 9782–9793.
22. Galvita, V.e.a., *Synthesis gas production by steam reforming of ethanol.* Appl. Catal., A., 2001. **220**(1-2): p. 123-127.
23. Zhang, M. and Y. Yu, *Dehydration of Ethanol to Ethylene.* Industrial & Engineering Chemistry Research, 2013. **52**(28): p. 9505-9514.
24. Pan, L.R., *Development review of catalysts for ethanol dehydration to produce ethylene.* Speciality Petrochem, 1986. **4**: p. 41-64.

25. Pearson, D.E.e.a., *Phosphoric acid systems. 2. Catalytic conversion of fermentation ethanol to ethylene.* Prod. Res. Dev., 1981. **20**(4): p. 734-740.

26. *Alumina: catalyst and support. I. Alumina, its intrinsic acidity and catalytic activity.* J. Am. Chem. Soc., 1960. **82**(10): p. 2471–2483.

27. Le Van Mao, R.e.a., *The Bioethanol-to-ethylene (B.E.T.E.) process.* Applied. Catalysis., 1989. **48**(2): p. 265–277.

28. Xu, M.e.a., *Catalytic dehydration of methanol to dimethyl ether (DME) over Pd/Cab-O-Sil catalysts.* Applied Catalysis A: General., 1997. **149**: p. 303-309.

29. Takahara, I., et al., *Dehydration of Ethanol into Ethylene over Solid Acid Catalysts.* Catalysis Letters, 2005. **105**(3-4): p. 249-252.

30. Chen, G., et al., *Catalytic dehydration of bioethanol to ethylene over TiO2/γ-Al2O3 catalysts in microchannel reactors.* Catalysis Today, 2007. **125**(1-2): p. 111-119.

31. Li, Y.e.a., *Experimental study of the catalytic dehydration of ethanol to ethylene on a γ-Al2O3 catalyst.* Beijing Univ. Chem. Technol., 2007. **34**(5): p. 449–452.

32. Varisli, D., T. Dogu, and G. Dogu, *Ethylene and diethyl-ether production by dehydration reaction of ethanol over different heteropolyacid catalysts.* Chemical Engineering Science, 2007. **62**(18-20): p. 5349-5352.

33. Wannaborworn, M., P. Praserthdam, and B. Jongsomjit, *A Comparative Study of Solvothermal and Sol-Gel-Derived Nanocrystalline Alumina Catalysts for Ethanol Dehydration.* Journal of Nanomaterials, 2015. **2015**: p. 1-11.

34. Zhang, D., R. Wang, and X. Yang, *Effect of P Content on the Catalytic Performance of P-modified HZSM-5 Catalysts in Dehydration of Ethanol to Ethylene.* Catalysis Letters, 2008. **124**(3-4): p. 384-391.

35. Ramesh, K., et al., *Structure and reactivity of phosphorous modified H-ZSM-5 catalysts for ethanol dehydration.* Catalysis Communications, 2009. **10**(5): p. 567-571.

36. Bi, J., et al., *High effective dehydration of bio-ethanol into ethylene over nanoscale HZSM-5 zeolite catalysts.* Catalysis Today, 2010. **149**(1-2): p. 143-147.

37. Han, Y., et al., *Molybdenum oxide modified HZSM-5 catalyst: Surface acidity and catalytic performance for the dehydration of aqueous ethanol.* Applied Catalysis A: General, 2011. **396**(1-2): p. 8-13.

38. Liu, D., et al., *Catalytic dehydration of methanol to dimethyl ether over modified γ-Al2O3 catalyst.* Fuel, 2011. **90**(5): p. 1738-1742.

39. Rahmanian, A. and H.S. Ghaziaskar, *Continuous dehydration of ethanol to diethyl ether over aluminum phosphate–hydroxyapatite catalyst under sub and supercritical condition.* The Journal of Supercritical Fluids, 2013. **78**: p. 34-41.

40. Valdez, R., et al., *Effect of the acidity of alumina over Pt, Pd, and Pt–Pd (1:1) based catalysts for 2-propanol dehydration reactions.* Fuel, 2013. **105**: p. 688-694.

41. *Aluminum*. Thermo Scientific XPS; Available from: http://xpssimplified.com/elements/aluminum.php.

42. *Phosphorus*. Thermo Sciencific XPS; Available from: http://xpssimplified.com/elements/phosphorus.php.

43. Jiang, H.-L. and Q. Xu, *Recent progress in synergistic catalysis over heterometallic nanoparticles.* Journal of Materials Chemistry, 2011. **21**(36): p. 13705.

44. E.J. Angueira, e.a., *Leading Edge Catalysis research*. 2005: Nova Science Publisher. 39.

45. Han, L., et al., *Fe doping Pd/AC sorbent efficiently improving the Hg0 removal from the coal-derived fuel gas.* Fuel, 2016. **182**: p. 64-72.

46. Hyde, T., *Final Analysis: Crystallite Size Analysis of Supported Platinum Catalysts by XRD.* Platinum Metals Review, 2008. **52**(2): p. 129-130.

47. *Ruthenium*. Thermo Sciencific XPS; Available from: http://xpssimplified.com/elements/ruthenium.php.

48. *Platinum*. Thermo Sciencific XPS; Available from: http://xpssimplified.com/elements/platinum.php.
49. *Palladium*. Thermo Sciencific XPS; Available from: http://xpssimplified.com/elements/palladium.php.

APPENDIX

APPENDIX A

CALIBRATION CURVES OF ALUMINA PHASE

The calibration curves of mixed γ- and χ-phase alumina determined from analyzed both pure γ-phase alumina and pure χ-phase alumina mixtures in the appropriate ratio in X-ray diffraction instrument, then reported the percent of χ-phase alumina in y-axis and area under the curves in x-axis as shown in **Fig.A.1**.

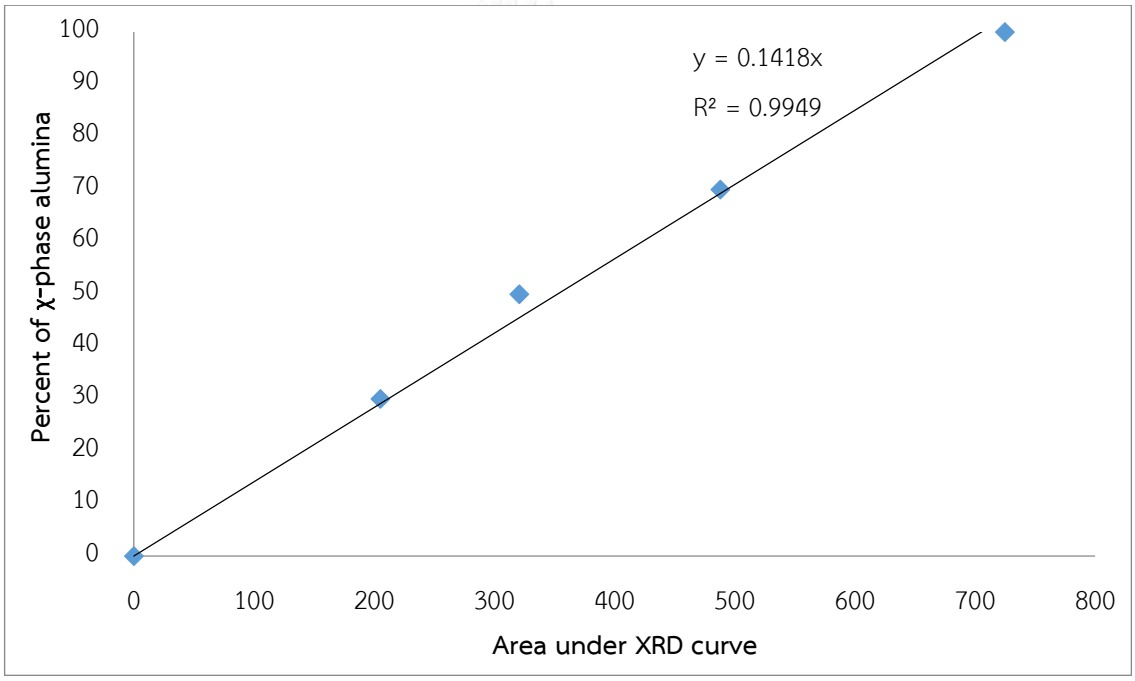

Fig.A.1 The calibration curve of mixed γ- and χ- phase alumina

APPENDIX B

CALCULATION FOR CATALYST PREPARATION

Calculation for preparation of phosphorus-modified Al_2O_3 catalyst by acid activation

1. Deposited of 5 wt% H_3PO_4 on Al_2O_3 support

Reagent – Phosphoric acid (H_3PO_4) 85%

Molecular weight = 98 g/mole

Phosphorus (P), atomic weight = 31 g/mole

– Al_2O_3 support

Based on 1 g of catalyst used;

There is 85 g of H_3PO_4 in 100 g of H_3PO_4 solution.

Thus, there is 5 g of H_3PO_4 in $\frac{100\times5}{85}$ g of H_3PO_4 solution.

or in 5.88 g of H_3PO_4 solution.

Density of H_3PO_4 = 1.685 g/mL

Thus, 5.88 g of H_3PO_4 solution equal to 3.49 mL.

Therefore, added 3.49 mL of H_3PO_4 solution into deionized water in amount of 94.12 mL, and then stirred the solution with Al_2O_3 support at room temperature for 30 min to obtain non-calcined 5 wt% H_3PO_4/Al_2O_3 catalyst.

2. Deposited of 10 wt% H_3PO_4 on Al_2O_3 support

Reagent – Phosphoric acid (H_3PO_4) 85%

Molecular weight = 98 g/mole

Phosphorus (P), atomic weight = 31 g/mole

– Al_2O_3 support

Based on 1 g of catalyst used;

There is	85 g	of H_3PO_4 in	100 g	of H_3PO_4 solution.
Thus, there is	10 g	of H_3PO_4 in	$\frac{100\times10}{85}$ g	of H_3PO_4 solution.
		or in	11.76 g	of H_3PO_4 solution.

Density of H_3PO_4 = 1.685 g/mL

Thus, 11.76 g of H_3PO_4 solution equal to 6.98 mL.

Therefore, added 6.98 mL of H_3PO_4 solution into deionized water in amount of 88.24 mL, and then stirred the solution with Al_2O_3 support at room temperature for 30 min to obtain non-calcined 10 wt% H_3PO_4/Al_2O_3 catalyst.

3. Deposited of 15 wt% H_3PO_4 on Al_2O_3 support

Reagent – Phosphoric acid (H_3PO_4) 85%

Molecular weight = 98 g/mole

Phosphorus (P), atomic weight = 31 g/mole

– Al_2O_3 support

Based on 1 g of catalyst used;

There is	85 g	of H_3PO_4 in	100 g	of H_3PO_4 solution.
Thus, there is	15 g	of H_3PO_4 in	$\frac{100\times15}{85}$ g	of H_3PO_4 solution.
		or in	17.65 g	of H_3PO_4 solution.

Density of H_3PO_4 = 1.685 g/mL

Thus, 17.65 g of H_3PO_4 solution equal to 10.47 mL.

Therefore, added 10.47 mL of H_3PO_4 solution into deionized water in amount of 82.35 mL, and then stirred the solution with Al_2O_3 support at room temperature for 30 min to obtain non-calcined 15 wt% H_3PO_4/Al_2O_3 catalyst.

4. Deposited of 20 wt% H_3PO_4 on Al_2O_3 support

Reagent – Phosphoric acid (H_3PO_4) 85%

Molecular weight = 98 g/mole

Phosphorus (P), atomic weight = 31 g/mole

– Al_2O_3 support

Based on 1 g of catalyst used;

There is 85 g of H_3PO_4 in 100 g of H_3PO_4 solution.

Thus, there is 20 g of H_3PO_4 in $\frac{100\times20}{85}$ g of H_3PO_4 solution.

or in 23.53 g of H_3PO_4 solution.

Density of H_3PO_4 = 1.685 g/mL

Thus, 23.53 g of H_3PO_4 solution equal to 13.96 mL.

Therefore, added 13.96 mL of H_3PO_4 solution into deionized water in amount of 76.47 mL, and then stirred the solution with Al_2O_3 support at room temperature for 30 min to obtain non-calcined 20 wt% H_3PO_4/Al_2O_3 catalyst.

Calculation for preparation of noble metal loading on P/Al_2O_3 catalysts by incipient wetness impregnation

1. Deposited of 0.5 wt% Ru on P/Al_2O_3 catalyst

Reagent – Ruthenium (III) nitrosyl nitrate ($N_4O_{10}Ru$); Ru 1.5%

Molecular weight = 317 g/mole

Ruthenium (Ru), atomic weight = 101 g/mole

– P/Al_2O_3 catalyst

Based on 1 g of catalyst obtained, the composition of catalyst would be as follow;

Ruthenium = 0.005 g

P/Al_2O_3 catalyst = 1.000-0.005 g

= 0.995 g

There is 1.5 g of Ru in 100 mL of $N_4O_{10}Ru$ solution.

Thus, there is 0.005 g of Ru in $\frac{100\times0.005}{1.5}$ mL of $N_4O_{10}Ru$ solution.

or in 0.333 mL (333µL) of $N_4O_{10}Ru$ solution.

Pore volume of P/Al_2O_3 catalyst = 487 µL

Therefore, added deionized water in amount of 154 µL into 333 µL of $N_4O_{10}Ru$ solution.

2. Deposited of 0.5 wt% Pt on P/Al_2O_3 catalyst

Reagent – Tetraammineplatinum (II) chloride hydrate ($PtCl_2(NH_3)_4.H_2O$) 99.99%

Molecular weight = 352 g/mole

Platinum (Pt), atomic weight = 195 g/mole

– P/Al_2O_3 catalyst

Based on 1 g of catalyst obtained, the composition of catalyst would be as follow;

Platinum = 0.005 g

P/Al_2O_3 catalyst = 1.000-0.005 g

= 0.995 g

There is 195 g of Pt in 352 g of $PtCl_2(NH_3)_4.H_2O$ 99.99%.

Thus, there is 0.005 g of Pt in $\frac{352\times0.005}{195}$ g of $PtCl_2(NH_3)_4.H_2O$ 99.99%.

or in 0.009 g of $PtCl_2(NH_3)_4.H_2O$ 99.99%.

Pore volume of P/Al_2O_3 catalyst = 487 µL

Therefore, added deionized water in amount of 487 µL into 0.009 g of $PtCl_2(NH_3)_4.H_2O$ 99.99% solution.

3. Deposited of 0.5 wt% Pd on P/Al_2O_3 catalyst

Reagent – Tetraamminepalladium (II) nitrate ($Pd(NH_3)_4(NO_3)_2$) 10%

Molecular weight = 298.5 g/mole

Platinum (Pt), atomic weight = 106.5 g/mole

– P/Al_2O_3 catalyst

Based on 1 g of catalyst obtained, the composition of catalyst would be as follow;

Palladium = 0.005 g

P/Al_2O_3 catalyst = 1.000-0.005 g

= 0.995 g

In 100 g of $Pd(NH_3)_4(NO_3)_2$ solution , there is 10 g of $Pd(NH_3)_4(NO_3)_2$ or 3.57 g of Pd.

Thus, there is 0.005 g of Pd in $\frac{100\times0.005}{3.57}$ g of $Pd(NH_3)_4(NO_3)_2$ solution.

or in 0.141 g of $Pd(NH_3)_4(NO_3)_2$ solution.

Density of $Pd(NH_3)_4(NO_3)_2$ solution = 1.038 g/mL

Thus, 0.141 g of $Pd(NH_3)_4(NO_3)_2$ solution equal to 0.136 ml (136 µL)

Pore volume of P/Al_2O_3 catalyst = 487 µL

Therefore, added deionized water in amount of 351 µL into 136 µL of $Pd(NH_3)_4(NO_3)_2$ solution.

APPENDIX C

CALIBRATION CURVES OF REACTANT AND PRODUCTS

The calibration curves of reactant and products shown in this appendix were used to calculate the amount of reactant and products obtained from ethanol dehydration reaction.

The calibration curves of the main reagent including ethanol, diethyl ether, ethylene and acetaldehyde are illustrated in **Fig.D.1-D.4** as follows;

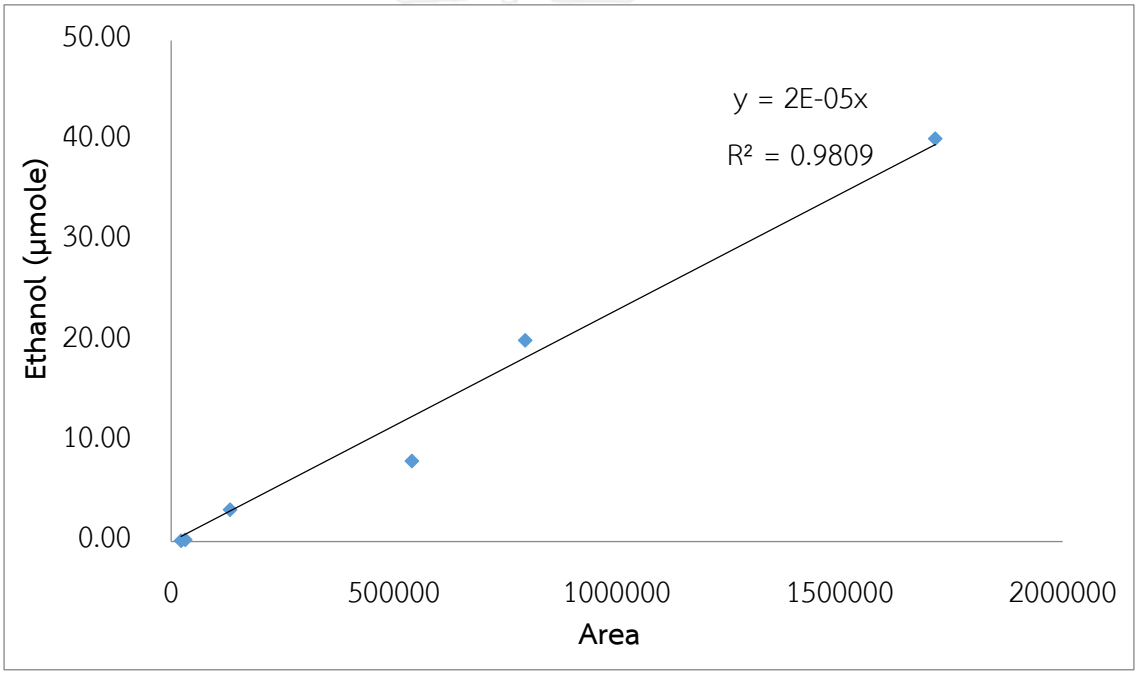

Fig.C.1 The calibration curve of ethanol

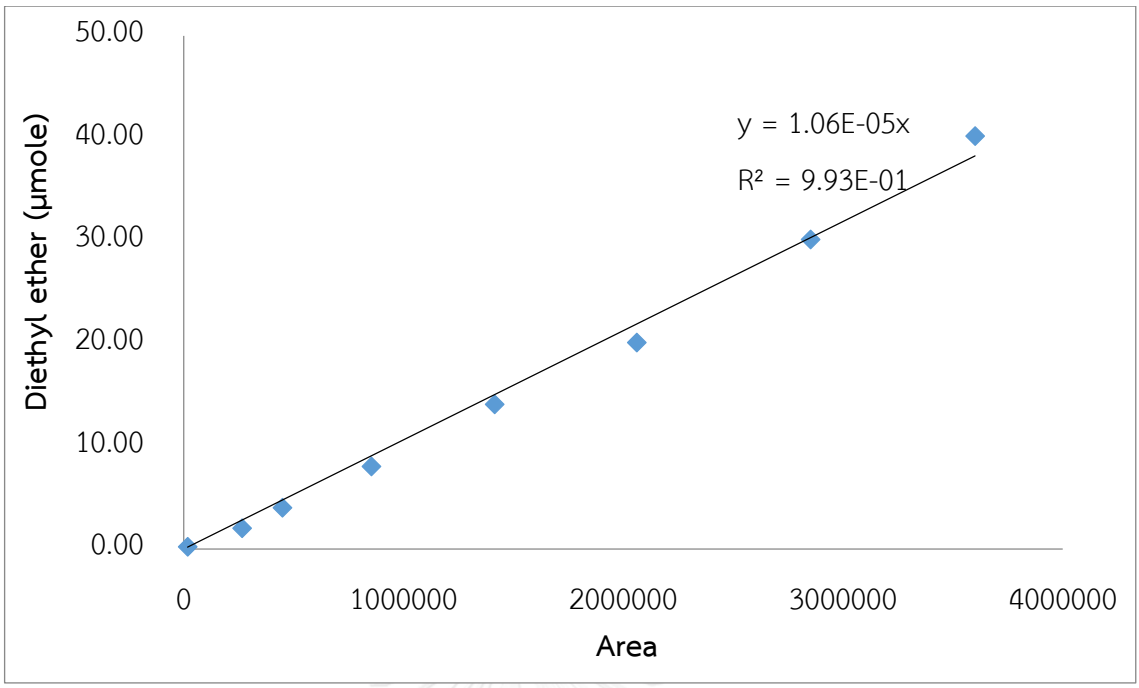

Fig.C.2 The calibration curve of diethyl ether

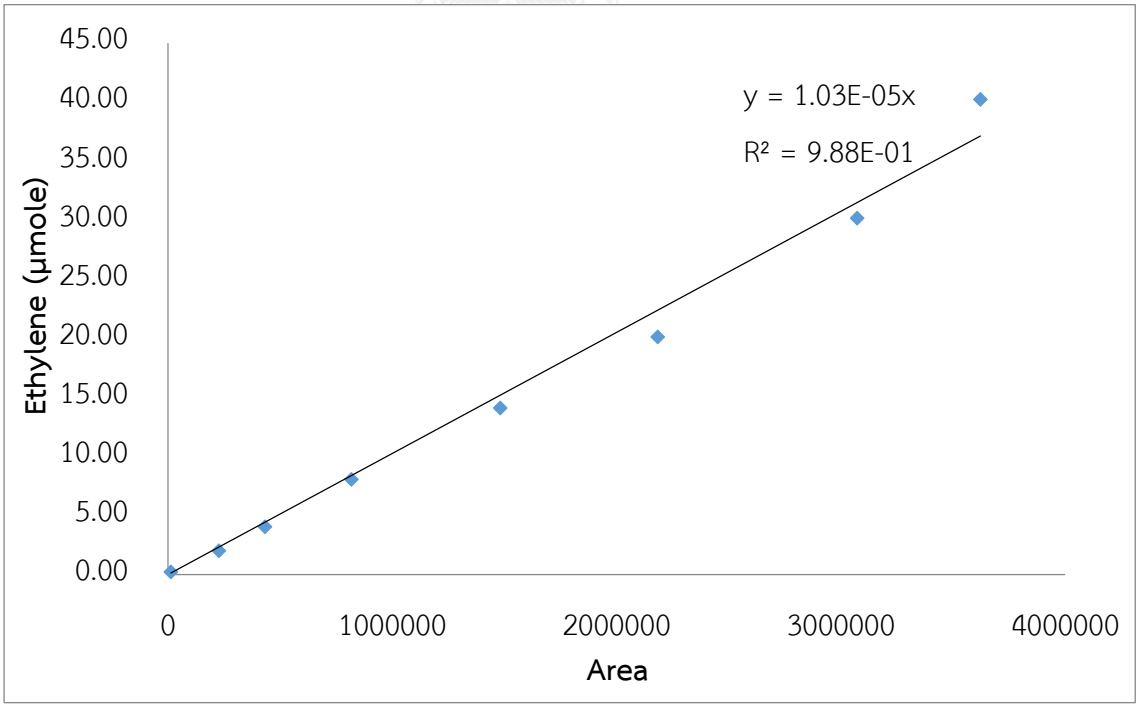

Fig.C.3 The calibration curve of ethylene

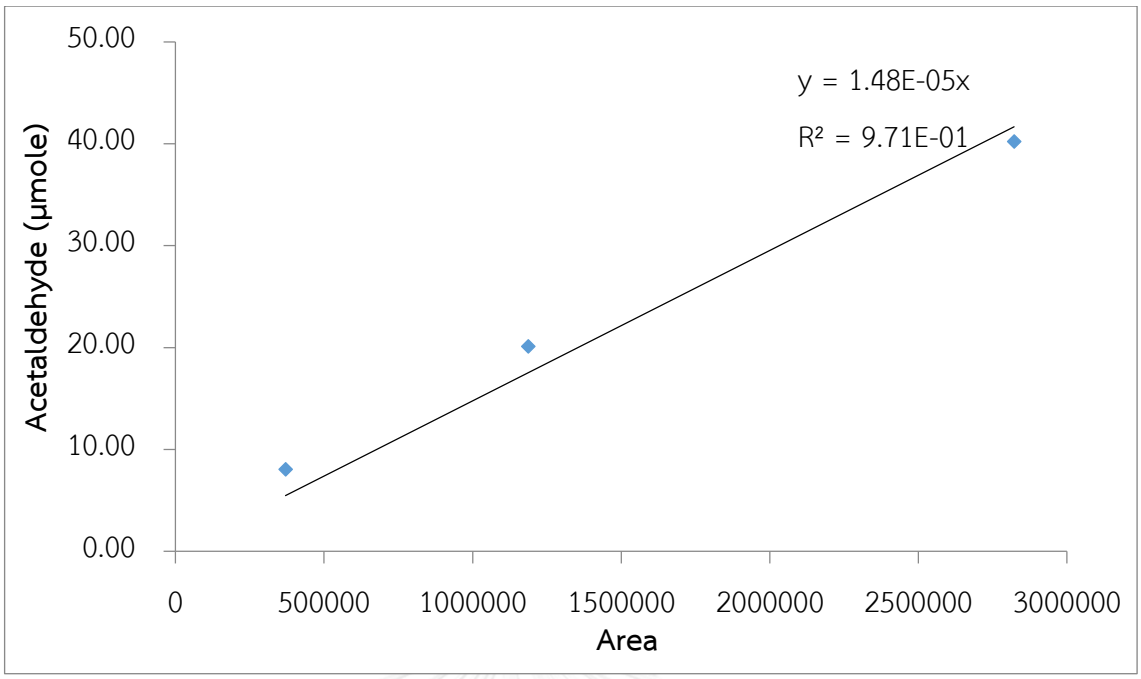

Fig.C.4 The calibration curve of acetaldehyde

APPENDIX E

CHROMATOGRAM

From the chromatograms depicted in **Fig.D.1** and **Fig.D.2**;

- Peak position of ethanol : 4.9 min
- Peak position of diethyl ether : 5.2 min
- Peak position of ethylene : 4.4 min
- Peak position of acetaldehyde : 4.6 min

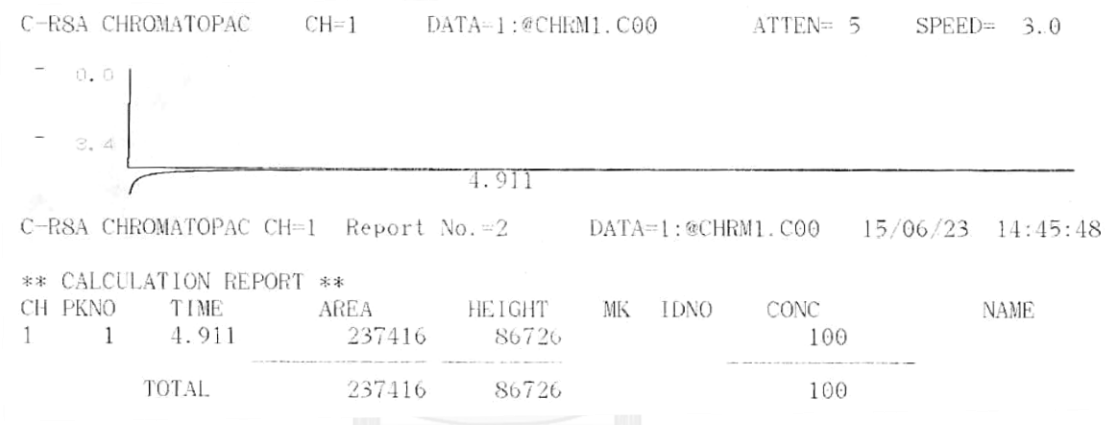

Fig.D.1 Chromatogram of the reagent before the reaction

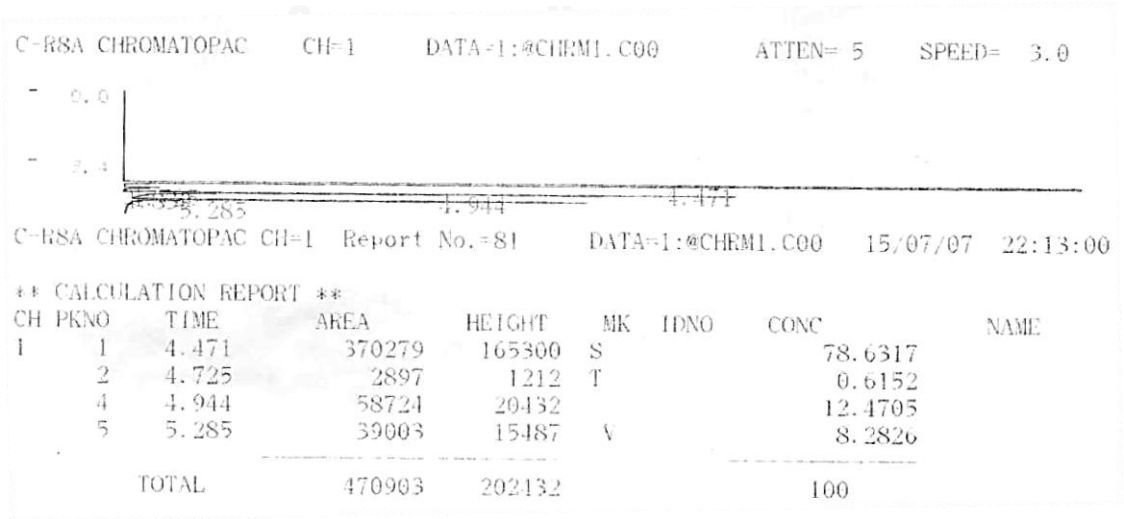

Fig.D.2 Chromatogram of the reagent after the reaction

APPENDIX E

CALCULATION OF ACIDITY

The acidity of the catalysts is determined from NH_3-TPD by calculating area under TCD signal curve as a functional of temperature as follows;

$$\text{Acidity of catalyst} = \frac{\text{Moles of desorbed } NH_3}{\text{Weight of dry catalyst}} \times 100$$

Where NH_3 desorbed (moles) = Area under the curve of TCD signal × 300 μmole (NH_3 desorbed in mole is calculated from the calibration curve of Micromeritics Pulse Chemisorp 2750 instrument.)

Weight of dry catalyst = 0.1 g

The unit of catalyst acidity is μmole/g cat.

APPENDIX F
CALCULATION OF REACTANT CONVERSION, PRODUCT SELECTIVITY, PRODUCT YIELD AND RATE OF REACTION

The catalytic performance in ethanol dehydration reaction can be demonstrated from reactant conversion, product selectivity, product yield and rate of reaction.

Reactant conversion

The conversion of reactant is defined as moles of reacted reactant with respect to moles of fed reactant;

$$\text{Reactant conversion (\%)} = \frac{\text{Moles of reacted reactant}}{\text{Moles of fed reactant}} \times 100$$

Product selectivity

The selectivity towards each product is defined as moles of product formed with respect to total moles of products;

$$\text{Product selectivity (\%)} = \frac{\text{Moles of each product}}{\text{Total moles of product}} \times 100$$

Product yield

Product yield (%) = Reactant conversion × Selectivity of each product

Rate of reaction

$$\text{Rate of reaction (mole ethanol/g cat. h)} = \frac{\text{Ethanol feed rate (mole ethanol/h)} \times \text{Ethanol conversion at studied temperature (\%)}}{\text{0.0821 (l.atm/mol.K)} \quad \text{Studied temperature (K)} \quad \text{Amount of catalyst used (g)}}$$

APPENDIX G
CATALYTIC TESTING RESULTS

Table G.1 Ethanol conversion, product selectivity, product yield and rate of reaction obtained from dehydration reaction of ethanol at 200°C

Catalysts	Ethanol Conversion (%)	Selectivity (%)		
		Diethyl ether	Ethylene	Acetaldehyde
Al_2O_3	14.05	100	0	0
$5P/Al_2O_3$	9.12	100	0	0
$12P/Al_2O_3$	8.12	100	0	0
$14P/Al_2O_3$	4.62	100	0	0
$20P/Al_2O_3$	0.00	100	0	0
$Ru5P/Al_2O_3$	5.27	100	0	0
$Pt5P/Al_2O_3$	2.55	100	0	0
$Pd5P/Al_2O_3$	10.60	100	0	0
Pd/Al_2O_3	5.44	37	12	51

Catalysts	Yield (%)			Rate of Reaction $\times 10^2$ (mole ethanol/g cat. h)
	Diethyl ether	Ethylene	Acetaldehyde	
Al_2O_3	14.05	0.00	0.00	7.24
$5P/Al_2O_3$	9.12	0.00	0.00	4.70
$12P/Al_2O_3$	8.12	0.00	0.00	4.18
$14P/Al_2O_3$	4.62	0.00	0.00	2.38
$20P/Al_2O_3$	0.00	0.00	0.00	0.00
$Ru5P/Al_2O_3$	5.27	0.00	0.00	2.71
$Pt5P/Al_2O_3$	2.55	0.00	0.00	1.31
$Pd5P/Al_2O_3$	10.60	0.00	0.00	5.46
Pd/Al_2O_3	2.01	0.65	2.77	2.80

Table G.2 Ethanol conversion, product selectivity, product yield and rate of reaction obtained from dehydration reaction of ethanol at 250°C

Catalysts	Ethanol Conversion (%)	Selectivity (%)		
		Diethyl ether	Ethylene	Acetaldehyde
Al_2O_3	40.13	68	32	0
$5P/Al_2O_3$	22.12	95	4	1
$12P/Al_2O_3$	19.28	97	2	1
$14P/Al_2O_3$	6.82	100	0	0
$20P/Al_2O_3$	0.00	100	0	0
$Ru5P/Al_2O_3$	19.81	97	2	1
$Pt5P/Al_2O_3$	6.10	99	1	0
$Pd5P/Al_2O_3$	23.88	97	0	3
Pd/Al_2O_3	18.16	75	10	15

Catalysts	Yield (%)			Rate of Reaction $\times 10^2$ (mole ethanol/g cat. h)
	Diethyl ether	Ethylene	Acetaldehyde	
Al_2O_3	27.29	12.84	0.00	18.69
$5P/Al_2O_3$	21.01	0.88	0.22	10.30
$12P/Al_2O_3$	18.70	0.39	0.19	8.98
$14P/Al_2O_3$	6.82	0.00	0.00	3.18
$20P/Al_2O_3$	0.00	0.00	0.00	0.00
$Ru5P/Al_2O_3$	19.22	0.40	0.20	9.23
$Pt5P/Al_2O_3$	6.04	0.06	0.00	2.84
$Pd5P/Al_2O_3$	23.16	0.00	0.72	11.12
Pd/Al_2O_3	13.62	1.82	2.72	8.46

Table G.3 Ethanol conversion, product selectivity, product yield and rate of reaction obtained from dehydration reaction of ethanol at 300°C

Catalysts	Ethanol Conversion (%)	Selectivity (%)		
		Diethyl ether	Ethylene	Acetaldehyde
Al_2O_3	60.38	12	87	1
$5P/Al_2O_3$	49.16	70	28	2
$12P/Al_2O_3$	40.03	80	20	0
$14P/Al_2O_3$	11.20	84	16	0
$20P/Al_2O_3$	3.49	92	8	0
$Ru5P/Al_2O_3$	28.74	95	5	0
$Pt5P/Al_2O_3$	31.95	70	30	0
$Pd5P/Al_2O_3$	31.61	96	1	3
Pd/Al_2O_3	50.25	72	26	2

Catalysts	Yield (%)			Rate of Reaction $\times 10^2$ (mole ethanol/g cat. h)
	Diethyl ether	Ethylene	Acetaldehyde	
Al_2O_3	7.25	52.53	0.60	25.67
$5P/Al_2O_3$	34.41	13.76	0.98	20.90
$12P/Al_2O_3$	32.02	8.01	0.00	17.02
$14P/Al_2O_3$	9.41	1.79	0.00	4.76
$20P/Al_2O_3$	3.21	0.28	0.00	1.48
$Ru5P/Al_2O_3$	27.30	1.44	0.00	12.22
$Pt5P/Al_2O_3$	22.37	9.59	0.00	13.58
$Pd5P/Al_2O_3$	30.35	0.32	0.95	13.44
Pd/Al_2O_3	36.18	13.07	1.01	21.36

Table G.4 Ethanol conversion, product selectivity, product yield and rate of reaction obtained from dehydration reaction of ethanol at 350°C

Catalysts	Ethanol Conversion (%)	Selectivity (%)		
		Diethyl ether	Ethylene	Acetaldehyde
Al_2O_3	84.87	2	96	2
$5P/Al_2O_3$	83.90	9	90	1
$12P/Al_2O_3$	61.88	41	59	0
$14P/Al_2O_3$	18.91	54	46	0
$20P/Al_2O_3$	9.55	58	42	0
$Ru5P/Al_2O_3$	40.76	78	22	0
$Pt5P/Al_2O_3$	49.27	80	20	0
$Pd5P/Al_2O_3$	70.34	82	13	5
Pd/Al_2O_3	86.68	11	87	2

Catalysts	Yield (%)			Rate of Reaction $\times 10^2$ (mole ethanol/g cat. h)
	Diethyl ether	Ethylene	Acetaldehyde	
Al_2O_3	1.70	81.48	1.70	33.19
$5P/Al_2O_3$	7.55	75.51	0.84	32.81
$12P/Al_2O_3$	25.37	36.51	0.00	24.20
$14P/Al_2O_3$	10.21	8.70	0.00	7.39
$20P/Al_2O_3$	5.54	4.01	0.00	3.73
$Ru5P/Al_2O_3$	31.79	8.97	0.00	15.94
$Pt5P/Al_2O_3$	39.42	9.85	0.00	19.27
$Pd5P/Al_2O_3$	57.68	9.14	3.52	27.50
Pd/Al_2O_3	9.53	75.41	1.73	33.89

Table G.5 Ethanol conversion, product selectivity, product yield and rate of reaction obtained from dehydration reaction of ethanol at 400°C

Catalysts	Ethanol Conversion (%)	Selectivity (%)		
		Diethyl ether	Ethylene	Acetaldehyde
Al_2O_3	88.48	0	99	1
$5P/Al_2O_3$	86.12	6	94	0
$12P/Al_2O_3$	72.86	21	79	0
$14P/Al_2O_3$	35.49	35	65	0
$20P/Al_2O_3$	17.16	49	51	0
$Ru5P/Al_2O_3$	48.04	38	62	0
$Pt5P/Al_2O_3$	70.29	36	63	0
$Pd5P/Al_2O_3$	81.97	38	51	11
Pd/Al_2O_3	99.35	0	98	2

Catalysts	Yield (%)			Rate of Reaction $\times 10^2$ (mole ethanol/g cat. h)
	Diethyl ether	Ethylene	Acetaldehyde	
Al_2O_3	0.00	87.60	0.88	32.03
$5P/Al_2O_3$	5.17	80.95	0.00	31.17
$12P/Al_2O_3$	15.30	57.56	0.00	26.37
$14P/Al_2O_3$	12.42	23.07	0.00	12.85
$20P/Al_2O_3$	8.41	8.75	0.00	6.21
$Ru5P/Al_2O_3$	18.26	29.78	0.48	17.39
$Pt5P/Al_2O_3$	25.30	44.28	0.00	25.44
$Pd5P/Al_2O_3$	31.15	41.80	9.02	29.67
Pd/Al_2O_3	0.00	97.36	1.99	35.96

Table G.6 Ethanol conversion and diethyl ether yield obtained from dehydration reaction of ethanol in time on stream system through Al_2O_3, $5P/Al_2O_3$ and $Pd5P/Al_2O_3$ at 250, 300 and 350°C, respectively

Time	Ethanol Conversion (%)			Diethyl Ether Yield (%)		
(h)	Al_2O_3	$5P/Al_2O_3$	$Pd5P/Al_2O_3$	Al_2O_3	$5P/Al_2O_3$	$Pd5P/Al_2O_3$
1	30.18	28.86	28.17	24.77	17.35	20.73
2	32.23	30.41	35.25	29.06	27.39	27.91
3	38.47	35.30	42.14	35.53	33.17	32.87
4	34.02	36.18	45.78	32.16	34.33	36.22
5	32.14	34.25	51.65	29.99	32.30	40.47
6	34.17	40.13	55.68	31.31	37.57	46.55
7	36.41	37.32	63.14	32.89	35.13	48.85
8	36.89	35.44	68.97	32.76	33.22	55.98
9	36.66	38.29	70.22	33.43	36.10	56.25
10	33.24	39.57	72.15	29.75	37.41	59.20

VITA

Miss Mutjalin Limlamthong was born on March 9th, 1993 in Bangkok province, Thailand. She finished high school from the Demonstration School of Ramkhamheang University in 2010 and received the bachelor's degree in Department of Chemical Engineering, Faculty of Engineering, Chulalongkorn University in 2015. She has continued her study in master's degree at Department of Chemical Engineering, Faculty of Engineering, Chulalongkorn University since 2015.